EP 2006-02

Assessment of the potential for orogenic gold deposits in the Abitibi

Documents complémentaires

Additional Files

Licence

License

Énergie et Ressources naturelles
Québec

Assessment of the potential for orogenic gold deposits in the Abitibi

Daniel Lamothe and Jeff R. Harris[1]

EP 2006-02

2006

[1] Geological Survey of Canada

ABSTRACT

The aim of this study is to determine the location of high-favourability zones for orogenic gold deposits in the Abitibi. It also describes 313 potential gold occurrences that were unstaked at the time of the study. High-favourability zones are defined using 19 parameters in 6 broad classes, that is: 1) lithological control; 2) structural control; 3) metal indices; 4) geophysical signature; 5) alteration indices; and 6) favourable geological setting.

The geological significance of each parameter is evaluated by the weights-of-evidence spatial analysis method. This technique is used to measure the degree of spatial association between a given parameter and the location of known occurrences. A binary map has been produced for each parameter, showing the areas of high favourability for gold deposits in the Abitibi. The different combinations of parameters are weighted using a radial basis neural network approach. The result is an overall favourability map for orogenic gold deposits in the Abitibi, available at 1:500,000 scale in PDF format.

A minimal favourability threshold value for defining high-favourability zones was determined using a statistical approach. These zones encompass 79% of the 179 gold mines and deposits with an estimated tonnage that were used to assess the spatial association of the parameters. From these zones, the authors eliminated the sectors staked on December 6, 2005 together with the unstakable sectors, thereby identifying 313 exploration targets. The targets have been grouped into four classes according to the number of parameters that went into defining them. The assessment of favourability, the high-favourability zones and the targets are shown on 132 maps (1:50,000 scale) available in PDF format on CD-ROM. Each target on a map is linked to a database containing a large amount of valuable information for assessing potential. The grid and vector data used to prepare the document are also provided on the CD-ROM.

DOCUMENT PUBLISHED BY GÉOLOGIE QUÉBEC

Director
Alain Simard

Service à la clientèle de l'exploration et du marketing
Chantal Dussault

Document accepted for publication on 2006/01/09

Translation
Barbara Chunn

Editing
Denis L. Lefebvre, eng.

Dépôt légal – Bibliothèque nationale du Québec
ISBN : 2-550-46418-4

TABLE DES MATIÈRES

1 Introduction

The advent of GIS (geographic information system) platforms in the early 1990s led to the development of approaches for processing and combining a variety of geological parameters in order to define zones favourable for the exploration of economic minerals (see Chung and Agterberg, 1980; Bonham-Carter et al., 1988; Harris, 1989; Agterberg et al. 1990; Chung and Moon, 1991; Bonham-Carter, 1994; Rencz et al., 1994; Harris et al., 1995; Wright and Bonham-Carter, 1996; Singer and Kouda, 1997a,b; Raines, 1999; Harris et al., 2001; Brown et al., 2000; D'Ercole et al., 2000; de Araujo and Macedo, 2002; Porwal et al., 2003a,b). A number of assessment studies based on georeferenced data integration have been published for several ore deposit models, specifically:

- volcanogenic massive sulphides (VMS) deposits (Wright and Bonham-Carter, 1996; Dion and Lamothe, 2002);
- mesothermal gold deposits (Harris et al., 2001; Groves et al., 2000; Knox-Robinson, 2000);
- epithermal gold deposits (Boleneus et al., 2001);
- Mississipi Valley-type deposits (D'Ercole et al., 2000);
- Olympic Dam-Kiruna-type deposits (Lamothe and Beaumier, 2001 and 2002);
- kimberlite potential (Labbé, 2002; Paganelli et al., 2002).

There are several steps in the production of a mineral potential map (Figure 1). First, an appropriate exploration model (e.g. VMS, or orogenic gold) must be selected for the targeted mineral(s). Using this model, geological parameters are chosen and combined to create a **favourability map**[1]. This step is crucial because it enables the modeller to evaluate the availability of sources of georeferenced data for each parameter and to calculate the time it will take to acquire new data sources, if needed. It is also during this step that an appropriate *geodetic reference system* and map projection will be chosen.

The second step consists in producing, for each parameter selected, a **digital evidence map**[1], which will be integrated when processing the exploration model. The map format is either binary (0 or 1), multi-class or continuous (See Harris et al., 1999, 2000, 2001). This processing step generally requires the use of spatial analysis or statistical processing software that is usually available as a GIS extension.

The third step involves integrating the different evidence maps in order to produce a favourability map. The integration approaches fall into two categories (Table 1): data-driven methods and knowledge-driven methods (See Bonham-Carter (1994) and Wright and Bonham-Carter (1996) for a detailed review). In order to use data-driven approaches, a sufficient number of mineralized zones of the type sought must be present in the study area. These methods analyse the spatial relationships between the evidence data (parameters) and the location of known deposits, allowing a weight to be assigned to each evidence map. The weights-of-evidence (*WofE*) method (Bonham-Carter, 1994),

[1] This term has come into increasing use in the scientific literature.

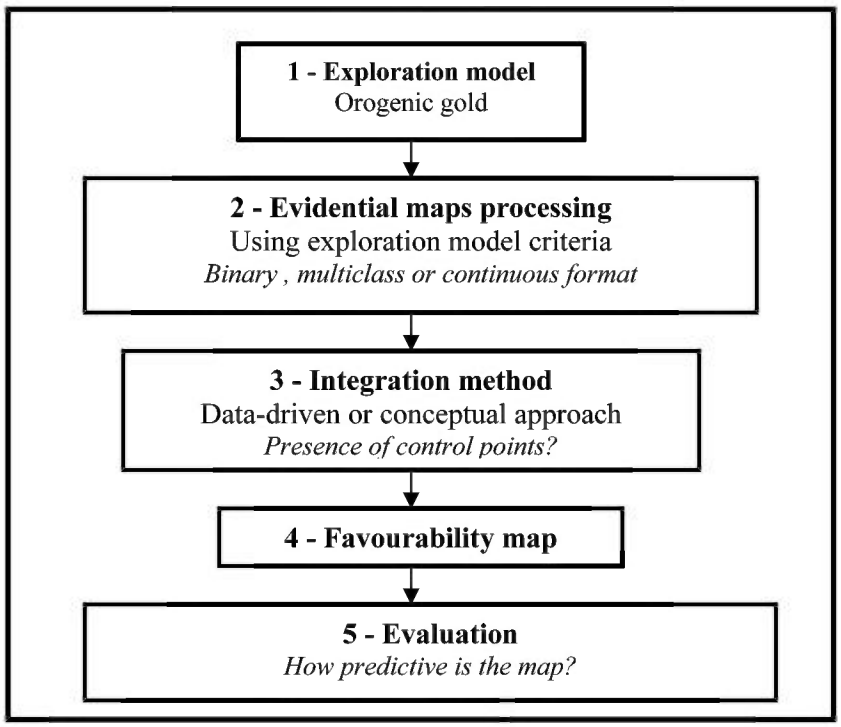

Figure 1 - Steps in creating a favourability map through georeferenced data integration (modified from Harris et al., 2005).

logistic regression (Chung and Agterberg, 1980) and neural network analysis (Singer and Kouda, 1996, 1999; Harris and Pan, 1999; Brown et al., 2000) are data-driven methods (Table 1).

Knowledge-driven (conceptual) approaches harness the modeller's expertise in assigning weight factors to the individual evidence maps based on the exploration model. Although subjective, these methods allow the geologist's knowledge and experience to be incorporated into the procedures. They include Boolean logic, multi-layer overlay (Harris, 1989), Dempster-Schafer belief theory functions (Chung and Moon, 1991; An et al., 1992) and fuzzy logic (An et al., 1991).

It is possible to develop hybrid models that combine the data-driven and knowledge-driven approaches. For example, to assess the potential for SEDEX deposits in India (Porwal et al., 2003b) or VMS deposits in the Abitibi (Lamothe et al., 2005), these authors used the weights-of-evidence approach to weight the parameters, converting these values into fuzzy weights and combining the evidence maps using fuzzy logic. In another case, Brown et al. (2003a) weighted evidence maps by fuzzy logic and combined them using neural networks in order to assess the orogenic gold potential of western Australia.

The result of the integration process is a georeferenced map of potential illustrating zones of high favourability for the type of mineral resource sought. In addition to correctly predicting the presence of known deposits, the map should also identify new exploration zones. The credibility of such a map is dependent on the effective measurement of favourability. Countervalidation techniques are used to confirm the reliability of the method. This validation step is important and should be integrated into any serious assessment of mineral potential.

Table 1 - Methods of integrating evidence maps in a GIS environment.

Method	Processing	Combination Criteria
Data-driven methods		
Weight of evidence (WofE)	Control points (known deposits or occurrences)	Determination of the spatial relationship between known occurrences and the variables being tested (use of Bayes' Theorem)
Logistic regression	Control points (known deposits or occurrences)	Use of spatial zones around known deposits to determine the statistical criteria for applying data layers to predict the presence or absence of mineral deposits
Neural networks	Control points (known deposits or occurrences)	Reproduction of an anomalous assemblage (i.e. deposits) through a shape recognition process
Knowledge-driven methods		
Boolean operations	Input of the geologist	Sum of binary maps
Multi-layer overlay	Input of the geologist	Sum of weighted binary maps
Inference network and decision tree used in an expert system	Input of the geologist	
Dempster-Shafer belief theory	Input of the geologist	
Fuzzy logic	Input of the geologist	Each prediction map is assigned a fuzzy weighting factor ranging from 0 to 1; maps are combined using a fuzzy operator (and, or, gamma)
Analytic Hierarchy Process (AHP)	Input of the geologist	Sum of weighted favourability (continuous maps)

1.1 Study objectives

The purpose of the present study was to determine the location of high-favourability zones for orogenic gold deposits in the Abitibi. Although many of these zones are already staked, the aim was to define a number of unstaked targets and provide a maximum of data to facilitate the assessment of each target. This will enable mining industry stakeholders to capitalize on the study findings quickly, while also allowing the authors to evaluate the benefits of the study by determining the number of targets staked after it is published.

The authors' second goal was to determine the usefulness and credibility of this type of approach by assessing the predictive value of the favourability map produced in the study.

1.2 Parameters

The assessment study covers 12 NTS sheets at 1:250,000 scale, i.e. an area of more than 177,000 km^2 (Figure 2). Since the region of interest lies in two UTM zones, all the data from zone 17 were projected into zone 18. All digital files generated in the study and included on the CD-ROM are in UTM projection, NAD 83, zone 18. Grid files for the evidence maps covering the Abitibi are composed of 50-m cells spread out on a grid of 9,002 rows by 11,294 columns. The final favourability map has a resolution of 100 m. Processing was performed with ArcView 3.2 and ArcGIS 8.3. Weight calculations and parameter combinations were done with Arc-SDM.

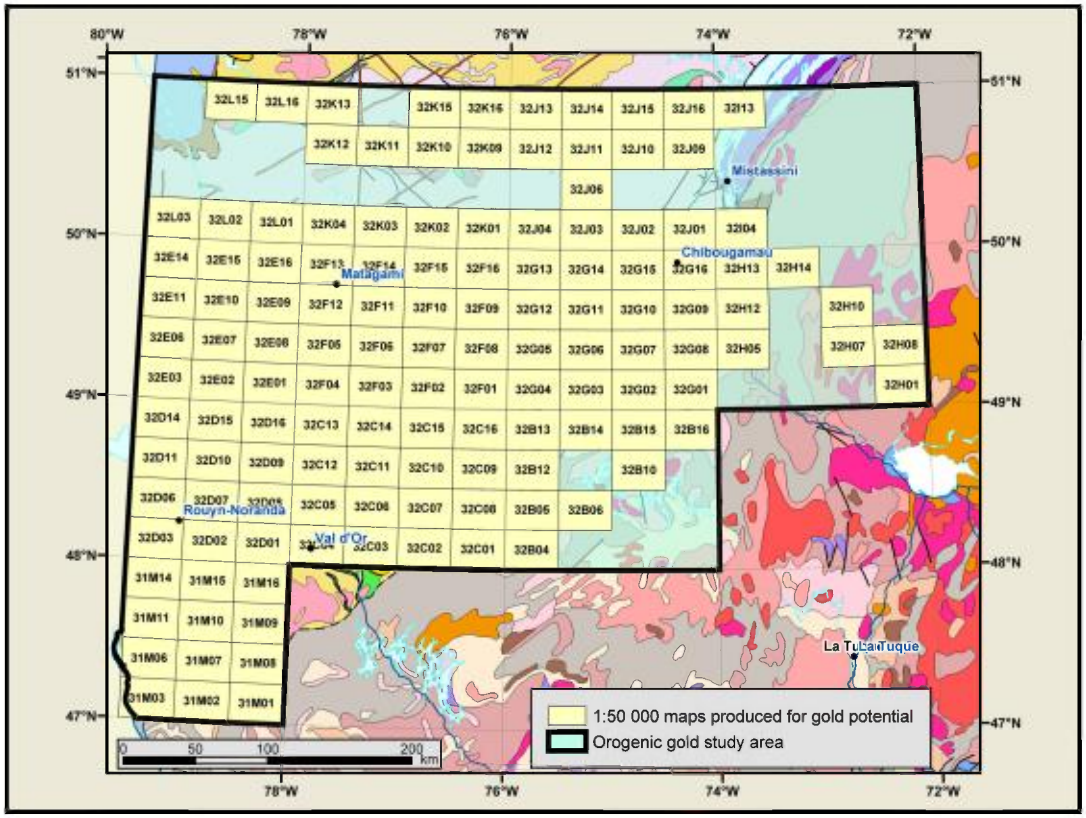

Figure 2 - Location of study area and list of 1:50,000-scale favourability maps available separately in PDF format.

In addition to this guide describing the processing of parameters for the orogenic gold model, other deliverables include:

- 132 maps at 1:50,000 scale in PDF format showing the calculated favourability, the location of the high-favourability zones defined in the study and the location of targets not yet staked at the time of publication;
- one map at 1:500,000 scale of the entire Abitibi in PDF format;
- all parameter evidence maps in ESRI vector format and/or ASCII grid format; this grid format can be imported in most widely used GIS. The final favourability map is available in UTM projection, NAD 83, zone 18, and in geographic projection.

- one vector file of Abitibi geology in polygons. The data for this file were taken from digital polyline maps available in SIGEOM databases as of June 2004. Whenever possible, 1:20,000-scale maps were used; otherwise 1:50,000- or 1:250,000-scale data were used. Given the limited time available for this study, no reinterpretation or standardization of lithologies or of stratigraphy was performed prior to data integration.
- An Access database composed of files summarizing the available information for each target defined in the study. Each file contains:
  - position in UTM coordinates (zone, easting and northing) from the central point of the target;
  - target dimensions in m^2;
  - target class based on the number of parameters used to define it;
  - geological units in contact with the target;
  - descriptive data on the gold deposits located within 2 km of the target;
  - descriptive data on drill holes located within 200 m of the target;
  - data from analyses of rocks located within 200 m of the target;
  - contribution of each parameter used to define the target;
  - descriptive list of MRNF documents related to the target; and
  - descriptive list of the mineral exploration documents dealing with the target.

2 Geological characteristics of Archean orogenic gold deposits

Archean orogenic gold deposits are generally defined as structurally controlled vein or shear margin deposits emplaced epigenetically in all lithologies occurring in volcanoplutonic belts of Archean age (Groves et al., 1998). These gold concentrations are the result of relatively homogeneous hydrothermal fluid flows of variable origin, including metamorphic devolatilization, felsic plutonism and mantle fluids (Hagemann and Cassidy, 2000).

Structural control is predominant at the mesocopic and macroscopic scales of mineralization. The deposits are typically located in second- and third-order structures, generally in proximity to large-scale compressive structures. The brittle to ductile nature of the structural controls is expressed in a wide variety of styles, including (a) brittle faults in ductile shear zones indicating low- to high-angle reverse movement, strike-slip or oblique movement; (b) a network of fractures, stockwerks or even brecciated zones in competent rocks; (c) foliated zones; or (d) fold hinges in ductile turbidite sequences (Groves et al., 1998).

Orogenic gold deposits exhibit strong hydrothermal alteration with lateral zoning composed of mineral assemblages indicative of proximal to distal alteration. These assemblages, composed generally of carbonates (ankerite, dolomite or calcite) and sulphides (mainly pyrite, pyrrhotite, arsenopyrite), vary with the type of host rock and crustal depth. Alkaline metasomatism is characterized by sericitization or albitization, or by the formation of fuchsite, biotite, alkaline feldspath and/or by chloritization of mafic minerals. Sulphidation reaches a peak in iron formations or in iron-rich host rocks. Greenschist facies alteration of host rocks implies the addition of significant quantities of CO_2, S, K, H_2O, SiO_2, ±Na and light lithophilic elements (Groves et al., 1998).

3 Methodology for assessing favourability

3.1 Assessment of potential using neural network analysis

Orogenic gold deposits share certain general parameters, such as rheological control linked to the competence of the host rock, structural control linked to regional tectonic constraints and synorogenic emplacement in a hydrothermal environment. However, owing to significant variability in local physical and chemical conditions, the individual characteristics of orogenic gold deposits vary greatly (Hagemann and Cassidy, 2000).

To overcome this complexity, a number of authors have recently tested the usefulness of artificial neural networks in assessing mineral potential (Harris and Pan, 1999; Singer and Kouda, 1999; Brown et al., 2000, 2003a,b; Koike et al., 2002). Artificial neural networks are a relatively new data-driven approach for this type of assessment. An outgrowth of artificial intelligence research, these analytical systems have properties that are particularly well suited to recognizing shapes and classifying data. For example, they can recognize non-linear patterns in multifactorial data sets that cannot be detected visually or by standard statistical analyses.

A neural network approach is especially useful for handling a large enough number of control points (deposits) in the absence of a robust metallogenic model. This is clearly the case for the Abitibi region because it has 1,367 documented orogenic gold deposits, including 211 mines (active or closed) or deposits with a tonnage estimate. Since a data-driven approach has been adopted in this study, 179 mines or deposits with a tonnage estimate out of a total of 211 occurrences were used as a training set, with the remainder (32 points) being used to validate the predictions of the final map.

The neural network-based assessment of potential was performed using the Arc-SDM module in ArcView. This module[1], which is distributed free of charge, can be used to produce mineral potential maps using three different data-driven methods (*Weights of Evidence* or *WofE*, logistic regression, neural network analysis) or a conceptual method (fuzzy logic). There are several types of neural network algorithms; the one used by Arc-SDM (called DataXplore; Looney and Yu, 1999) belongs to the **radial basis function (RBF)** class. RBF networks are a special type of **multilayer Perceptron** networks that belong to the feedforward category of supervised networks. The input layer consists of relevant geological parameters selected intuitively by the geologist. RBF networks use Gaussian functions in a hidden layer (Figure 3) to determine the weight of the connections between the hidden layer and the output layer.

This study uses 19 geological parameters (Table 2). Each parameter gives rise to a binary grid file (composed of cells with a value of 0 or 1) made up of cells, each covering an area of 50 metres by 50 metres. When these 19 binary maps are combined, a grid file is generated comprising 9,031 combinations. The resulting grid file is called a "**unique conditions" map**. The 179 points of the training set are distributed among 167 different combination values ("unique conditions"). The DataXplore module in Arc-SDM uses these 167 unique values as **training vectors** in a hidden layer (Figure 3). RBF processing seeks to optimize the weighting around each vector by adjusting the weight factor, the central points and the spread (Gaussian distribution) in a reiterative manner.

[1] Available at the following Web site: http://ntserv.gis.nrcan.gc.ca/sdm/

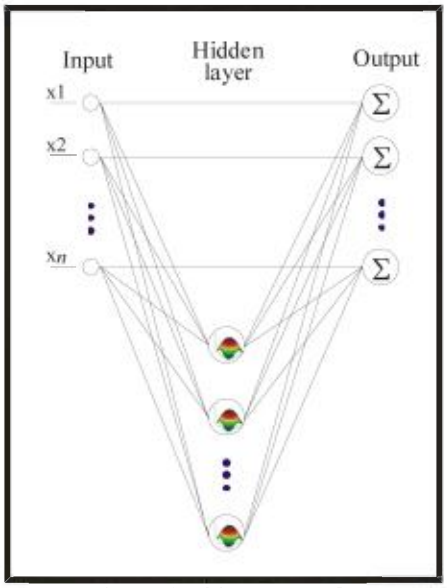

Figure 3 - Architecture of an RBF network.

3.2 Parameters

Most of the parameters useful for processing a mineral potential map can be obtained directly from the ***e-SIGEOM à la carte*** tool on the MRNF's Web site. This tool can be used to query the different digital databases making up the Système d'information géominière (SIGEOM), which includes more than 92,600 drill holes, 81,700 whole rock analyses and 180,000 outcrops compiled for the Abitibi.

The first step in any assessment of potential consists in selecting parameters that will be effective predictors of orogenic gold deposits from all the possible geological parameters available in digital format for the study area. The "weights-of-evidence" method (Bonham-Carter et al., 1989; Harris et al., 2001; Lamothe et al., 2005) was used to evaluate the spatial association of the individual parameters with the known orogenic gold occurrences, i.e. the group of 179 mines/deposits with a tonnage estimate. Only those parameters with contrast (C) values greater than 1.5 were retained. The list of parameters is given in Table 2.

Table 2 - Parameters used to assess the potentiel for orogenic gold deposits in the Abitibi.

Family of parameters	Parameters used
Lithological control	Association with a favourable lithology Lithological diversity Competence contrast Reactivity
Structural control	Proximity to an Archean fault Archean fault density Proximity to a ductile lineament Proximity to quartz veins
Metal indices	Proximity to an Au anomaly Proximity to an As anomaly Proximity to an Sb anomaly Proximity to an S anomaly
Geophysical evidence	Favourable value for total magnetic field Favourable value for vertical magnetic gradient
Alteration indices	Proximity to an anomalous ISER index Proximity to an ICHLOR index Proximity to an anomalous IPAF index Proximity to a mineralization indicator
Favourable metallogenic context	Association with a favourable zone for VMS

3.3 Parameter processing strategy

The approach generally adopted with neural networks is to use the raw data for each parameter (distance around a fault, point or interpolated value for arsenic, etc.) to train the system. However, in view of the fairly high number of parameters involved and the vast study region, such an approach cannot be used with the RBF network in Arc-SDM, because it generates too many unique conditions which impede processing. To reduce the number of unique conditions, the following modifications were made:

- Cell size was enlarged from 50 m to 100 m during the creation of the unique conditions map;
- Multi-class maps were transformed into binary evidence maps. The threshold between predictive values (=1) and non-predictive values (=0) for a parameter is determined by the weights-of-evidence method (see Section 3.4).

These two changes made it possible to reduce the number of unique conditions to 9,031 once all the evidence maps were combined. This number is low enough that the DataXplore module can run the RBF network analysis.

3.4 Weights-of-evidence method

The weights-of-evidence method, developed by Bonham-Carter et al. (1988) and Agterberg (1989), is a data-driven technique that incorporated concepts developed by Spiegelhalter (1986) and was later applied to mineral exploration (Bonham-Carter, 1994; Harris et al., 1995 and 2001; Wright, 1996; Raines, 1999). This approach measures the probability that a spatial association exists between a set of predictors (evidence maps) and the location of known deposits. The degree of spatial association is assessed using a pair of weight factors (W^+ et W^-) calculated from the amount of overlap between known deposits and evidence maps. If there is no spatial association between the training set and the evidence maps, then $W^+ = W^- = 0$. A positive W^+ value indicates a positive association between the training set and the predictor, whereas a negative W^- value points to a negative association. The contrast value ($C = W^+ - W^-$), introduced by Agterberg (1989) and Agterberg et al. (1990), is also an indicator of spatial association. A contrast value of 0 indicates an absence of spatial association (random distribution) between a set of points and an evidence map, whereas a higher C value (typically ≥ 1.0) indicates a stronger association. The anomaly threshold of a data set is generally obtained by identifying the break point for the contrast curve relative to the class intervals (Figure 4).

The studentized contrast value, or Stud(Cnt), which is obtained by dividing the C value by its standard deviation, is a measure of its significance. Studentized contrast values greater than 1.5 indicate that the C value is significant (Bonham-Carter, 1994). The different parameters of the weight-of-evidence method calculated using Arc-SDM are presented in Table 3.

Table 3 - Parameters calculated by the *WofE* module in Arc-SDM.

Factor	Description
Class	Identifier for specific classes or attribute values
Area_km²	Area of each class in km²
No_Points	Number of training points that fall within the area of the class
W+	Value of *W+*
s(W+)	Standard deviation of *W+*
W-	Value of *W-*
s(W-)	Standard deviation of *W-*
C	Contrast (difference between *W+* and *W-*)
s(C)	Standard deviation of C
Stud(Cnt)	Studentized contrast (C divided by *s(C)*)

In creating a mineral potential map, this method assumes conditional independence of the data making up the different evidence maps with respect to orogenic gold deposits. Violation of the conditional independence assumption tends to result in favourability maps for which the posterior probability values are overestimated. Since the processes involved in the generation of gold-bearing deposits are usually interdependent (the Au, As and Sb levels generally have a strong positive correlation; the demarcation line between geological contacts is often based on the contours of magnetic field maps in zones with few outcrops, etc.), the conditional independence requirement generally precludes the use of the weights-of-evidence method to create favourability maps. The method is nonetheless valid for measuring the spatial association of the parameters considered individually.

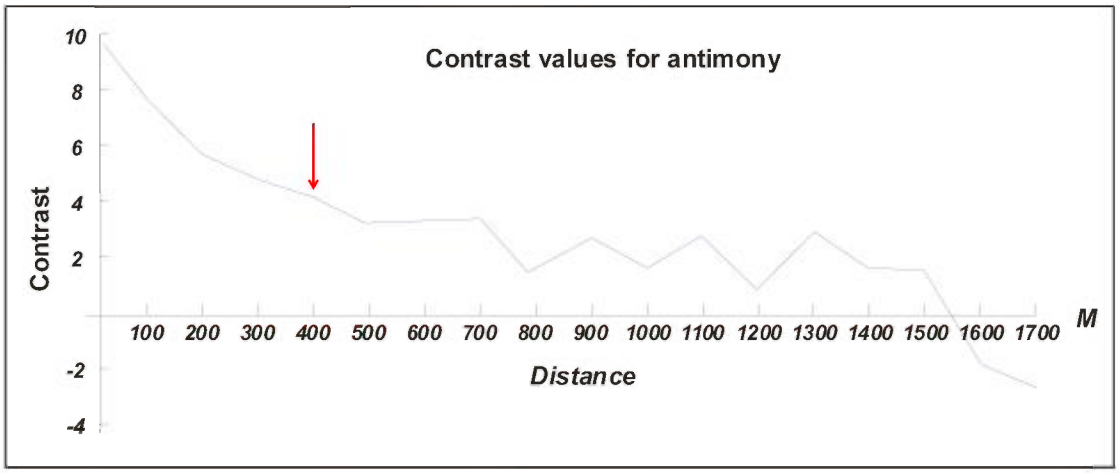

Figure 4 - Determination of the anomaly threshold of contrast values (C) for antimony. In this example, the antimony concentrations exhibit a strong correlation up to a distance of 400 m distance from the sampling point.

4 Processing of evidence maps

All the binary evidence maps described in this section have been created by the weights-of-evidence method. This approach evaluates the probability of association between a geological parameter and a set of points representing the targeted type of mineralization (Bonham-Carter et al., 1989; Harris et al., 2001). The Abitibi region has 1,367 documented orogenic gold deposits; these include active or closed mines, deposits with a tonnage estimate, exploited deposits and showings (Table 4). In this study, only the mines and the deposits with a tonnage estimate were used to evaluate the spatial association between the parameters and orogenic gold deposits. These types of ore bodies are generally well documented, and studies show that the favourability maps produced based on mines or deposits with a tonnage estimate have a greater predictability (Lamothe et al., 2005; Harris et al., 2005). Of the 211 occurrences of these two types available in SIGEOM, 32 were extracted randomly to create a validation set and set aside for testing purposes. The rest (179 ore bodies) were used to create a set of training data (*training set*), used to measure the spatial association of the parameters and to weight the RBF network processing.

Table 4 - Orogenic gold deposits in the Abitibi from SIGEOM.

Type of ore body	Number
Active or closed mines	99
Deposits with a tonnage estimate	112
Exploited deposits	638
Showings	518
Total	**1367**

4.1 Lithological control

4.1.1 Association with a favourable lithology

Several assessment studies on potential for mesothermal gold in Ontario have shown that certain lithologies are preferentially associated with gold-bearing deposits (Harris et al., 2001; Harris et al., 2005). To validate this hypothesis in the Abitibi context, the weights of evidence method was used to measure the spatial association between the different lithologies of the Abitibi and a set of 179 mines and deposits with a tonnage estimate corresponding to orogenic gold deposits (Table 5). The approach consists in determining the probability that a lithology will contain a gold deposit; the notion of proximity is therefore not pertinent to this approach. Processing is performed using an ArcView file consisting of closed polygons associated with a database containing lithological and stratigraphic information for the Abitibi (shapefile). The data making up this file come from the polyline digital maps available in the databases of SIGEOM. Where present, 1:20,000-scale maps were used, and the data from 1:50,000- or 1:250,000-scale maps were used as a complement. Given the time constraints imposed on the study, no reinterpretation or standardization of lithologies or of stratigraphy was performed prior to data integration. By generalizing the information contained in the lithological code field of the file, it is possible to create a lithological map of the Abitibi (shapefile) (Figure 5).

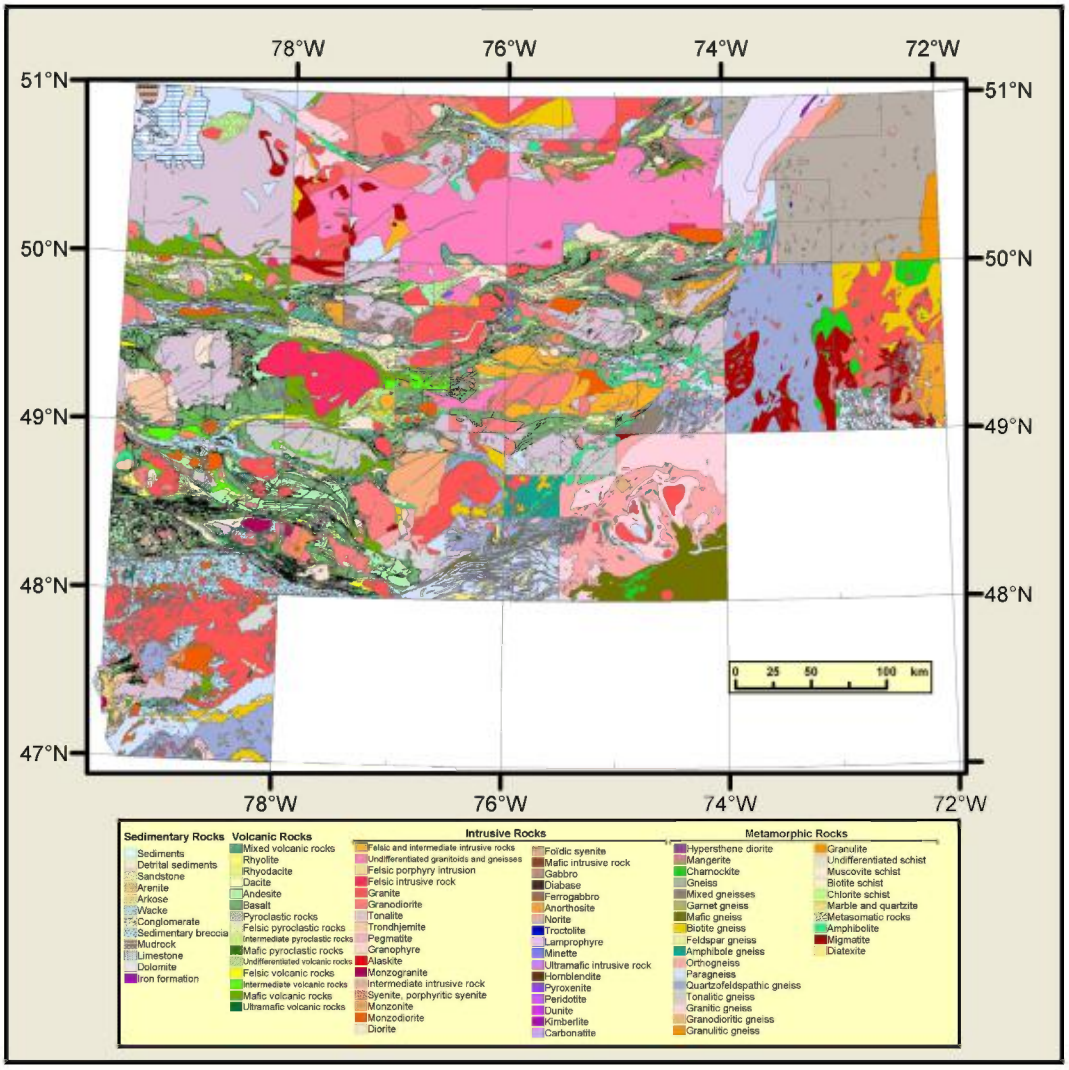

Figure 5 - Lithological map of the Abitibi obtained by generalizing the lithological codes in the Abitibi polygon file.

Hodgson (1993) clearly showed that gold deposits can be found in any type of rock. However, certain types of rocks contain substantially more gold than would normally be inferred on the basis of their statistical distribution in a greenstone belt. Among other hypotheses, two factors are currently put forward to explain this situation:

- Iron-rich lithologies are known to be effective traps for hydrothermal solutions carrying gold. The high or extreme Fe content of lithologies 1 to 4 in Table 5 confirm this point.

- Highly competent lithologies (i.e., lithologies 2 to 5, 8 and 11) are more likely to contain gold deposits because they generally have a high fracturation index conducive to the circulation of hydrothermic fluids.

Table 5 - Contrast values (C) and studentized contrast values (StudCnt) calculated for the lithologies of the Abitibi region. The lithologies were classified in descending order of contrast. The zones corresponding to the lithologies in yellow are considered favourable (value of 1 on the binary evidence map).

#	Code	Lithology	C	Stud(Cnt)
1	V3T	Mafic pyroclastics	3.4737	3.4095
2	I3	Intrusive mafic or ultramafic rocks	3.4717	4.8064
3	V4	Ultramafic lava	2.4893	5.4565
4	S9	Iron formation	2.3772	3.3254
5	V1B	Rhyolite	2.0572	4.9356
6	S4	Conglomerate	2.0315	3.4761
7	VT	Pyroclastics	1.9256	3.2962
8	I2J	Diorite	1.8799	6.9491
9	I1E	Trondhjemite	1.8065	4.3376
10	S	Detrital sediments	1.8012	3.9595
11	I3A	Gabbro	1.7191	6.3576
12	V2J	Andesite	1.5806	6.3468
13	V2T	Intermediate pyroclastics	1.5425	3.0434
14	I4B	Pyroxenite	1.3539	1.3475
15	V1	Felsic volcanics	1.3519	1.8975
16	V1T	Felsic pyroclastics	1.2738	2.1838
17	V3B	Basalt	1.1066	5.5956
18	I2D	Syenite	0.9716	0.9676
19	V1D	Dacite	0.9669	0.9629
20	V2	Intermediate volcanics	0.6019	0.8456
21	S6	Mudrock	0.5608	0.5587
22	V3	Mafic volcanics	0.5325	1.4708
23	S1	Sandstone	0.4939	0.9759
24	V	Mixed volcanic rocks	0.3322	0.732
25	I2F	Monzonite	0.1663	0.1657
26	I1C	Granodiorite	0.0865	0.2655
27	S3	Wacke	0.0109	0.0262
28	M16	Amphibolite	-0.2166	-0.3045

All lithologies with a C value greater than 1.5 were considered predictive and are represented by a value of 1 on the binary evidence map of favourable lithologies (Figure 6).

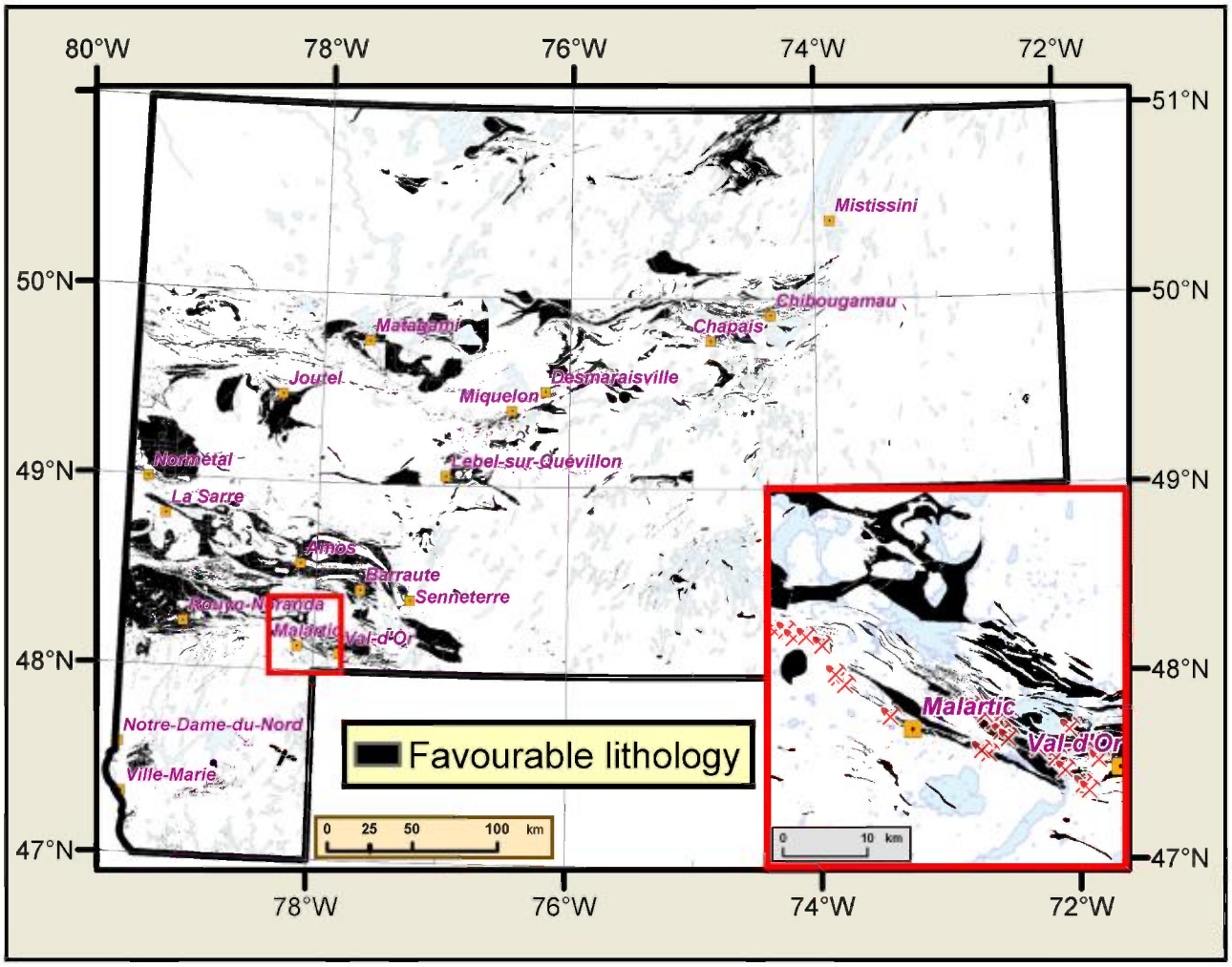

Figure 6 - Favourable lithologies for orgenic gold mineralization.

4.1.2 Lithological diversity

Some researchers have shown that there is a direct relationship between the geological complexity of a sector and the diversity of occurrences in that sector, especially with respect to potential for gold (Mihalasky and Bonham-Carter, 2001; Hagemann and Cassidy, 2000). The concept of lithological diversity (or lithodiversity), defined as the frequency of rock types per unit area, was also used by Brown et al. (2003a and b) to assess the potential for orogenic gold deposits in the Kalgoorlie Terrane of Western Australia.

Lithological diversity is measured in a manner similar to competence contrast, except that the *Variety* option of the *"neighborhood statistics"* function in *"Spatial Analyst"* (an ArcGIS extension) is used. This processing performed on a grid file obtained by conversion of a vector file of lithologies, assigns to each cell of the image a value indicating the number of unique lithologies counted inside a window whose size is determined by the modeller. Tests with windows of 6¼, 25 and 100 km² showed that a size of 25 km² was optimal, given the variable map scales characterizing the polygon file of Abitibi geology. The assessment of favourability using *WofE* shows that maximal optimization of the results (Figure 7) is obtained by a grouping in 5 classes using Jenks natural breaks scheme (1967). *WofE* analysis of mineral potential favourability shows that only the 2 classes of cells with a density equal to or greater than 15 unique lithologies per 25

km² exhibit a significant contrast value (Table 6). The binary evidence map for lithodiversity is created by assigning a value of 1 to these two classes (Figure 8).

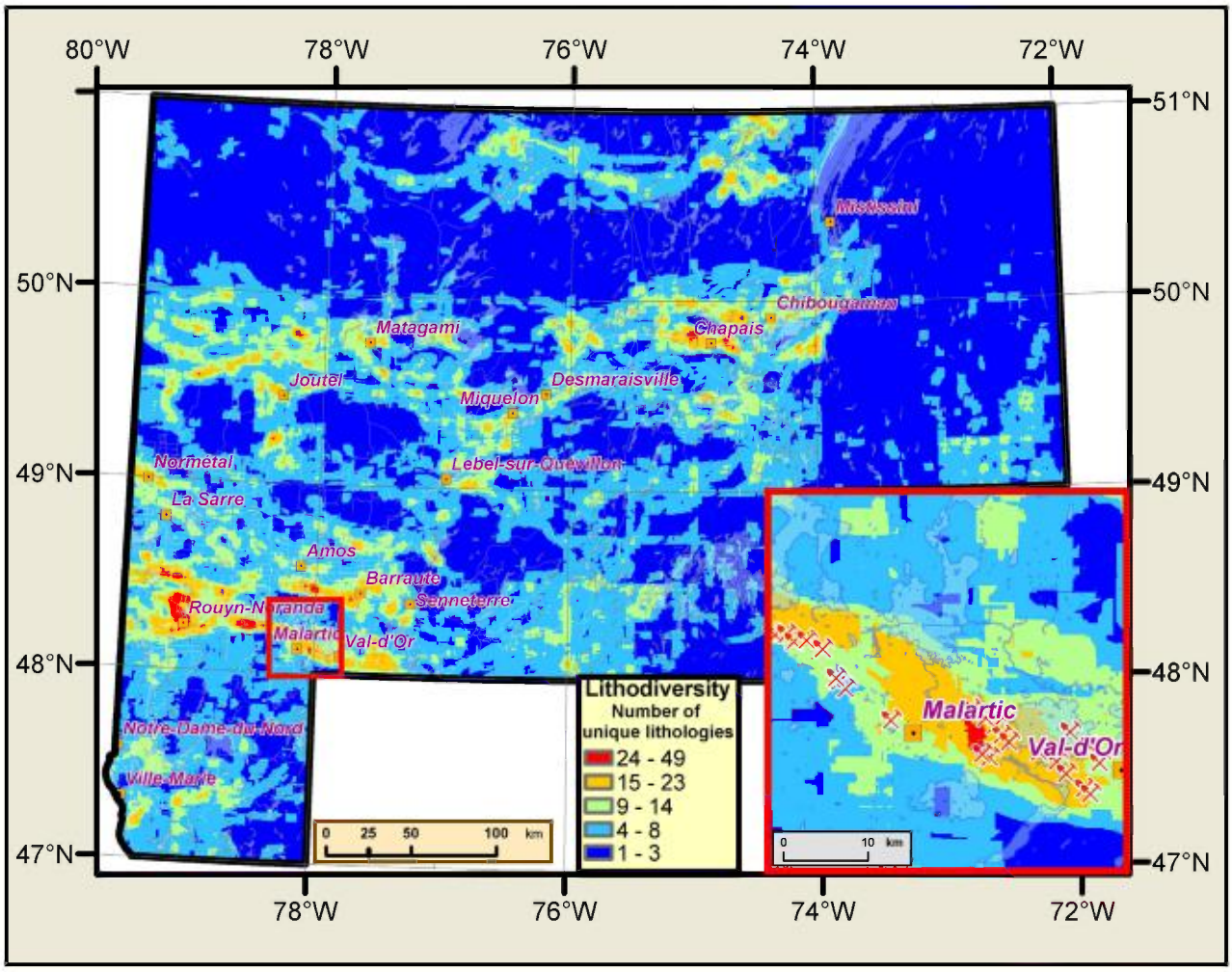

Figure 7 - Lithodiversity of the Abitibi. The contrast values were grouped into 5 classes by the natural breaks method.

Table 6 - Results of *WofE* processing for the favourability of lithodiversity. Cells showing a density of 15 or more unique lithologies per 25 km² are considered favourable for gold-bearing deposits. The high studentized contrast values for the two higher classes confirm the reliability of the calculated contrast values (see Table 3 for the definitions of the parameters).

Class	Area_km²	No_Points	*W+*	*s(W+)*	*W-*	*s(W-)*	C	*s(C)*	Stud(Cnt)
24 - 49	417	22	4.0121	0.2191	-0.1289	0.0798	4.141	0.2332	17.7607
15 - 23	4096	63	2.7408	0.127	-0.4108	0.0929	3.1516	0.1573	20.0341
9 - 14	18799	54	1.0502	0.1363	-0.2475	0.0895	1.2977	0.163	7.96
4 - 8	64891	40	-0.4911	0.1582	0.2015	0.0849	-0.6925	0.1795	-3.8582
1 - 3	89575	0							

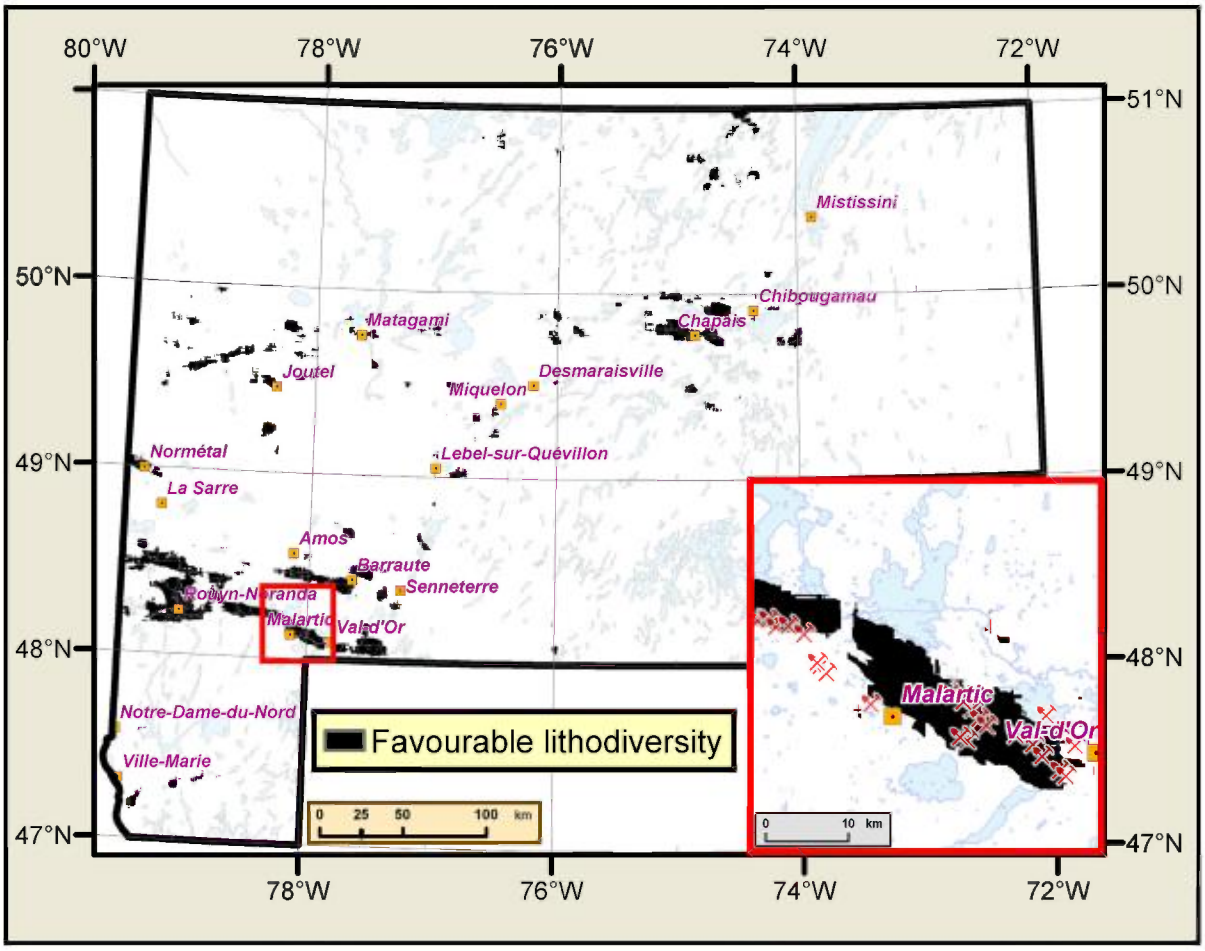

Figure 8 - Zones with a favourable lithodiversity index.

4.1.3 Competence contrast

Many orogenic gold deposits are characterized by a mineralized vein system bordering an intense shear zone. These veins form in the most competent portions of the lithological assemblage subjected to deformation in a fragile or fragile-ductile regime. The competent portions of the assemblage serve as structural traps, and the development of a network of fractures substantially increases the interactive surface between the fluids and the host rock, favouring the precipitation of gold (Mikucki, 1998; Hagemann and Cassidy, 2000). The sectors with the most pronounced competence contrast between rock units are the most promising ones for gold exploration.

Groves (2002) proposed a diagram that can be used to assign a reactivity index and a competence index to lithologies[1] (Figure 9). With this diagram, a competence index was assigned to Archean lithologies in the Abitibi (shapefile) (view table). A favourability test performed on a grid file using only lithological competence shows a favourability contrast value of close to 1.6 for competence indices greater than 30. A competence contrast file was created using a function for analysing differences in the statistical values of neighbouring cells ("Range" option in the

[1] Although the competence indices shown in Figure 9 were established for greenschist facies metamorphic rocks, it is postulated that the competence contrasts will remain essentially unchanged for the amphibolite facies, which account for about 3% to 5% of the Archean rocks of the Abitibi.

"*neighborhood statistics*" function of "*Spatial Analyst*" in ArcGIS). This method can be used to assign to each cell the maximum variance calculated within a radius determined by the modeller. Four tests were carried out using windows of 150, 500, 1,000 and 2,000 metres. The best favourability result for the competence contrast was obtained after reclassifying the standard deviation values in 4 classes with a 150-m window and a maximum contrast value of 2.49 for contrast variances greater than 9 (Table 7). A binary evidence map (Figure 10) of the favourability associated with competence contrast was produced by assigning a value of 1 to the cells in class 4 (Table 7).

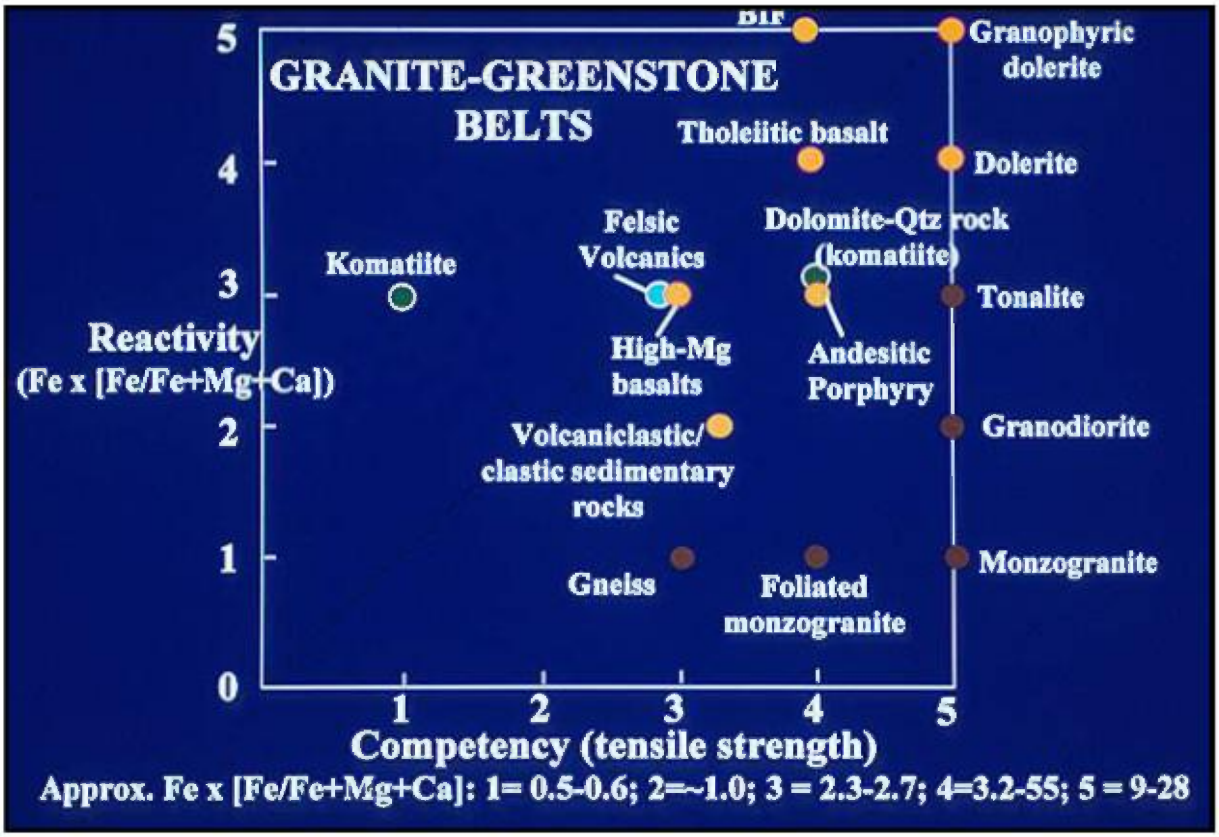

Figure 9 - Reactivity and competence contrast indices for the principal lithologies of the Archean greenstone belts (Groves, 2002).

Table 7 - Results of *WofE* processing for the favourability associated with competence contrasts. The competence contrast values were grouped into 4 classes based on their standard deviation. Only class 4 was considered significant with a C value of 2.4929 and a studentized contrast value of 16.7188 (See Table 3 for the definition of parameters).

Class	Competence contrast	Area_km²	No_Points	W+	s(W+)	W-	s(W-)	C	s(C)	Stud(Cnt)
1	0 - 2	141890	112	-0.5426	0.0945	2.0967	0.1048	-2.6394	0.1412	-18.698
2	3 - 5	2145	22	2.0315	0.2143	-0.0999	0.0742	2.1314	0.2268	9.3988
3	6 - 9	238	2	1.8311	0.7101	-0.0083	0.0704	1.8394	0.7136	2.5777
4	10 - 30	6026	68	2.128	0.122	-0.365	0.0858	2.4929	0.1491	16.7188
-99		27481	7							

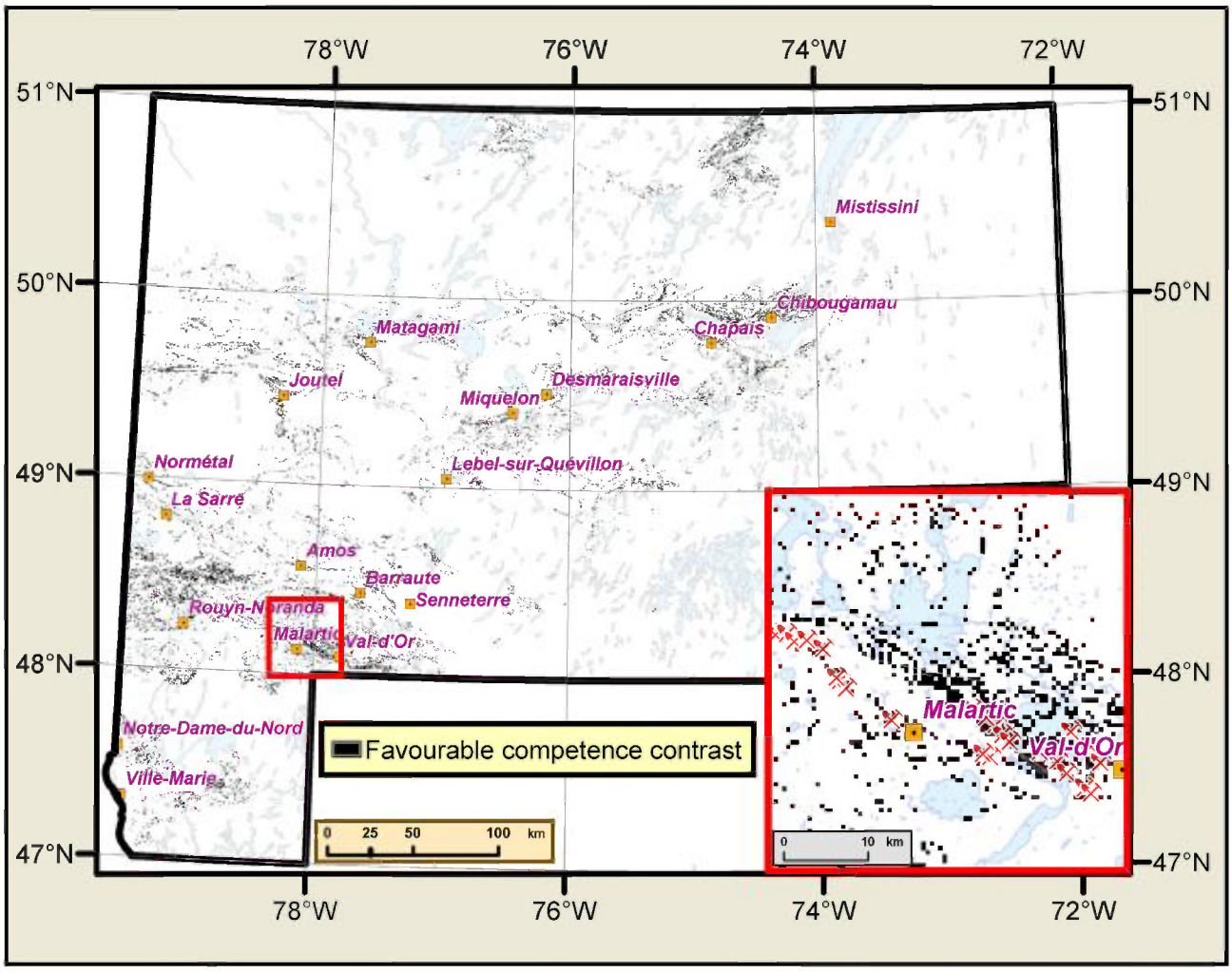

Figure 10 - Zones with a competence contrast favourable for gold mineralization.

4.1.4 Reactivity

In some cases, gold precipitation from hydrothermal fluids is caused by a change in physico-chemical conditions occurring during the interaction between these fluids and the host rock (Mikucki, 1998; Hagemann and Cassidy, 2000). For example, sulphidation of Fe-enriched wall rock has been shown to be an effective mechanism in the creation of major deposits in mafic rocks and iron formations (Phillips and Groves, 1983; Hagemann and Cassidy, 2000). This mechanism has been put forward primarily in relation to gold deposits that formed in alteration halos around hydrothermal conduits. The reactivity of a lithology is therefore directly related to its iron content and determines its potential for gold precipitation.

Using the diagram in Figure 9, a reactivity index was assigned to the Archean lithologies of the Abitibi (shapefile) (view table). For the *WofE* analysis, the reactivity values were reclassified in 5 classes based on their standard deviation. Only the last class (reactivity ≥ 47) shows a clear association with the gold mines and deposits of the Abitibi (Table 8). A binary evidence map (Figure 11) of the lithologies showing a reactivity favourable for gold mineralization was produced by assigning a value of 1 to class 5 rocks.

Table 8 - Results of *WofE* processing for favourability associated with reactivity. The contrast values have been grouped into 5 classes based on their standard deviation. Only class 5 was deemed significant with a C value of 2.0519 (See Table 3 and Figure 9 for the definitions of parameters and reactivity).

Class	Reactivity	Area_km²	No_Points	W+	s(W+)	W-	s(W-)	C	s(C)	Stud(cnt)
1	10-19	45378	2	-3.4503	0.7071	0.3472	0.0694	-3.7975	0.7105	-5.3447
2	19-29	45185	43	-0.377	0.1526	0.1255	0.0774	-0.5025	0.1711	-2.9369
3	29-38	42211	93	0.4637	0.1038	-0.2585	0.0925	0.7222	0.139	5.1938
4	38-47	18459	70	1.0083	0.1198	-0.2758	0.0846	1.2841	0.1466	8.7596
5	47-50	189	2	2.0435	0.7109	-0.0083	0.0694	2.0519	0.7143	2.8727
-99		26357	1							

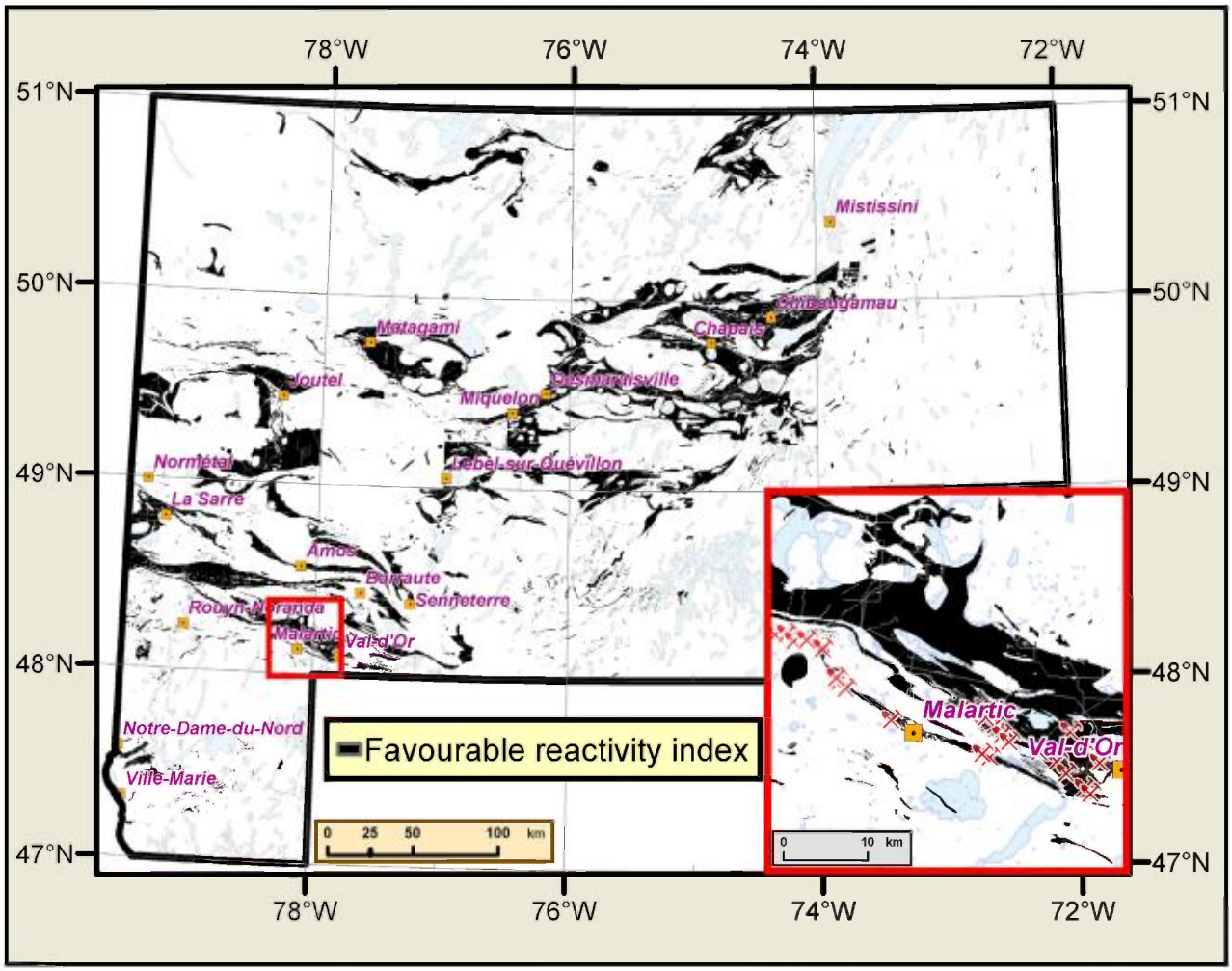

Figure 11 - Lithologies with a reactivity index (≥ 47) favourable for gold mineralization.

4.2 Structural control

Orogenic gold deposits are emplaced along active convergent margins during compressive tectonic regimes (Groves et al., 1998). This type of setting promotes the flow of hydrothermal fluids along major shear zones, which serve as structural traps for gold that precipitates out of solution. The importance of these structures is very clear in the Abitibi, where 87% of mines are located within 5 km of the Cadillac and Porcupine-Destor faults.

4.2.1 Proximity to an Archean fault

This processing was performed on a shapefile of the Abitibi faults from which Proterozoic faults preferentially oriented between N000° and N060° were manually removed. To determine the favourability associated with proximity to Archean faults, an initial buffering at 100-m intervals was performed up to a distance of 2 km (Figure 12). The *WofE* module in Arc-SDM was used to obtain an initial assessment of the weighting for each 100-m class (Table 9).

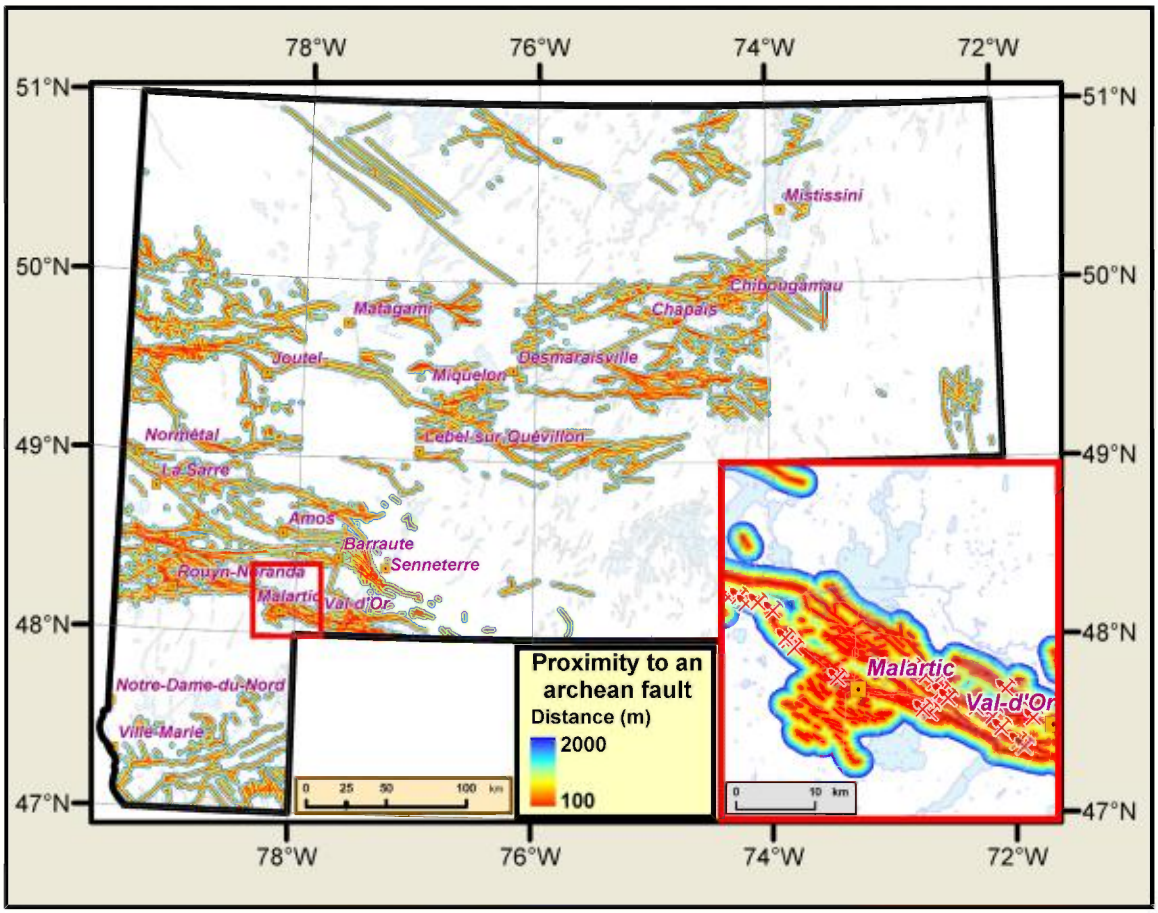

Figure 12 - Buffering around Archean faults by 100-m intervals up to a distance of 2 km.

Table 9 - Contrast values as a function of proximity to Archean faults (see Table 3 for the definition of parameters).

Distance	Area_km²	No_Points	W+	s(W+)	W-	s(W-)	C	s(C)	Stud(Cnt)
100	3918	81	3.0419	0.1123	-0.5806	0.101	3.6225	0.1511	23.982
200	2896	20	1.9314	0.2244	-0.1022	0.0793	2.0336	0.238	8.5445
300	2908	14	1.5684	0.2679	-0.065	0.0779	1.6334	0.279	5.8546
400	2597	15	1.7517	0.2589	-0.0729	0.0781	1.8246	0.2705	6.7458
500	2683	3	0.1048	0.5777	-0.0017	0.0754	0.1065	0.5826	0.1829
600	2197	6	0.9996	0.4088	-0.0217	0.0761	1.0213	0.4158	2.4561
700	2463	8	1.1736	0.3541	-0.0318	0.0765	1.2054	0.3623	3.3272
800	2163	7	1.1698	0.3786	-0.0277	0.0763	1.1975	0.3862	3.1009
900	2138	5	0.8439	0.4477	-0.0162	0.0758	0.8602	0.4541	1.8942
1000	2106	2	-0.0586	0.7074	0.0007	0.0752	-0.0593	0.7114	-0.0833
1100	1945	3	0.4269	0.5778	-0.0059	0.0754	0.4328	0.5827	0.7428
1200	1790	2	0.1039	0.7075	-0.0011	0.0752	0.105	0.7115	0.1476
1300	1915	1	-0.6568	1.0003	0.0052	0.075	-0.6621	1.0031	-0.66
1400	1723	1	-0.5511	1.0003	0.0041	0.075	-0.5553	1.0031	-0.5536
1500	1749	2	0.1271	0.7075	-0.0013	0.0752	0.1285	0.7115	0.1805
1600	1643	0							
1700	1628	0							
1800	1495	0							
1900	1509	2	0.2749	0.7076	-0.0027	0.0752	0.2777	0.7116	0.3902
2000	1540	1	-0.4392	1.0003	0.0031	0.075	-0.4423	1.0031	-0.4409
2001	134772	6	-3.1196	0.4083	1.3881	0.0762	-4.5077	0.4153	-10.854

The *WofE* analysis shows that favourability is not significant beyond a distance of 400 m, and that contrast drops off sharply beyond that point (Table 9). A binary evidence map is created by assigning a value of 1 to cells located up to 400 m from a fault (Figure 13).

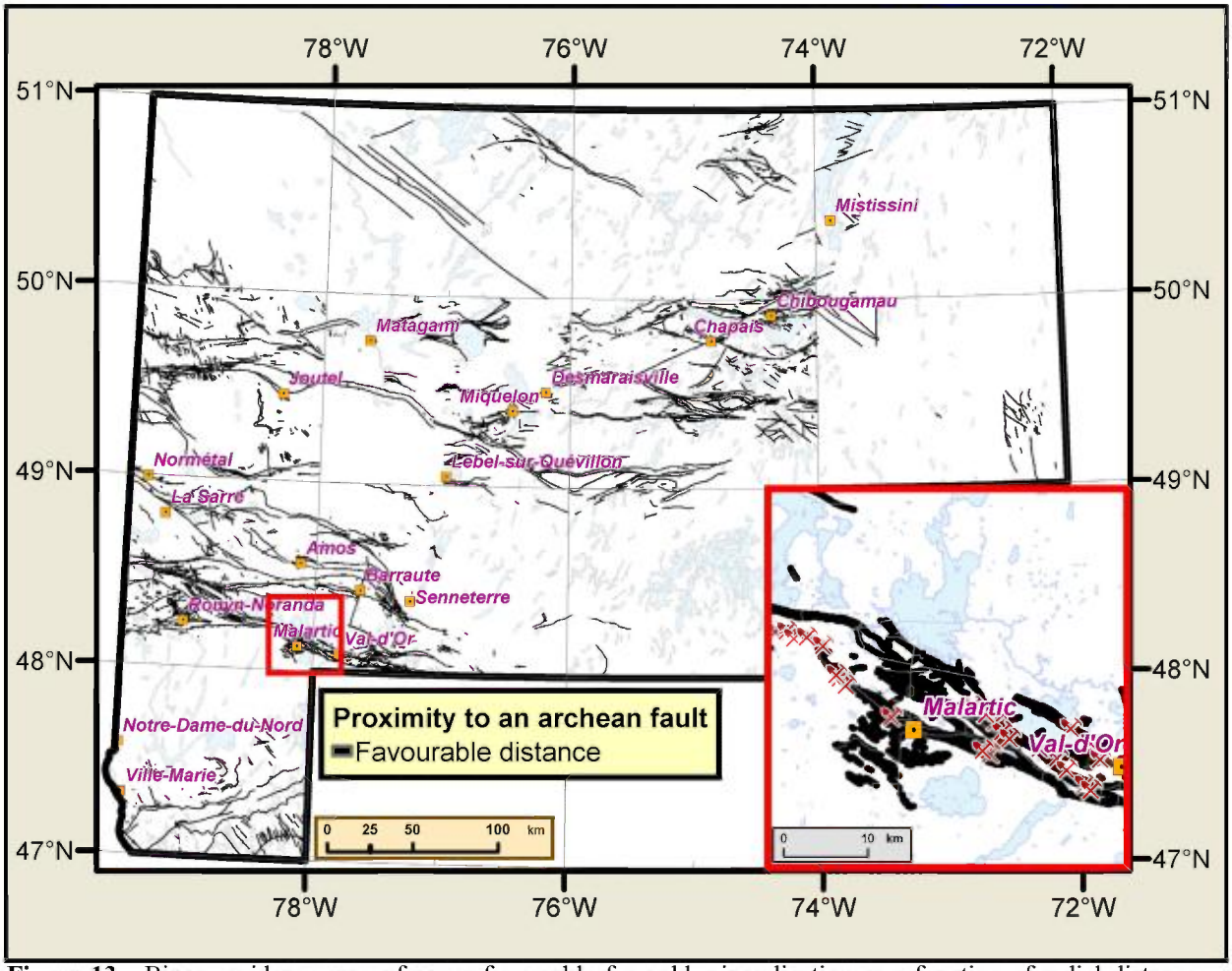

Figure 13 - Binary evidence map of zones favourable for gold mineralization as a function of radial distance from Archean faults.

4.2.2 Archean fault density

Fault density (number of faults per unit area) is an indicator of regional deformation in a fragile regime. A high fault density is conducive to hydrothermal circulation and the formation of structural traps for gold precipitation (Hagemann and Cassidy, 2000).

A number of studies suggest that second- and third-order structures within the regional fracture network are preferential deposition sites, whereas relatively few deposits are located at the heart of the main conduits (Eisenlohr et al., 1989; Groves et al., 1989; Robert, 1990). Although it is theoretically possible to use spatial analysis to assess the relative hierarchy of faults, this approach cannot be applied to the entire Abitibi region because of variability in the detail of the maps available for the study area. Nonetheless, the concept of density is applicable and provides a means of targeting sectors in the region most likely to contain deposits.

A grid image of fault density per square kilometre was generated by using a 4 km-by-4 km window (Figure 14). The values were grouped into 10 classes by the natural breaks method.

Classes 6 to 10 were selected for their significant favourability (Table 10) and used to create the binary evidence map (Figure 15).

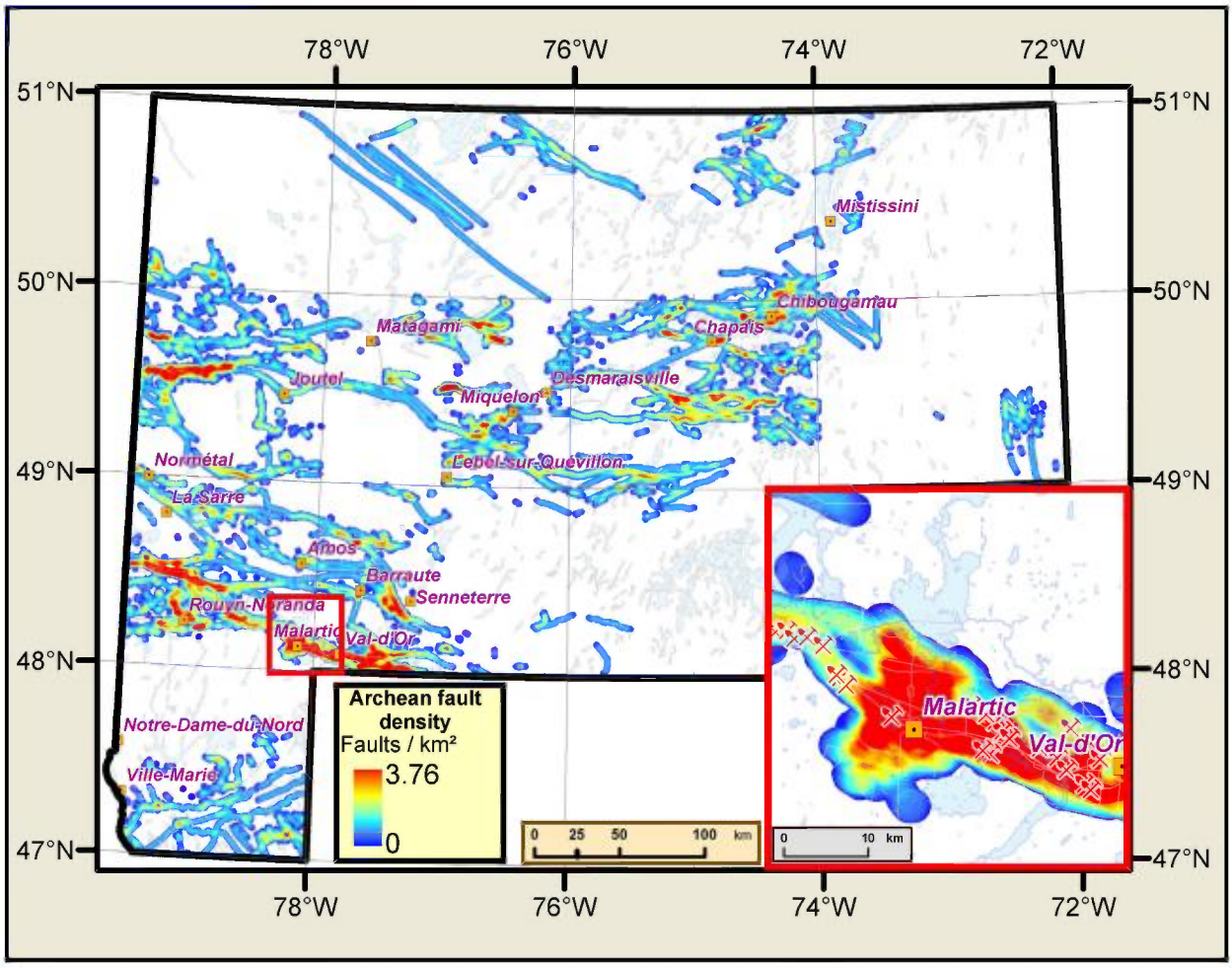

Figure 14 - Fault density per km² measured with a 16 km² window moving from cell to cell.

Table 10 - Grouping of density values in 10 classes by the natural breaks method (See Table 3 for the definition of parameters).

Class	Area_km²	No_Points	W+	s(W+)	W-	s(W-)	C	s(C)	Stud(cnt)
1	139067	13	-2.5424	0.2774	1.4647	0.0712	-4.0072	0.2864	-13.993
2	10887	18	0.3319	0.2359	-0.026	0.072	0.3579	0.2466	1.4511
3	14241	21	0.2174	0.2184	-0.0214	0.0726	0.2387	0.2301	1.0373
4	6985	34	1.415	0.1719	-0.1358	0.0752	1.5507	0.1876	8.2641
5	3208	25	1.8885	0.2008	-0.108	0.0734	1.9966	0.2138	9.3399
6	1757	24	2.4555	0.2055	-0.1109	0.0732	2.5665	0.2182	11.7637
7	859	31	3.4499	0.1829	-0.1542	0.0746	3.6041	0.1976	18.2438
8	476	22	3.7072	0.2183	-0.1075	0.0728	3.8148	0.2301	16.5778
9	239	11	3.7049	0.3087	-0.0523	0.0708	3.7571	0.3167	11.8629
10	59	12	5.3796	0.3238	-0.0583	0.0709	5.4379	0.3314	16.4074

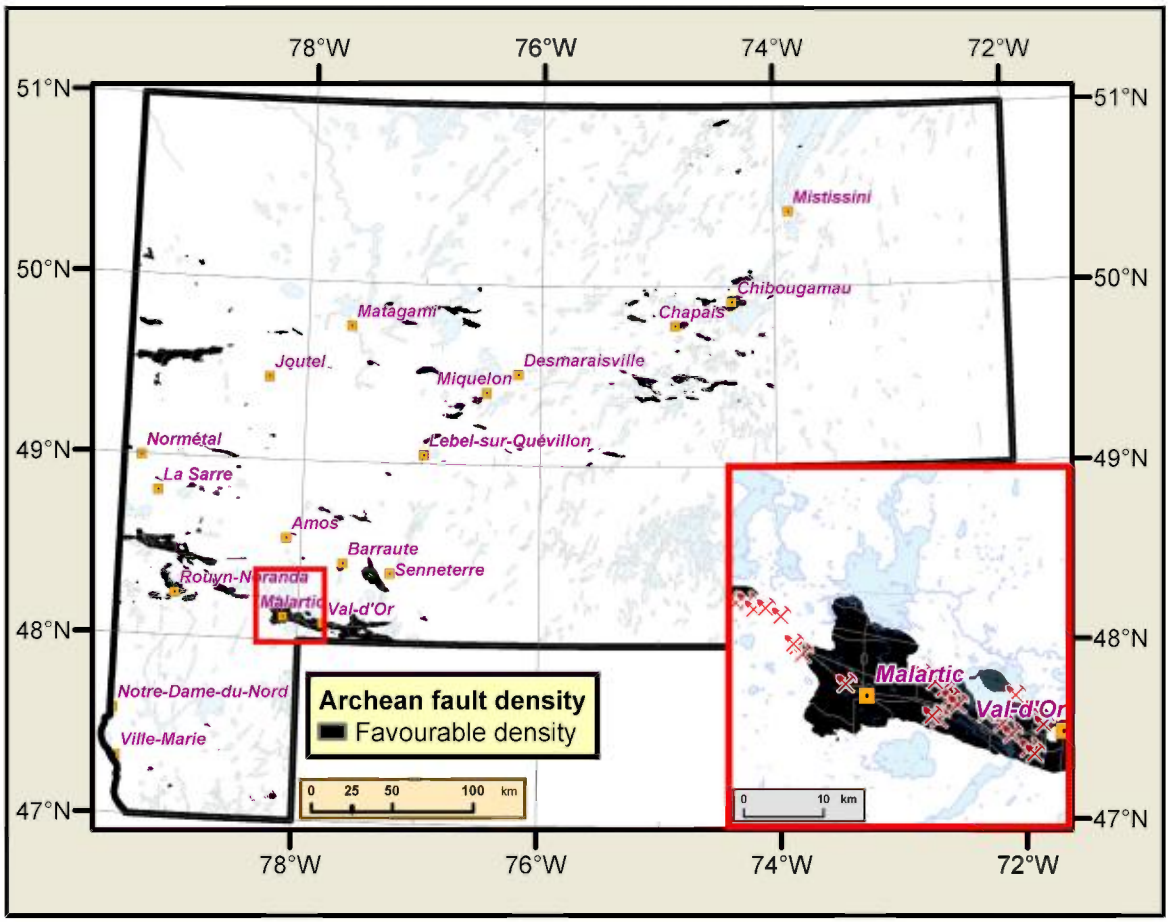

Figure 15 - Binary evidence map of fault density favourable for gold deposits.

4.2.3 Proximity to a ductile lineament

Many shear zones are not fully documented in the geological database for the Abitibi, either because the original geological surveys were conducted before high-resolution geophysical surveys began to be used routinely or because of extensive Quaternary deposits. That is why ductile lineaments (shapefile) derived on the basis of geophysical data for the Abitibi (Faure, 2004) were used as a proximity parameter. These lineaments generally correspond to major shear zones likely to have a secondary network of branching faults.

Buffers consisting of 100-m intervals were established up to a distance of 2 km (Figure 16) and their favourability was assessed with *WofE* (Table 11). The analysis showed that the parameter remains favourable up to a distance of 600 m, beyond which the contrast decreases rapidly. The binary evidence map was generated by assigning a value of 1 to all the cells located up to 600 m away from a ductile lineament (Figure 17).

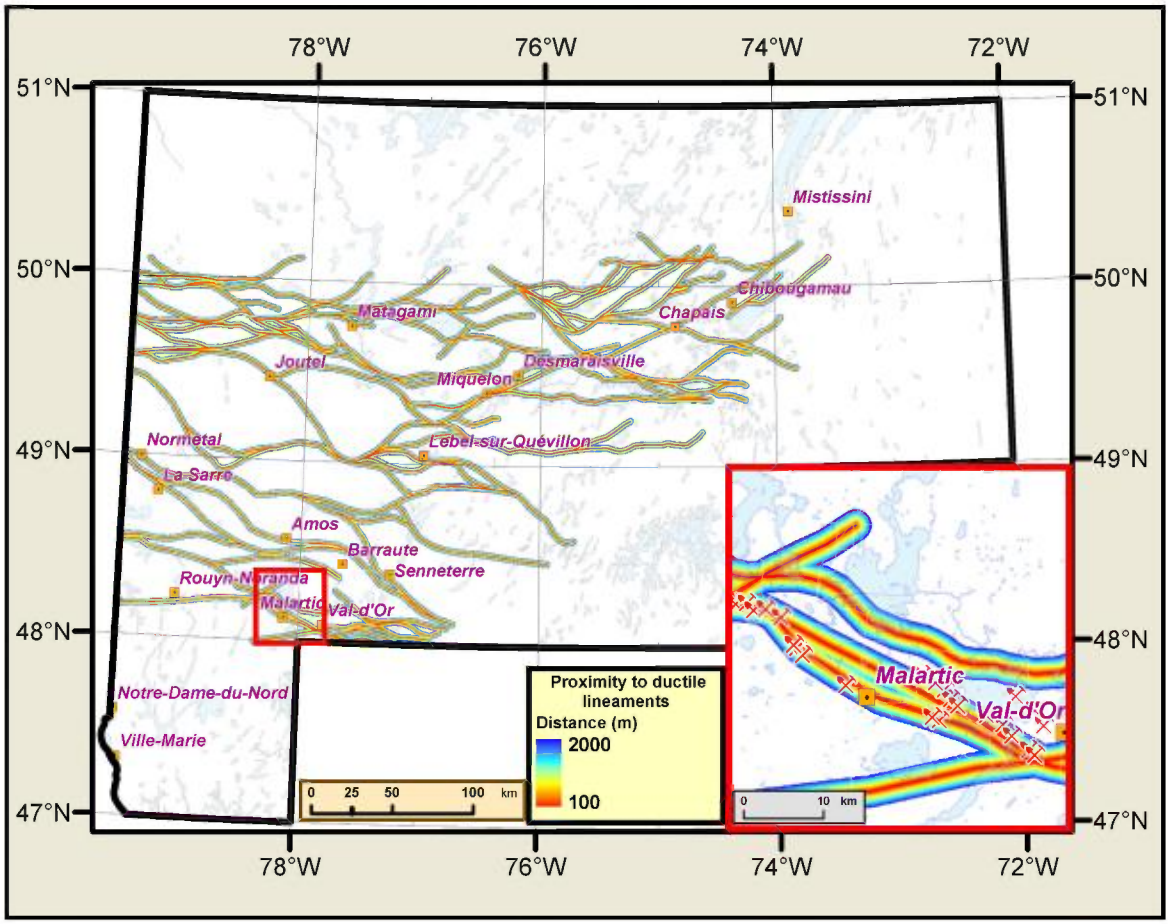

Figure 16 - Proximity to the ductile lineaments of the Abitibi. The lineaments were buffered by 100-m intervals up to a distance of 2 km.

Table 11 - Assessment of the favourability associated with proximity to ductile lineaments. The contrast is significant up to a distance of about 600 m (See Table 3 for the definition of parameters).

Class	Area_km²	No_Points	W+	s(W+)	W-	s(W-)	C	s(C)	Stud(cnt)
100	1618	8	1.4307	0.3544	-0.0295	0.0702	1.4602	0.3613	4.0414
200	1261	9	1.8001	0.3345	-0.0365	0.0704	1.8366	0.3419	5.3725
300	1315	9	1.7575	0.3345	-0.0362	0.0704	1.7938	0.3418	5.2478
400	1225	10	1.9357	0.3175	-0.0417	0.0706	1.9774	0.3253	6.0792
500	1301	13	2.1396	0.2787	-0.0563	0.0711	2.196	0.2877	7.6335
600	1116	6	1.5146	0.4093	-0.0226	0.0699	1.5372	0.4153	3.7016
700	1273	5	1.1999	0.4481	-0.0168	0.0697	1.2167	0.4535	2.683
800	1149	1	-0.3109	1.0004	0.0017	0.069	-0.3126	1.0028	-0.3117
900	1170	3	0.772	0.5781	-0.0077	0.0694	0.7797	0.5822	1.3391
1000	1183	6	1.4562	0.4093	-0.0222	0.0699	1.4784	0.4152	3.5605
1100	1123	6	1.5085	0.4093	-0.0225	0.0699	1.5311	0.4153	3.687
1200	1057	5	1.386	0.4483	-0.018	0.0697	1.404	0.4537	3.0949
1300	1144	2	0.3881	0.7077	-0.0031	0.0692	0.3912	0.7111	0.5501
1400	1048	4	1.1706	0.501	-0.0132	0.0695	1.1839	0.5058	2.3407
1500	1087	1	-0.2548	1.0005	0.0014	0.069	-0.2561	1.0028	-0.2554
1600	1034	9	2.0003	0.3348	-0.0378	0.0704	2.0381	0.3421	5.9574
1700	1049	4	1.1698	0.501	-0.0132	0.0695	1.183	0.5058	2.3391
1800	973	4	1.2451	0.501	-0.0137	0.0695	1.2587	0.5058	2.4885
1900	997	2	0.526	0.7078	-0.0039	0.0692	0.5299	0.7112	0.7451
2000	1016	2	0.5071	0.7078	-0.0038	0.0692	0.5109	0.7112	0.7183
2001	154642	102	-0.588	0.099	1.3821	0.096	-1.9701	0.1379	-14.282

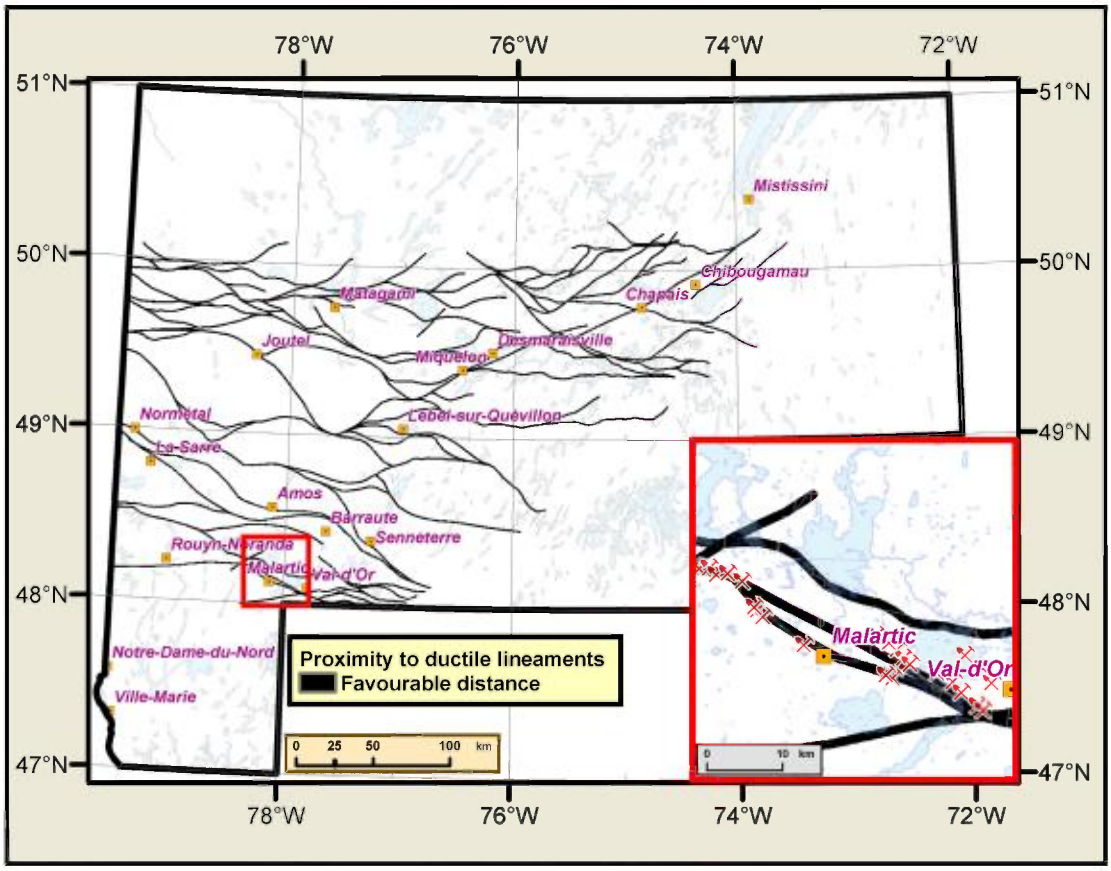

Figure 17 - Binary evidence map of favourability associated with proximity to ductile lineaments.

4.2.4 Proximity to quartz veins

Quartz vein deposits are the most common type of gold deposit in the Abitibi (Robert, 1990). This spatial association was evaluated by extracting all the point occurrences of quartz veins from databases of compilation outcrops, géofiches, whole-rock analyses and drill holes. The data from drill holes were projected onto the surface. The resulting vector file can be seen in Figure 18.

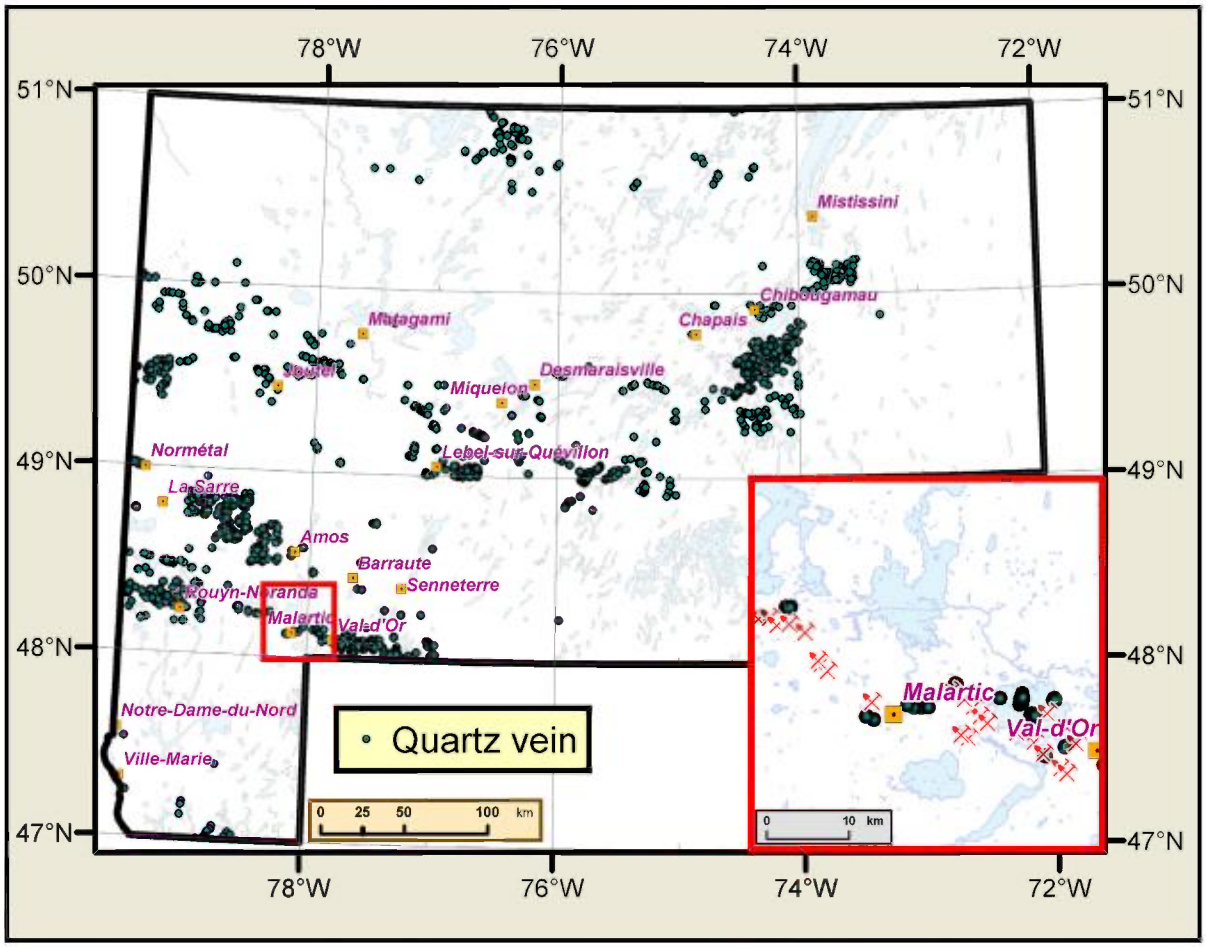

Figure 18 - Point occurrences of quartz veins in the Abitibi.

An initial processing step aimed at testing the density of the veins (number of veins per square kilometre) showed that the favourability of this factor remains the same regardless of the density value. A second approach for testing proximity associated with individual occurrences yielded more significant results (Table 12). The contrast values remain significant up to a distance of 800 m and become irregular beyond that. The binary evidence map for the parameter shows a value of 1 for cells up to a radial distance of 800 m from quartz vein occurrences (Figure 19).

Table 12 - *WofE* analysis of favourability associated with proximity to quartz veins. The parameter remains favourable up to a distance of 800 m (See Table 3 for the definition of parameters).

Class	Area_km²	No_Points	W+	s(W+)	W-	s(W-)	C	s(C)	Stud(cnt)
100	74	17	5.6833	0.2761	-0.0995	0.0786	5.7828	0.2871	20.1419
200	158	10	4.2032	0.3267	-0.0567	0.077	4.2598	0.3357	12.691
300	234	5	3.074	0.4521	-0.027	0.0758	3.1011	0.4584	6.7653
400	267	7	3.2833	0.383	-0.0384	0.0763	3.3217	0.3905	8.5055
500	336	7	3.0491	0.382	-0.038	0.0763	3.0871	0.3895	7.9257
600	314	5	2.7749	0.4508	-0.0266	0.0758	2.8015	0.4571	6.1283
700	398	8	3.0137	0.3572	-0.0435	0.0765	3.0572	0.3653	8.3698
800	392	8	3.03	0.3572	-0.0436	0.0765	3.0735	0.3653	8.4132
900	418	2	1.5621	0.7088	-0.0089	0.0752	1.571	0.7128	2.204
1000	451	7	2.7496	0.3809	-0.0374	0.0763	2.787	0.3885	7.1739
1100	441	3	1.9154	0.5793	-0.0144	0.0754	1.9298	0.5842	3.3033
1200	441	0							
1300	496	0							
1400	476	2	1.4326	0.7086	-0.0086	0.0752	1.4412	0.7126	2.0225
1500	500	3	1.7893	0.5791	-0.0141	0.0754	1.8034	0.584	3.0882
1600	500	3	1.7906	0.5791	-0.0141	0.0754	1.8047	0.584	3.0903
1700	509	3	1.7712	0.5791	-0.014	0.0754	1.7852	0.5839	3.0571
1800	499	3	1.7913	0.5791	-0.0141	0.0754	1.8054	0.584	3.0915
1900	513	2	1.356	0.7085	-0.0084	0.0752	1.3644	0.7125	1.915
2000	546	4	1.9908	0.5018	-0.0195	0.0756	2.0104	0.5075	3.9613
2001	169813	80	-0.7601	0.1118	2.5246	0.1011	-3.2846	0.1508	-21.7846

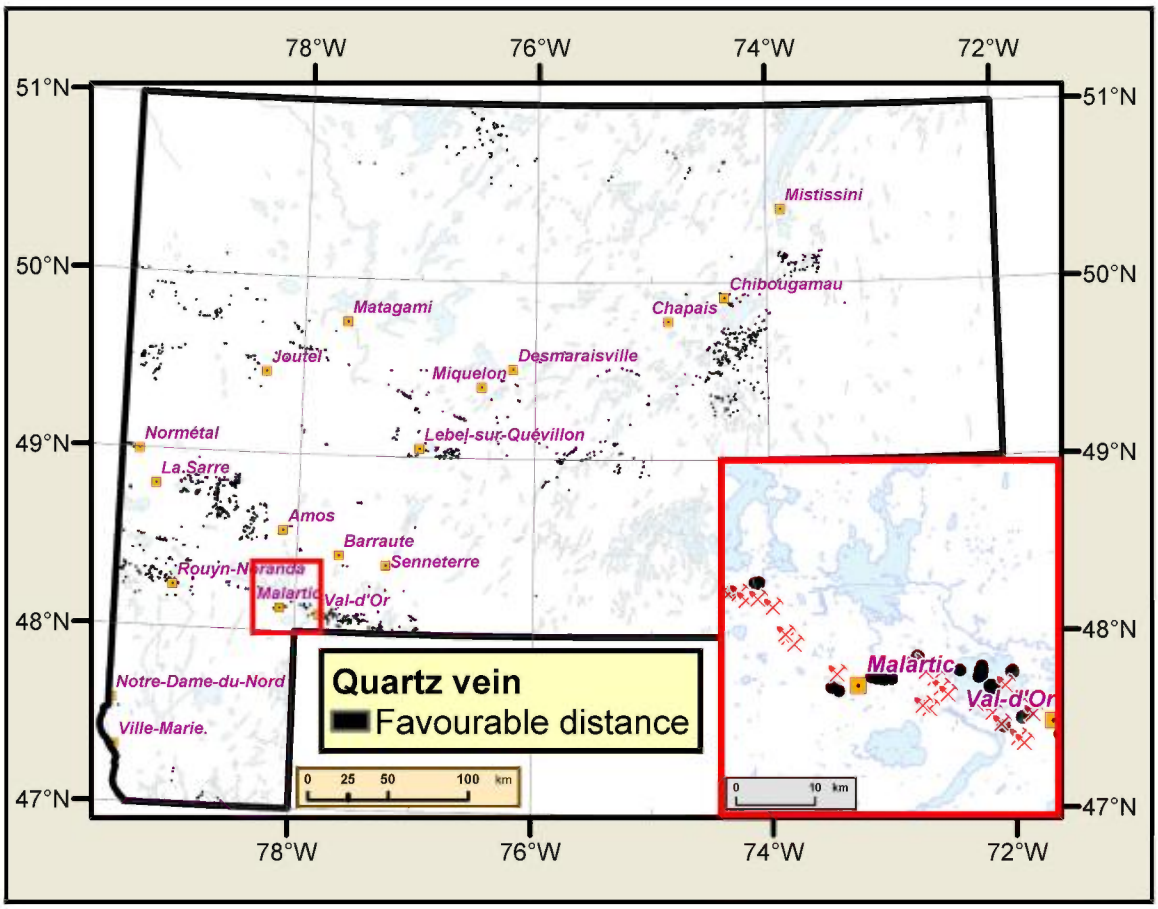

Figure 19 - Binary evidence map of the radial distance from quartz veins favourable for gold mineralization.

4.3 Metal indicators

Most of the deposits exhibit a metal association with Au, Ag ± As, B, Bi, Sb, Te and W (Hagemann and Cassidy, 2000). From this list, gold, arsenic and antimony have been retained, and sulphur has been added as an indicator of the presence of sulphide minerals. Processing is aimed at assessing the spatial association between an anomalous level of one of these elements and proximity to a gold occurrence.

4.3.1 Proximity to an Au anomaly

All of the Au analyses from drill holes and rock samples were extracted from SIGEOM. The data from drill holes were projected onto the surface and the grades were converted to ppb. The data for Au in the rock samples were extracted for all the analytical methods. The data were combined in a shapefile and the result is shown in Figure 20.

For this processing step, the anomaly threshold for Au contents was arbitrarily set at 16 ppb. All of the occurrences with contents equal to or higher than this value were buffered by 100-m intervals up to a distance of 2000 m. *WofE* analysis showed that the parameter remains favourable up to a distance of 400 m, and the high contrast values for proximal distances (< 200 m) confirm (not surprisingly) the importance of the parameter (Table 13). The binary evidence map shows a value of 1 for cells up to a radial distance of 400 m from the anomalous Au concentrations (Figure 21).

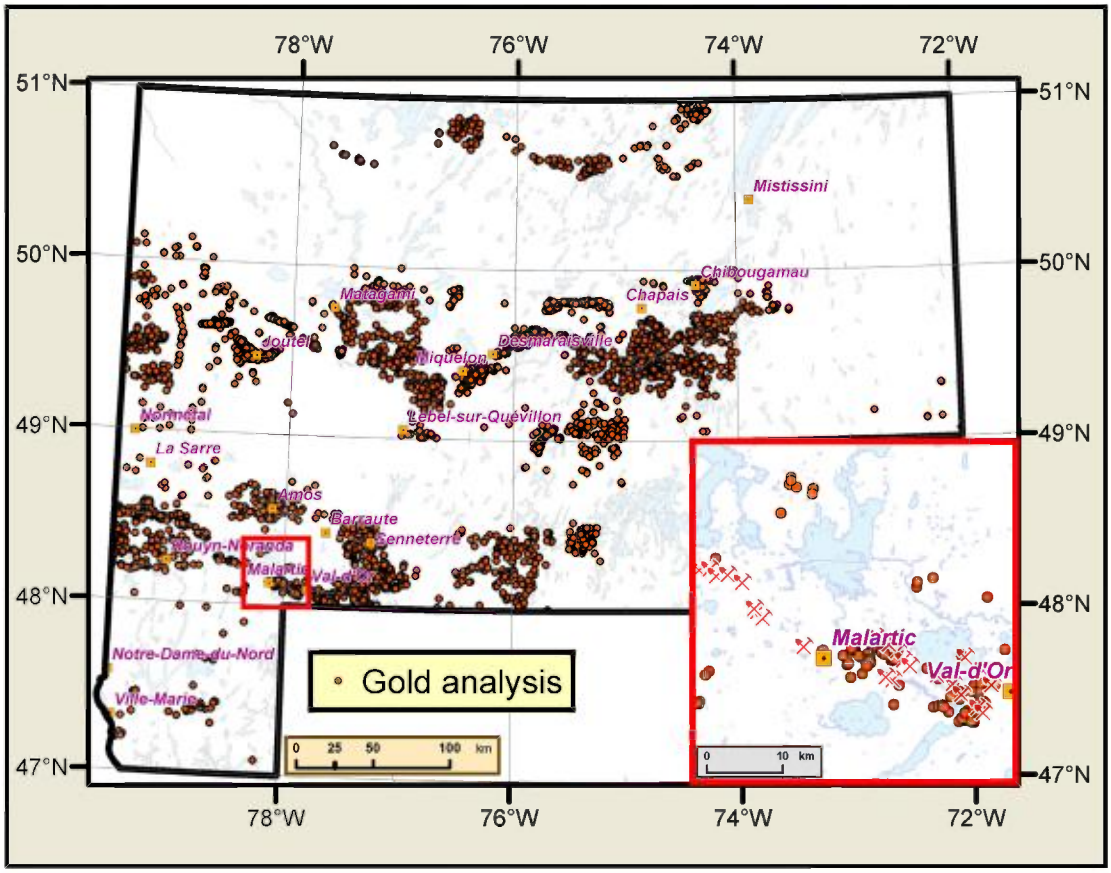

Figure 20 - Location of Au analyses in the Abitibi.

Table 13 - Assessment of the favourability associated with proximity to anomalous Au analyses (See Table 3 for the definition of parameters).

Classe	Aire_km²	No_Points	*W+*	*s(W+)*	*W-*	*s(W-)*	C	*s(C)*	*Stud(Cnt)*
100	521	126	5.7572	0.1023	-1.2149	0.1374	6.9721	0.1713	40.7026
200	886	30	3.5483	0.1857	-0.1786	0.082	3.7269	0.203	18.357
300	1130	6	1.6673	0.4093	-0.0277	0.0761	1.6951	0.4163	4.0714
400	1160	7	1.7958	0.3791	-0.0334	0.0763	1.8291	0.3867	4.73
500	1362	5	1.2966	0.448	-0.0207	0.0758	1.3173	0.4544	2.8988
600	1206	0							
700	1457	0							
800	1372	3	0.7768	0.578	-0.0092	0.0754	0.7859	0.5829	1.3483
900	1414	1	-0.3539	1.0004	0.0024	0.075	-0.3563	1.0032	-0.3552
1000	1488	0							
1100	1416	0							
1200	1373	0							
1300	1499	0							
1400	1395	0							
1500	1426	0							
1600	1389	0							
1700	1382	0							
1800	1321	0							
1900	1323	0							
2000	1373	0							
2001	151885	1	-5.031	1	1.9268	0.0752	-6.9578	1.0028	-6.9382

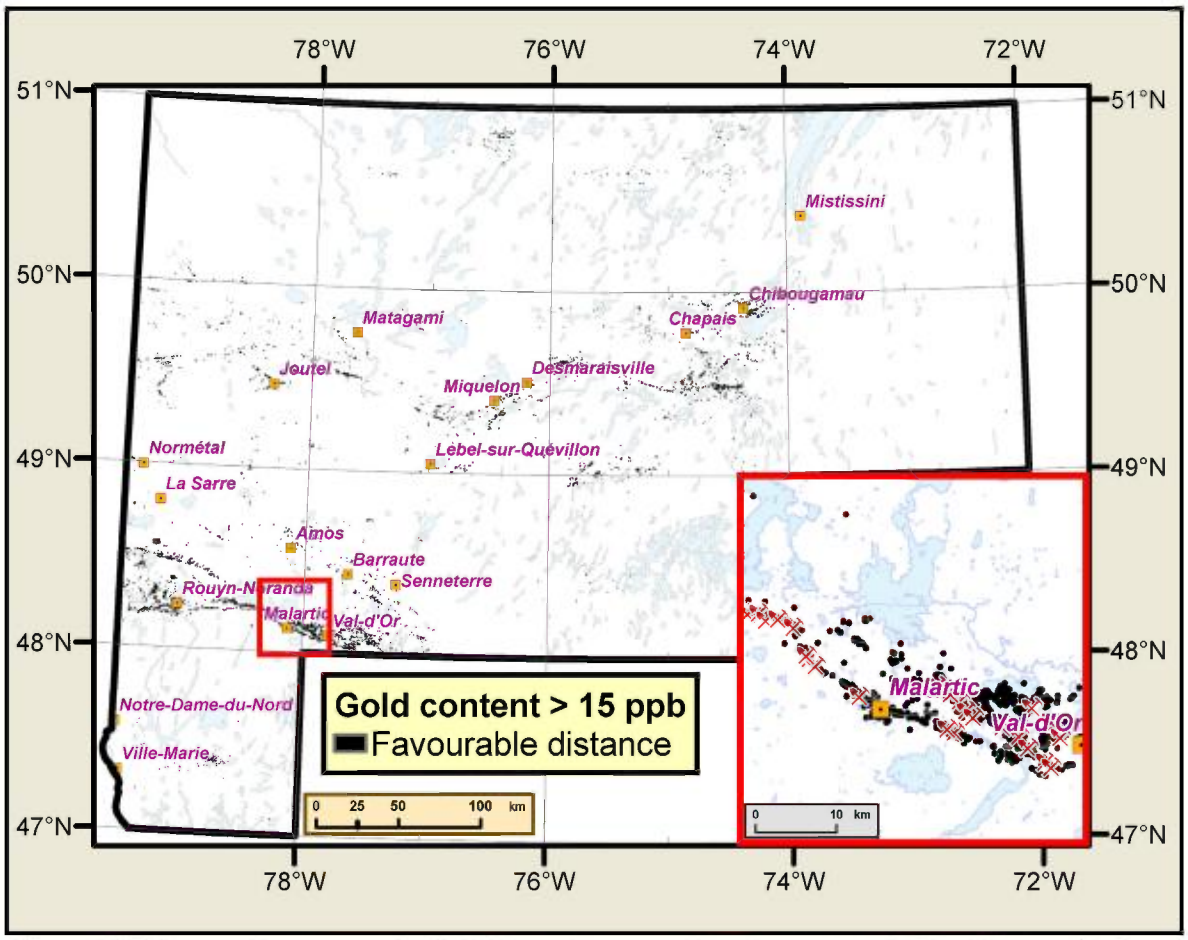

Figure 21 - Binary evidence map of radial distance from anomalous Au contents (>15 ppb) favourable for gold mineralization.

4.3.2 Proximity to an As anomaly

Only analyses derived from rock samples were used for this parameter because of the very small number of As analyses in drill holes. Extraction of As for all analytical methods made it possible to create the vector file shown in Figure 22. For this analysis, the anomaly threshold for As contents was arbitrarily set at 3 ppm. All occurrences with concentrations equal to or greater than this value were buffered by 100-m intervals up to a distance of 1000 m. *WofE* analysis showed that this parameter remains favourable up to a distance of 900 m, with a substantial contrast value for the first 200 m (Table 14). The binary evidence map shows a value of 1 for cells up to a radial distance of 900 m from anomalous As levels (Figure 23).

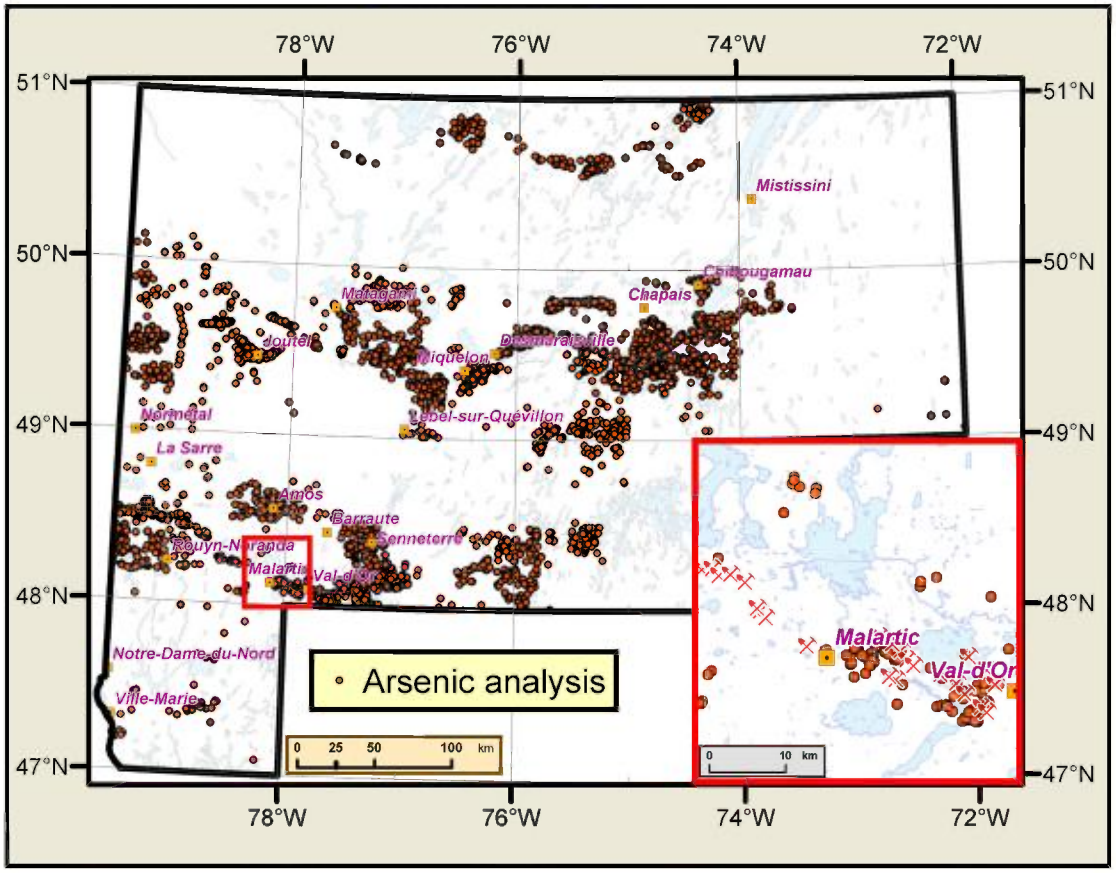

Figure 22 - Location of As analyses in the Abitibi.

Table 14 - *WofE* assessment of favourability associated with proximity to anomalous As analyses (See Table 3 for the definition of parameters).

Class	Area_km²	No_Points	W+	s(W+)	W-	s(W-)	C	s(C)	Stud(cnt)
100	97	25	5.837	0.232	-0.15	0.0806	5.987	0.2456	24.3775
200	193	11	4.0927	0.3105	-0.0624	0.0772	4.155	0.3199	12.9874
300	264	6	3.1379	0.413	-0.0326	0.0761	3.1706	0.4199	7.5505
400	291	4	2.6264	0.5035	-0.021	0.0756	2.6474	0.5091	5.1999
500	363	2	1.7029	0.7091	-0.0092	0.0752	1.7121	0.713	2.4011
600	339	5	2.6986	0.4505	-0.0264	0.0758	2.7251	0.4569	5.9644
700	429	3	1.9446	0.5794	-0.0145	0.0754	1.9591	0.5843	3.3531
800	422	5	2.4763	0.4499	-0.026	0.0758	2.5023	0.4562	5.4846
900	452	6	2.5918	0.411	-0.0316	0.0761	2.6234	0.418	6.2766
1000	493	1	0.7017	1.001	-0.0028	0.075	0.7045	1.0038	0.7019
1001	174435	111	-0.4592	0.0949	3.0252	0.1225	-3.4844	0.155	-22.4795

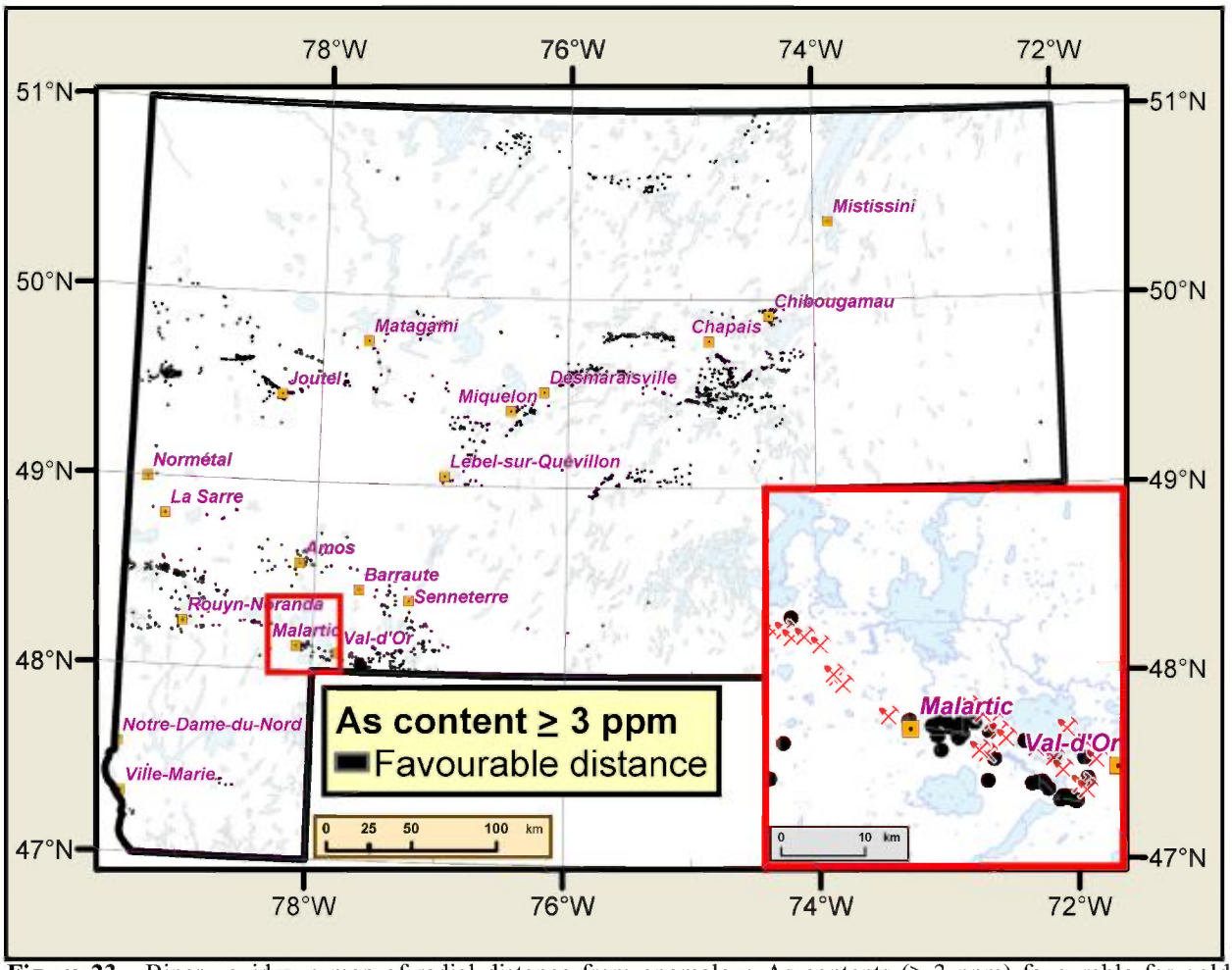

Figure 23 - Binary evidence map of radial distance from anomalous As contents (≥ 3 ppm) favourable for gold mineralization.

4.3.3 Proximity to an Sb anomaly

Extraction of antimony values was identical with that for arsenic. The vector file of the Sb analyses of the Abitibi is shown in Figure 24. The anomaly threshold value (≥ 2.5 ppm) was determined using a probability diagram. This value is very similar to that obtained by Harris et al. (2005) for this element in the Red Lake region of Ontario. Samples with Sb levels equal to or greater than 2.5 ppm were buffered using 100-m intervals up to a distance of 3 km. The *WofE* assessment of favourability shows a significant decrease in contrast beyond a distance of 700 m (Table 15). In addition, the spatial association of antimony for very proximal distances around the gold deposits shows a very high contrast (from 6.0 to 9.7), indicating that this element is generally an excellent indicator of the presence of proximal gold occurrences. The binary evidence map shows a value of 1 for cells up to a distance of 700 m around anomalous Sb concentrations (Figure 25).

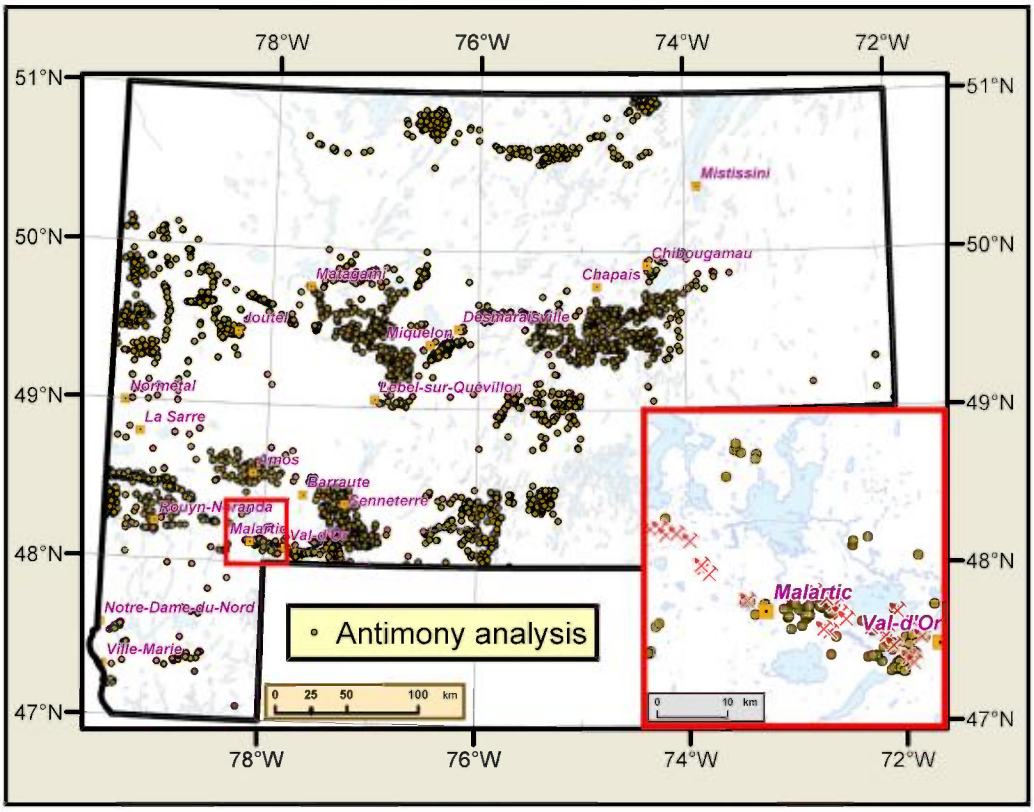

Figure 24 - Location of Sb analyses in the Abitibi.

Table 15 - Assessment of favourability associated with proximity to anomalous Sb analyses. The contrast values become erratic beyond a distance of 700 m (See Table 3 for the definition of parameters).

Class	Area_km²	No_Points	W+	s(W+)	W-	s(W-)	C	s(C)	Stud(cnt)
100	15	14	9.6142	1.0722	-0.0814	0.0779	9.6957	1.075	9.0191
200	33	10	6.0796	0.3795	-0.0574	0.077	6.1369	0.3872	15.8481
300	49	4	4.4762	0.5217	-0.0223	0.0756	4.4986	0.5271	8.534
400	58	3	3.9999	0.593	-0.0166	0.0754	4.0165	0.5978	6.7188
500	75	2	3.2994	0.7167	-0.0108	0.0752	3.3102	0.7206	4.5935
600	73	2	3.3264	0.717	-0.0108	0.0752	3.3372	0.7209	4.6293
700	95	3	3.4732	0.5867	-0.0164	0.0754	3.4896	0.5915	5.8998
800	96	1	2.343	1.0052	-0.0051	0.075	2.3481	1.008	2.3294
900	106	1	2.2501	1.0048	-0.005	0.075	2.2552	1.0076	2.2382
1000	117	3	3.2616	0.5849	-0.0163	0.0754	3.2779	0.5897	5.5582
1100	117	1	2.1486	1.0043	-0.005	0.075	2.1536	1.0071	2.1384
1200	118	1	2.1357	1.0043	-0.0049	0.075	2.1406	1.0071	2.1256
1300	135	0							
1400	131	0							
1500	141	5	3.5988	0.4554	-0.0276	0.0758	3.6264	0.4617	7.8553
1600	144	3	3.0525	0.5835	-0.0161	0.0754	3.0686	0.5883	5.2158
1700	149	1	1.9024	1.0034	-0.0048	0.075	1.9072	1.0062	1.8955
1800	148	1	1.9062	1.0034	-0.0048	0.075	1.911	1.0062	1.8993
1900	155	2	2.5635	0.7117	-0.0104	0.0752	2.5739	0.7157	3.5964
2000	167	3	2.8985	0.5826	-0.016	0.0754	2.9145	0.5875	4.9611
2100	159	2	2.5368	0.7116	-0.0104	0.0752	2.5472	0.7156	3.5597
2200	171	1	1.7639	1.0029	-0.0046	0.075	1.7685	1.0057	1.7584
2300	166	2	2.4932	0.7114	-0.0103	0.0752	2.5035	0.7154	3.4996
2400	174	3	2.8562	0.5824	-0.0159	0.0754	2.8722	0.5873	4.8908
2500	183	2	2.3948	0.711	-0.0102	0.0752	2.405	0.715	3.3638
2600	185	0							
2700	181	1	1.709	1.0028	-0.0046	0.075	1.7136	1.0056	1.7041
2800	192	3	2.7575	0.5819	-0.0158	0.0754	2.7734	0.5868	4.7264
2900	192	1	1.6493	1.0026	-0.0045	0.075	1.6538	1.0054	1.6449
3000	193	2	2.3383	0.7108	-0.0102	0.0752	2.3484	0.7148	3.2856
3001	173861	102	-0.5405	0.099	2.9902	0.1151	-3.5308	0.1518	-23.2526

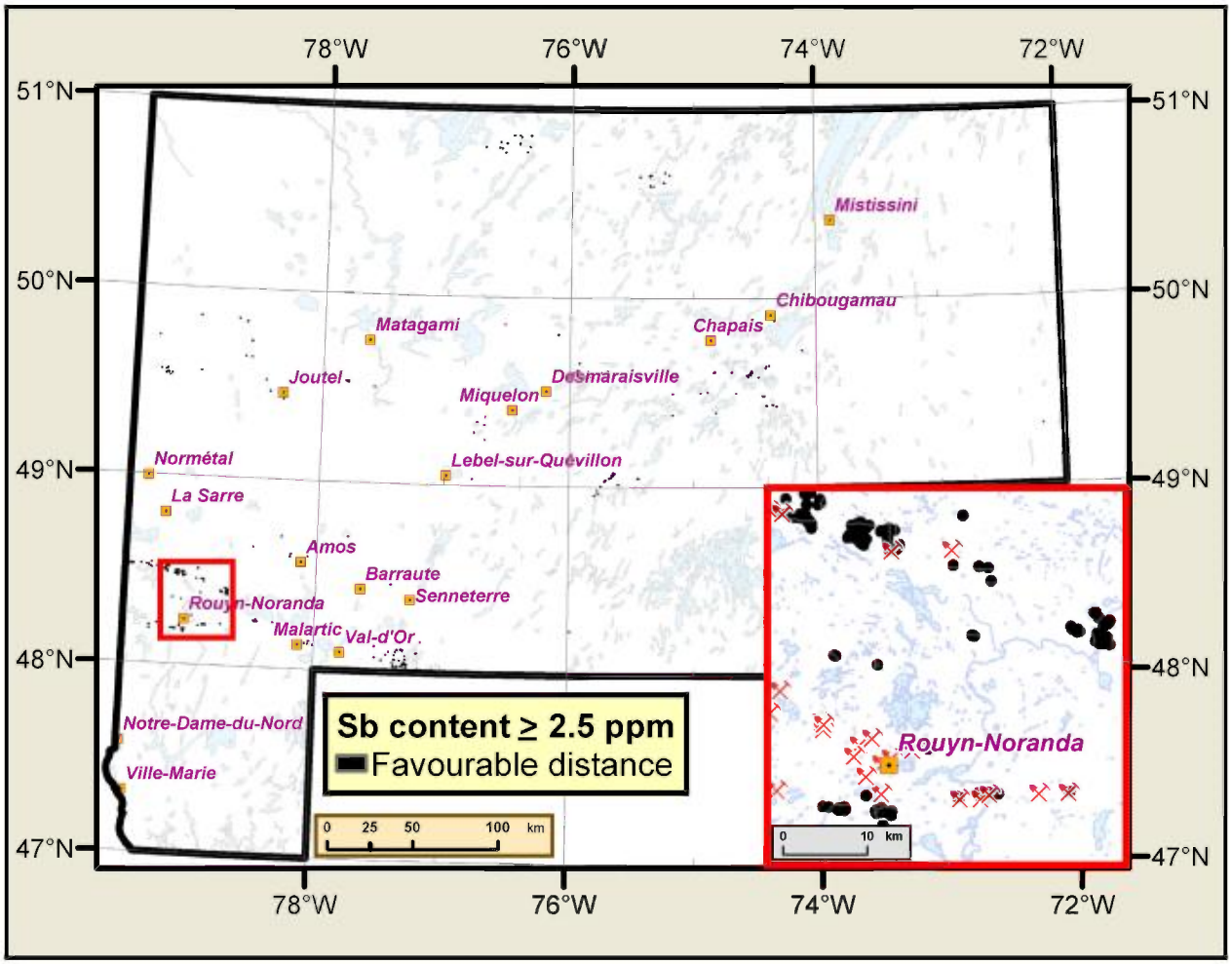

Figure 25 - Binary evidence map of radial distance from anomalous Sb concentrations (≥ 2.5 ppm) favourable for gold mineralization.

4.3.4 Proximity to an S anomaly

The sulphur concentration of a sample is a quantitative indicator of the levels of sulphide minerals, which are widely associated with gold. The study area comprises 3,801 sulphide analyses, which were used to create the vector file presented in Figure 26. The anomaly threshold value (≥ 0.42%) was determined by means of a probability diagram. Samples with S concentrations equal to or greater than the threshold were buffered by 100-m intervals up to a distance of 3 km. For this threshold, association with gold occurrences remains significant up to a distance of 1,500 m but becomes erratic beyond that (Table 16). Of all the parameters tested, this is the one that shows the strongest association with gold deposits (C ≅ 12). The binary evidence map shows a value of 1 for cells up to a radial distance of 1,500 m from anomalous S concentrations (Figure 27).

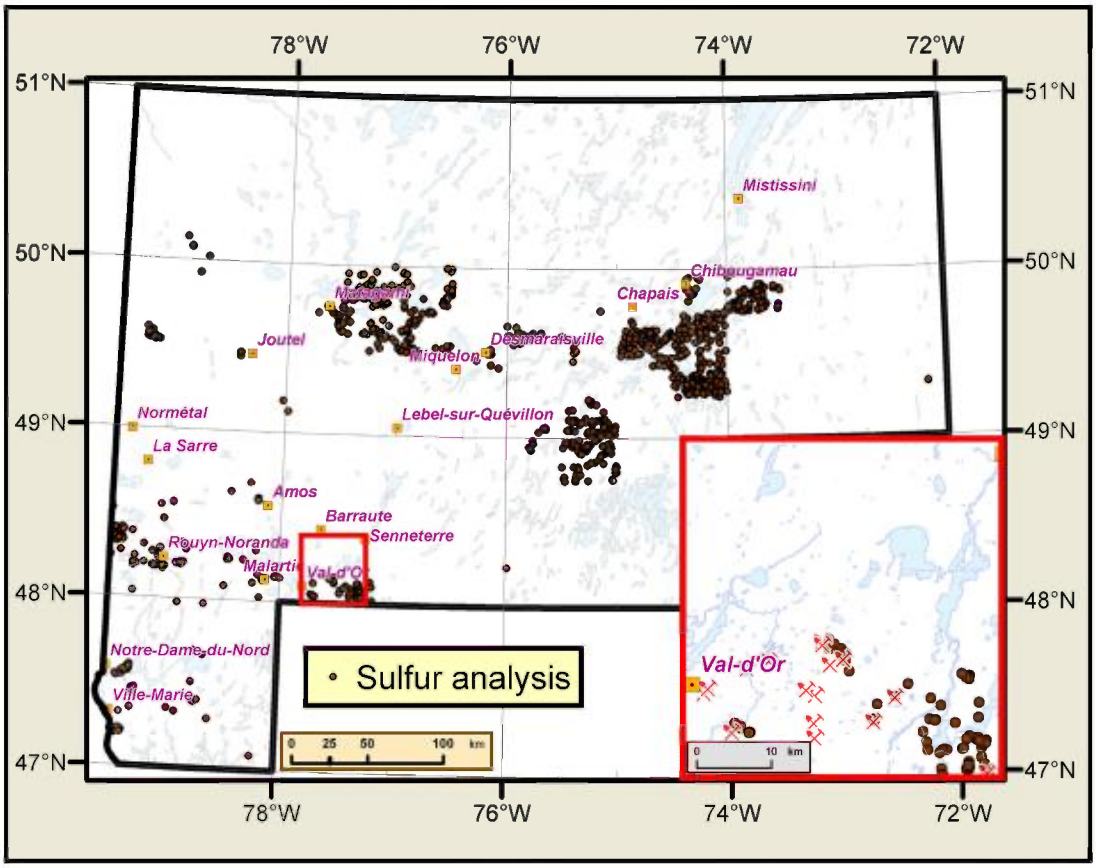

Figure 26 - Location of sulphur analyses in the Abitibi.

Table 16 - *WofE* analysis of favourability. The parameter's contrast remains significant up to a distance of 1,500 m (See Table 3 for the definition of parameters).

Class	Area_km²	No_Points	W+	s(W+)	W-	s(W-)	C	s(C)	Stud(cnt)
100	11	15	11.9105	2.6579	-0.0875	0.0781	11.9981	2.6591	4.5121
200	25	6	5.6807	0.4485	-0.034	0.0761	5.7147	0.4549	12.5632
300	40	2	3.946	0.7199	-0.011	0.0752	3.957	0.7238	5.467
400	49	4	4.4561	0.515	-0.0223	0.0756	4.4785	0.5205	8.6043
500	66	1	2.7177	1.0053	-0.0052	0.075	2.7229	1.0081	2.701
600	66	2	3.4306	0.7148	-0.0109	0.0752	3.4415	0.7187	4.7884
700	88	2	3.1319	0.7128	-0.0107	0.0752	3.1427	0.7168	4.3846
800	91	5	4.0395	0.4561	-0.0278	0.0758	4.0674	0.4623	8.7972
900	102	2	2.9852	0.712	-0.0107	0.0752	2.9958	0.716	4.1842
1000	115	1	2.1597	1.0031	-0.005	0.075	2.1647	1.0059	2.1521
1100	117	1	2.1413	1.003	-0.0049	0.075	2.1463	1.0058	2.1339
1200	121	0							
1300	139	4	3.3703	0.5051	-0.0218	0.0756	3.3922	0.5107	6.6417
1400	136	0							
1500	147	2	2.614	0.7105	-0.0104	0.0752	2.6244	0.7145	3.6732
1600	151	1	1.8898	1.0023	-0.0048	0.075	1.8945	1.0051	1.8849
1700	158	1	1.844	1.0022	-0.0047	0.075	1.8488	1.005	1.8395
1800	158	1	1.8392	1.0022	-0.0047	0.075	1.844	1.005	1.8348
1900	166	2	2.487	0.7101	-0.0103	0.0752	2.4973	0.7141	3.4972
2000	181	0							
2100	173	2	2.4468	0.71	-0.0103	0.0752	2.4571	0.714	3.4415
2200	187	0							
2300	182	1	1.7019	1.0019	-0.0046	0.075	1.7065	1.0047	1.6984
2400	191	1	1.654	1.0018	-0.0045	0.075	1.6585	1.0046	1.6509
2500	200	2	2.3002	0.7096	-0.0101	0.0752	2.3103	0.7136	3.2377
2600	202	0							
2700	197	2	2.3175	0.7096	-0.0101	0.0752	2.3276	0.7136	3.2618
2800	209	3	2.6655	0.5803	-0.0157	0.0754	2.6813	0.5851	4.5822
2900	209	4	2.9572	0.5034	-0.0214	0.0756	2.9786	0.509	5.8516
3000	211	0							
3001	173690	112	-0.4459	0.0945	2.8005	0.1229	-3.2463	0.155	-20.9413

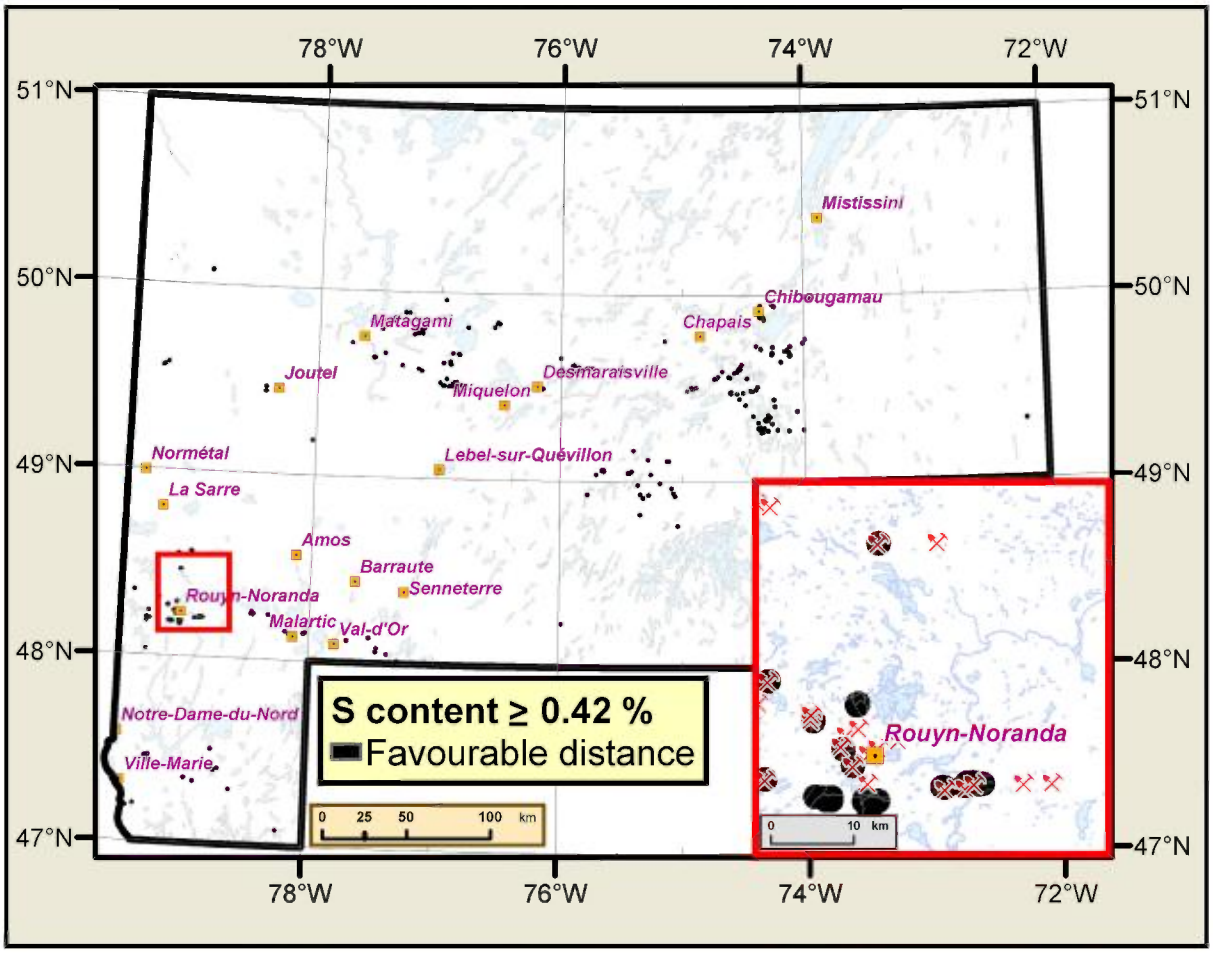

Figure 27 - Binary evidence map of the radial distance from anomalous S concentrations (≥ 0.42%) favourable for gold mineralization.

4.4 Geophysical signature

Digital data for the total magnetic field data and the vertical magnetic gradient reveal certain lithological properties that may be relevant for the present study. As indicated in Section 4.1.4, the reactivity of rocks likely to "fix" gold contained in hydrothermal solutions is directly related to their Fe content. In most cases, the Fe content also has a proportional influence on the magnetic signature of the rock. This processing step is aimed at determining whether there is a natural relationship between the intensity of the magnetic signature of host lithologies and the presence of gold-bearing deposits.

4.4.1 Favourability associated with the total magnetic field

To process this parameter, digital data for the total magnetic field obtained from MRNF surveys (pixels with a 50-m resolution) were combined with residual magnetic field data from the federal survey (pixels with a 200-m resolution). The latter were converted into total field data for this purpose. Figure 28 presents the results. The values were reclassified by ¼ of a standard deviation into 26 classes and analysed using the *WofE* approach (Table 17). As expected, the most magnetic classes exhibit a higher probability of association with gold deposits; these classes generally correspond to iron formation units and tholeiitic basalt units, as well as intrusions and ultramafic

volcanics. Although the latter lithologies host gold mineralization only occasionally, the presence of komatiitic units in a volcanosedimentary assemblage appears to typify the most important gold mining camps (Robert, 2005). The cells of classes with a magnetic field greater than 59768 nT were used to create the binary evidence map (Figure 29).

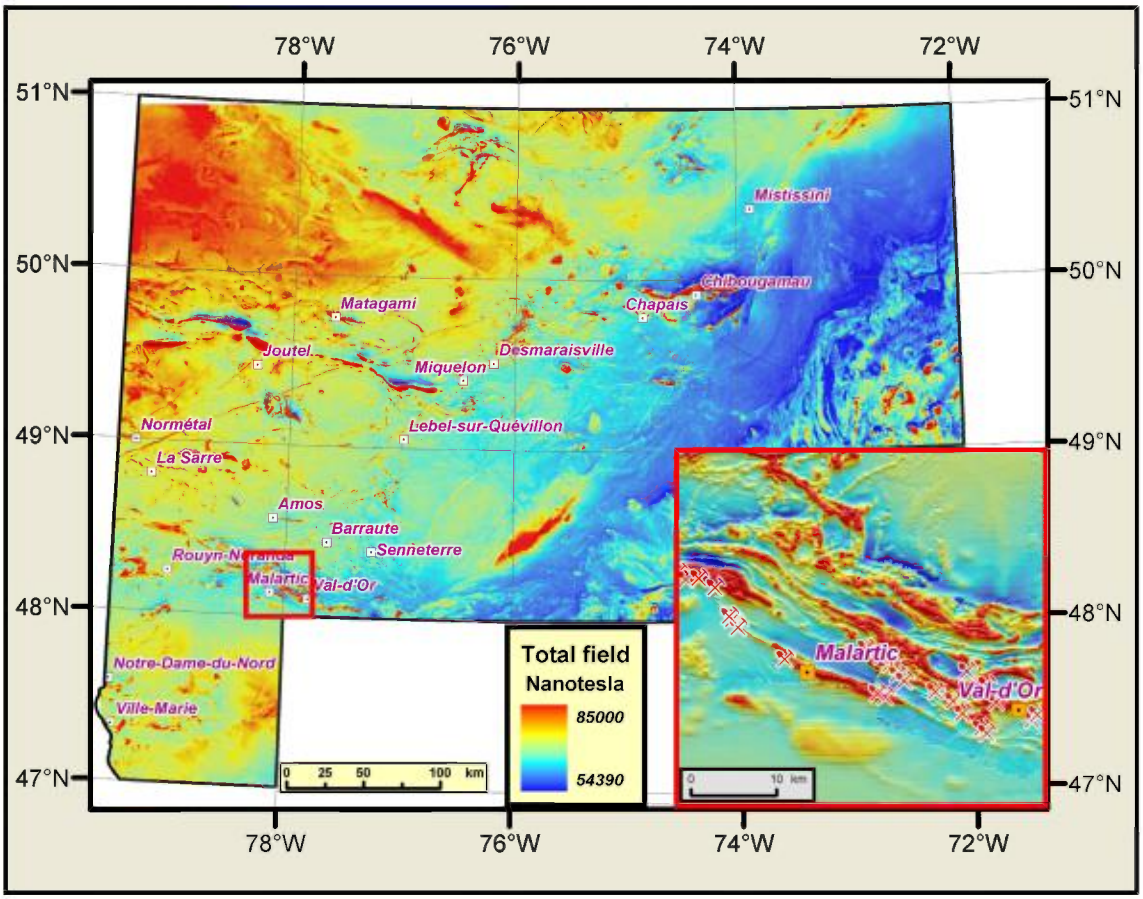

Figure 28 - Total magnetic field of the Abitibi.

Table 17 - Assessment of favourability of the magnetic signature of the total magnetic field. Classes greater than 59768 nT are preferentially associated with gold deposits (See Table 3 for the definition of parameters).

Class	Total MAG field	Area_km²	No_Points	W+	s(W+)	W-	s(W-)	C	s(C)	Stud(cnt)
1	54392,8 - 57770,1	28	0							
2	57770,1 - 57875,3	18	0							
3	57875,3 - 57980,5	24	0							
4	57980,5 - 58085,6	53	0							
5	58085,6 - 58190,8	140	0							
6	58190,8 - 58295,9	332	0							
7	58295,9 - 58401,1	1243	0							
8	58401,1 - 58506,2	5012	0							
9	58506,2 - 58611,4	13681	0							
10	58611,4 - 58716,6	13111	8	-0.5036	0.3537	0.0311	0.0765	-0.5347	0.3618	-1.4778
11	58716,6 - 58821,7	14817	17	0.1284	0.2427	-0.0126	0.0786	0.1409	0.2551	0.5525
12	58821,7 - 58926,9	18990	14	-0.3143	0.2674	0.0318	0.0779	-0.3461	0.2785	-1.2429
13	58926,9 - 59032,0	23529	27	0.1286	0.1926	-0.0212	0.0812	0.1498	0.209	0.7166
14	59032,0 - 59137,2	25862	23	-0.1266	0.2086	0.0201	0.0801	-0.1467	0.2235	-0.6564
15	59137,2 - 59242,3	21035	20	-0.0597	0.2237	0.0078	0.0793	-0.0675	0.2374	-0.2842
16	59242,3 - 59347,5	14251	15	0.0421	0.2583	-0.0038	0.0781	0.0459	0.2699	0.1699
17	59347,5 - 59452,7	9053	14	0.4273	0.2675	-0.0291	0.0779	0.4564	0.2786	1.6383
18	59452,7 - 59557,8	6535	7	0.0596	0.3782	-0.0024	0.0763	0.062	0.3858	0.1607
19	59557,8 - 59663,0	4633	7	0.404	0.3783	-0.0134	0.0763	0.4175	0.3859	1.0819
20	59663,0 - 59768,1	2102	3	0.347	0.5778	-0.005	0.0754	0.352	0.5827	0.6041
21	59768,1 - 59873,3	823	6	1.9832	0.4097	-0.0295	0.0761	2.0127	0.4167	4.8295
22	59873,3 - 59978,5	455	5	2.3977	0.4497	-0.0258	0.0758	2.4235	0.456	5.3142
23	59978,5 - 60083,6	265	2	2.0196	0.7098	-0.0098	0.0752	2.0294	0.7138	2.8432
24	60083,6 - 60188,8	186	1	1.6752	1.0027	-0.0046	0.075	1.6797	1.0055	1.6706
25	60188,8 - 60293,9	152	0							
26	60293,9 - 85004,8	1033	10	2.27	0.3178	-0.0517	0.077	2.3217	0.327	7.1009

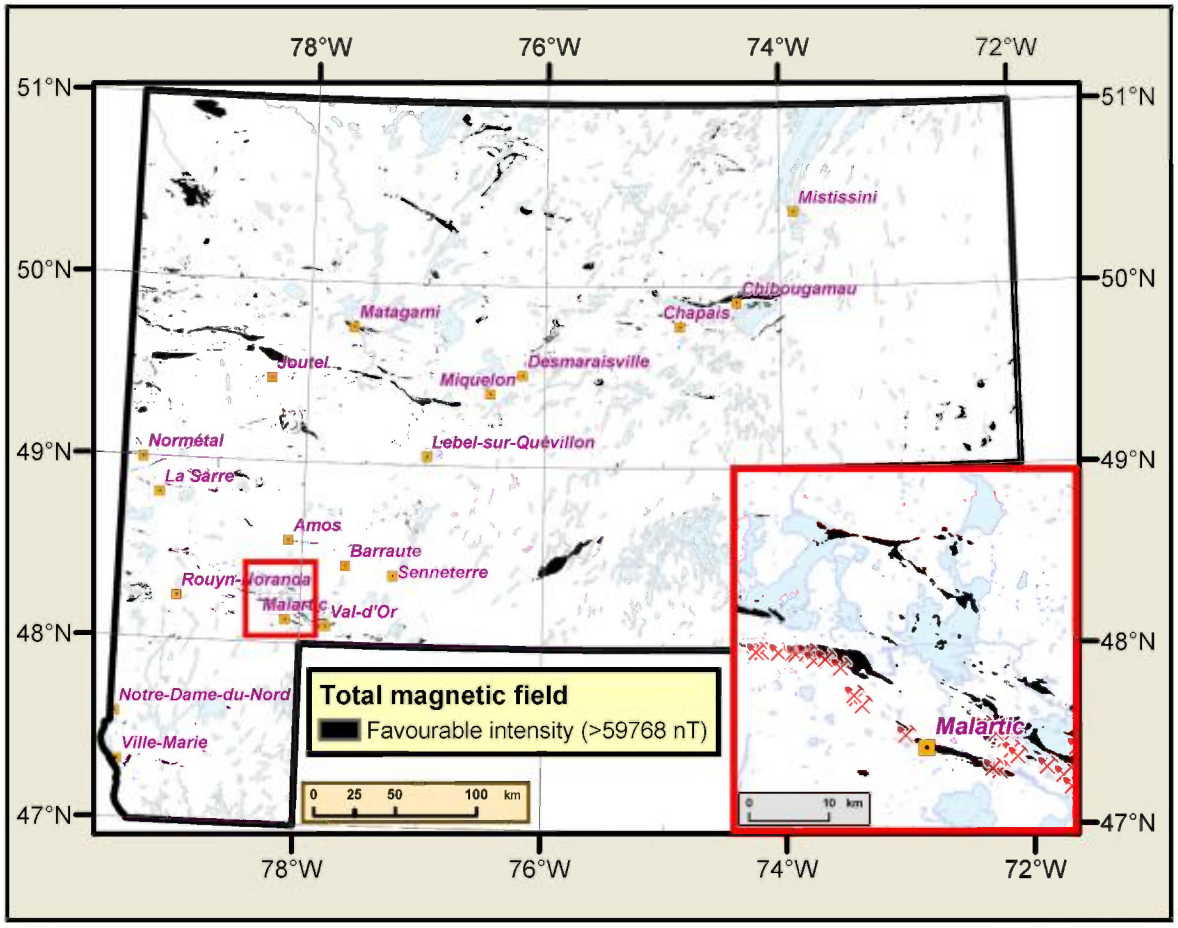

Figure 29 - Binary evidence map of magnetic signatures favourable for gold mineralization.

4.4.2 Favourability associated with the vertical magnetic gradient

Processing for this parameter is similar to that for the total magnetic field. The compiled image is shown in Figure 30. *WofE* analysis of the spatial association shows that two major groupings of gradient value classes are preferentially associated with gold deposits, that is, values lower than –0.726 nT/m and values higher than 0.909 nT/m (Table 18). The cells of these two classes were used to create the binary evidence map in Figure 31.

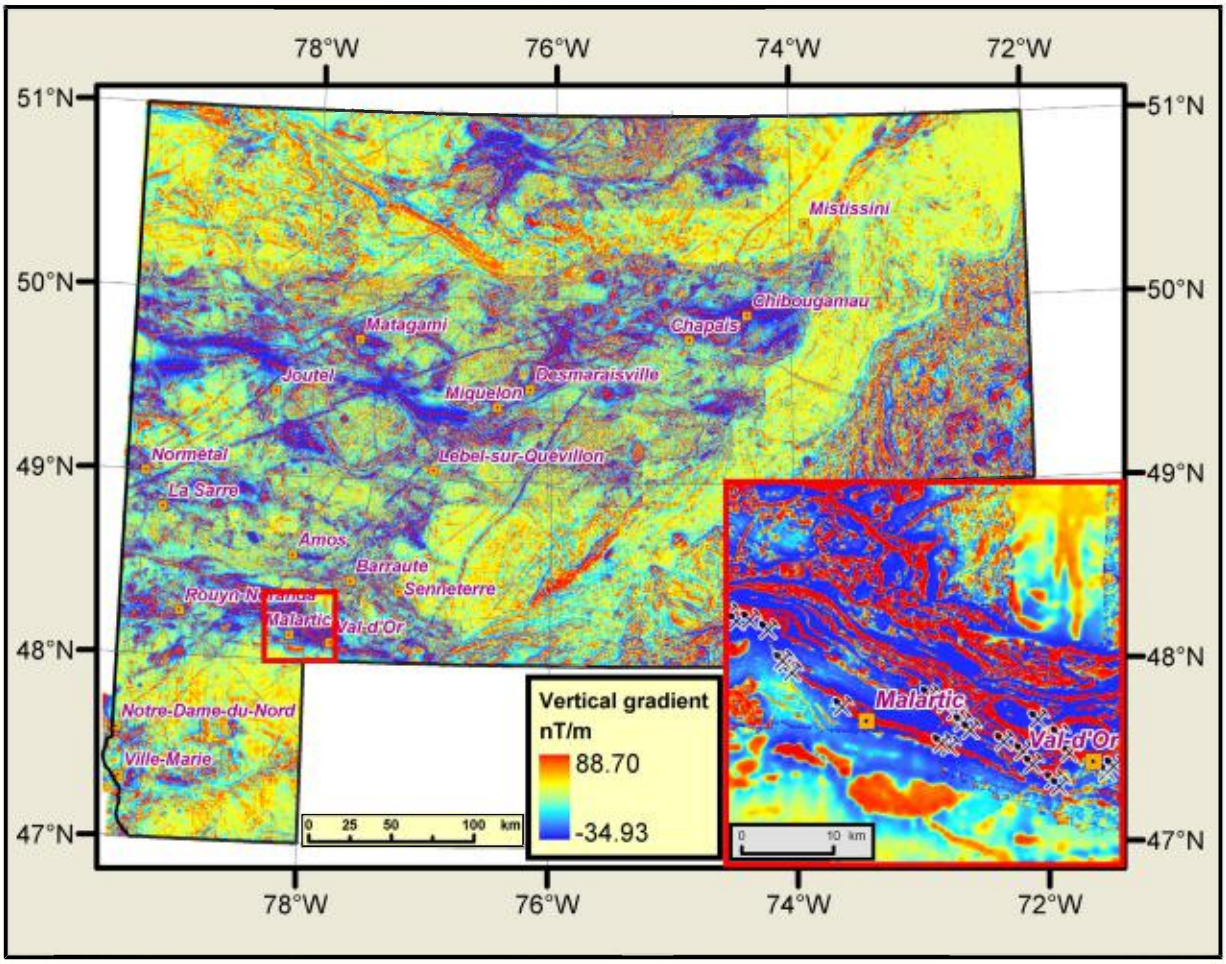

Figure 30 - Vertical magnetic gradient of the Abitibi.

Table 18 - Vertical magnetic gradient values favourable for gold mineralization (See Table 3 for the definition of parametres).

Class	Vert. Mag. grad.	Area_km²	No_Points	W+	s(W+)	W-	s(W-)	C	s(C)	Stud(cnt)
1	-34,93 à -2,18	501	5	2.3033	0.4495	-0.0255	0.0758	2.3289	0.4558	5.1092
2	-2,18 à -1,998	75	0							
3	-1,998 à -1,817	93	0							
4	-1,817 à -1,635	118	2	2.8387	0.7132	-0.0106	0.0752	2.8492	0.7171	3.9731
5	-1,635 à -1,453	153	2	2.5741	0.7118	-0.0104	0.0752	2.5845	0.7157	3.611
6	-1,453 à -1,272	209	2	2.2582	0.7105	-0.0101	0.0752	2.2683	0.7145	3.1747
7	-1,272 à -1,09	296	2	1.9082	0.7095	-0.0096	0.0752	1.9178	0.7135	2.6879
8	-1,09 à -0,908	447	4	2.1931	0.5023	-0.0201	0.0756	2.2132	0.5079	4.3574
9	-0,908 à -0,726	747	5	1.8995	0.4487	-0.0241	0.0758	1.9236	0.4551	4.2269
10	-0,726 à -0,545	1416	5	1.2573	0.448	-0.0204	0.0758	1.2776	0.4544	2.8118
11	-0,545 à -0,363	3326	8	0.8722	0.354	-0.0269	0.0765	0.899	0.3622	2.4825
12	-0,363 à -0,181	11309	22	0.6595	0.2134	-0.0655	0.0798	0.725	0.2279	3.1819
13	-0,181 à 0	91537	46	-0.6955	0.1475	0.4269	0.0868	-1.1223	0.1711	-6.559
14	0 à 0,182	53592	19	-1.0445	0.2295	0.2468	0.0791	-1.2913	0.2427	-5.3203
15	0,182 à 0,364	7121	11	0.4286	0.3017	-0.0226	0.0772	0.4512	0.3115	1.4485
16	0,364 à 0,546	2491	11	1.4818	0.3022	-0.0494	0.0772	1.5312	0.3119	4.9096
17	0,546 à 0,727	1200	6	1.607	0.4093	-0.0274	0.0761	1.6343	0.4163	3.926
18	0,727 à 0,909	704	2	1.0388	0.7081	-0.0073	0.0752	1.046	0.7121	1.4689
19	0,909 à 1,091	464	3	1.8652	0.5792	-0.0143	0.0754	1.8795	0.5841	3.2177
20	1,091 à 1,272	328	2	1.8066	0.7093	-0.0094	0.0752	1.816	0.7132	2.5461
21	1,272 à 1,454	243	3	2.5197	0.581	-0.0156	0.0754	2.5352	0.5858	4.3276
22	1,454 à 1,636	185	3	2.7933	0.5821	-0.0159	0.0754	2.8092	0.5869	4.7861
23	1,636 à 1,818	144	1	1.9347	1.0035	-0.0048	0.075	1.9395	1.0063	1.9274
24	1,818 à 1,999	114	1	2.172	1.0044	-0.005	0.075	2.177	1.0072	2.1614
25	1,999 à 2,181	94	3	3.4929	0.5868	-0.0164	0.0754	3.5093	0.5917	5.9313
26	2,181 à 88,706	871	11	2.5407	0.3034	-0.0586	0.0772	2.5993	0.3131	8.3018

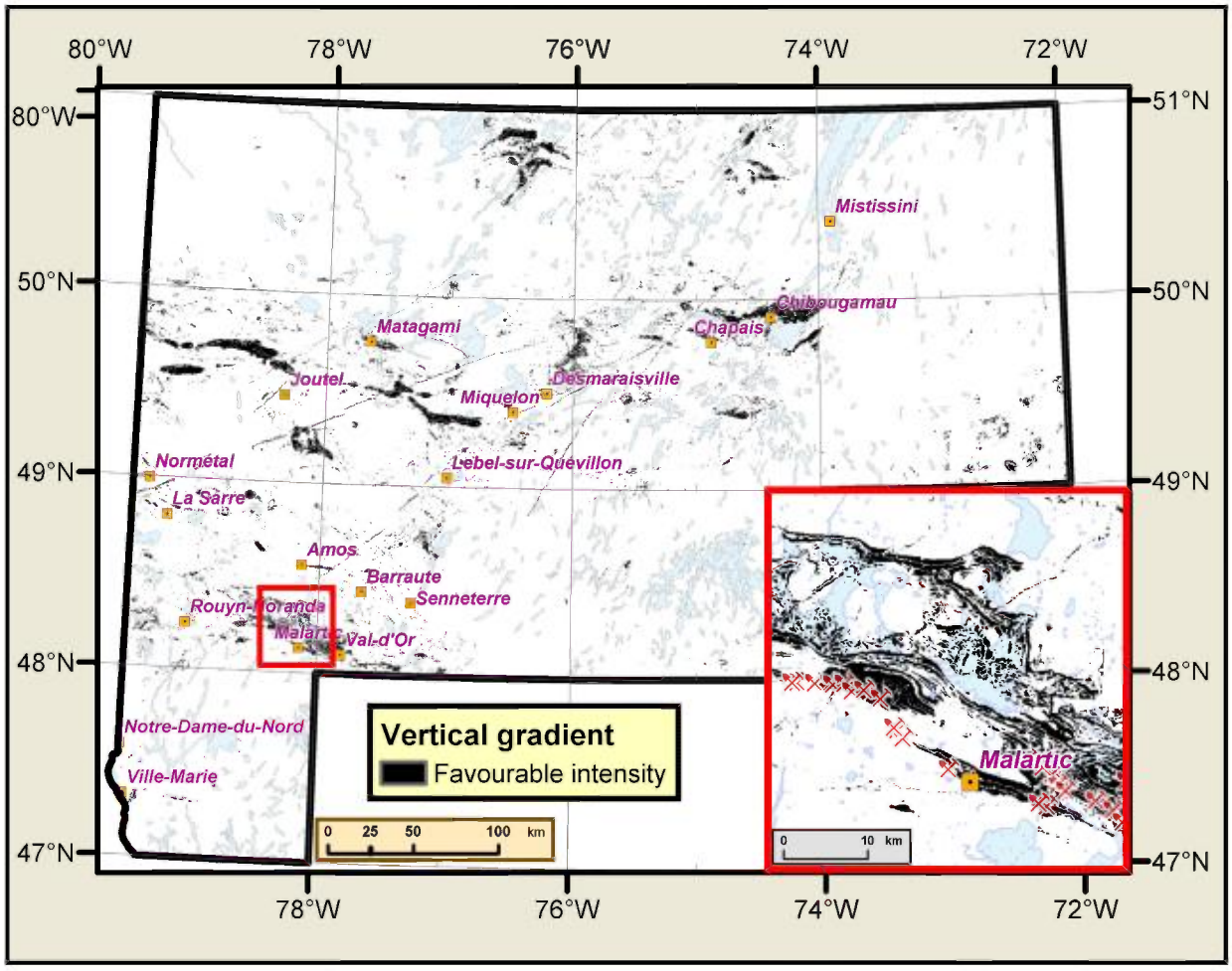

Figure 31 - Binary evidence map of vertical magnetic gradient signatures favourable for gold mineralization.

4.5 Alteration and mineralization evidence

Geochemical alteration indices, observations in drill holes and géofiches for the minerals associated with these deposits can be used to locate the zones in which hydrothermal fluids flowed and were discharged, leading to the formation of gold deposits. Alteration phenomena can be identified through certain normative mineral indices calculated with the NORMAT program (Piché and Jébrak, 2004). These indices can be used to quantify alteration regardless of the original composition of the rocks. The indices used to target alteration zones are ISER (index of sericitization), ICHLOR (index of chloritization) and IPAF (index of loss-on-ignition); the latter is used to quantify carbonatization alteration (Piché and Jébrac, 2004). Processing is aimed at quantifying the spatial association of anomalous values of these three alteration indices with gold deposits in the Abitibi. NORMAT calculation of the alteration indices was performed using about 47,425 analyses of magmatic rocks in the Abitibi. These analyses were used to create a vector file of NORMAT indices (Figure 32).

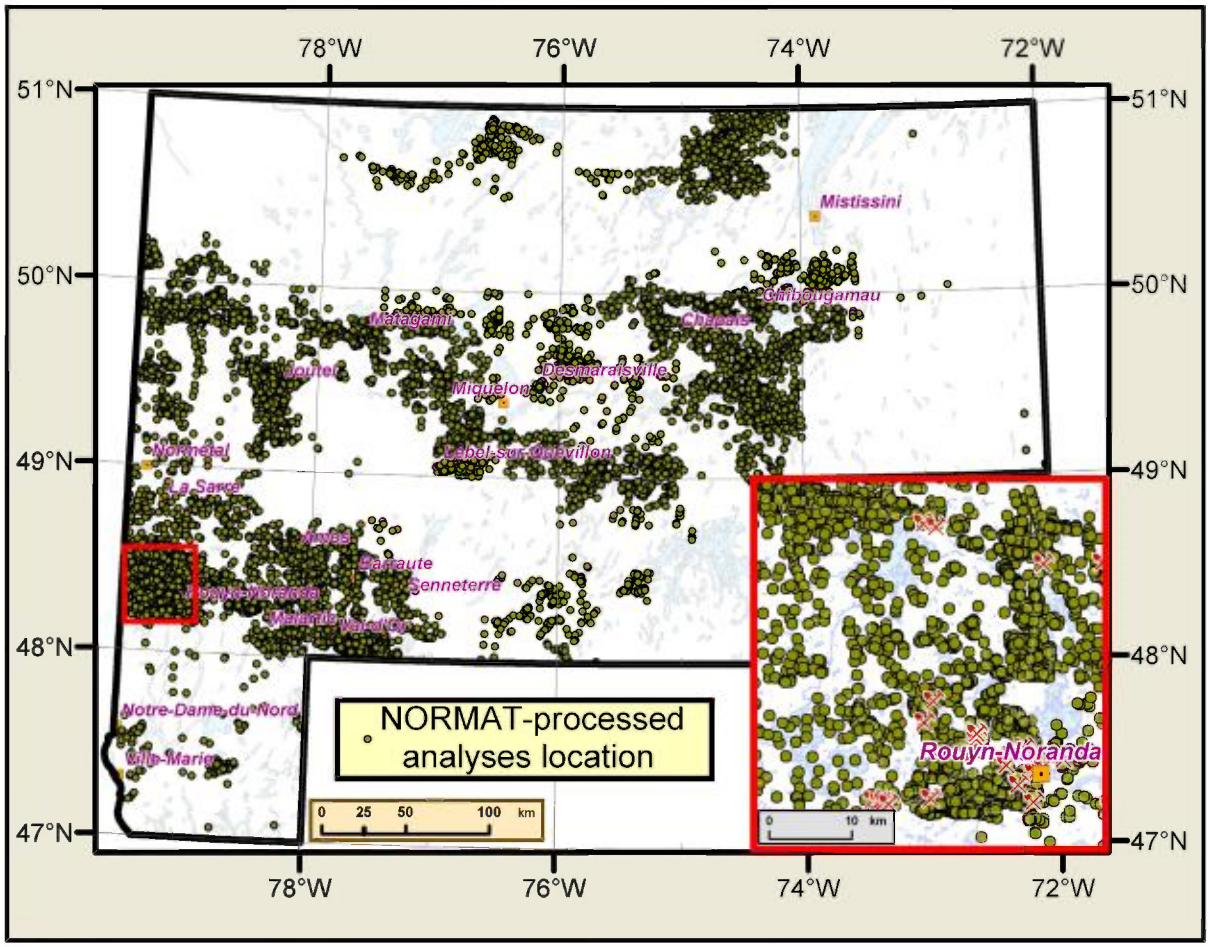

Figure 32 - Location of analyses processsed with NORMAT.

4.5.1 Proximity to an anomalous ISER index

The anomaly threshold of the ISER index has been estimated at 19% using a quantile-quantile plot[1] of the log-normal distribution of the values of the ISER index (Figure 33). The values higher than this threshold correspond to lithologies abnormally altered by sericite, which are generally found on the margins of alteration zones. The estimated value is fairly close to the anomaly threshold (ISER = 25%) determined by Piché (2000) for the Poirier mine, a VMS deposit. The difference between the threshold values probably results from the lower temperatures sometimes found in gold-bearing hydrothermal solutions, that is, 375°-550°C (Hagemann and Cassidy, 2000) versus ~400°C for VMS deposits (Franklin, 1993). Buffering at 100-m intervals up to a distance of 3000 m was performed around points corresponding to an ISER index equal to or greater than the threshold, and favourability associated with proximity was measured with *WofE* (Table 19). The contrast values decreased steadily up to a distance of 1,000 m, becoming erratic beyond this distance. The binary evidence map shows a value of 1 for cells up to a radial distance of 1,000 m from anomalous ISER indices (Figure 34).

[1] A quantile-quantile plot shows the quantile values of the normal distribution of the population on the X-axis, and the quantile values of the data on the Y-axis. This type of plot allows one to distinguish between the different populations in a set by a break in the curve.

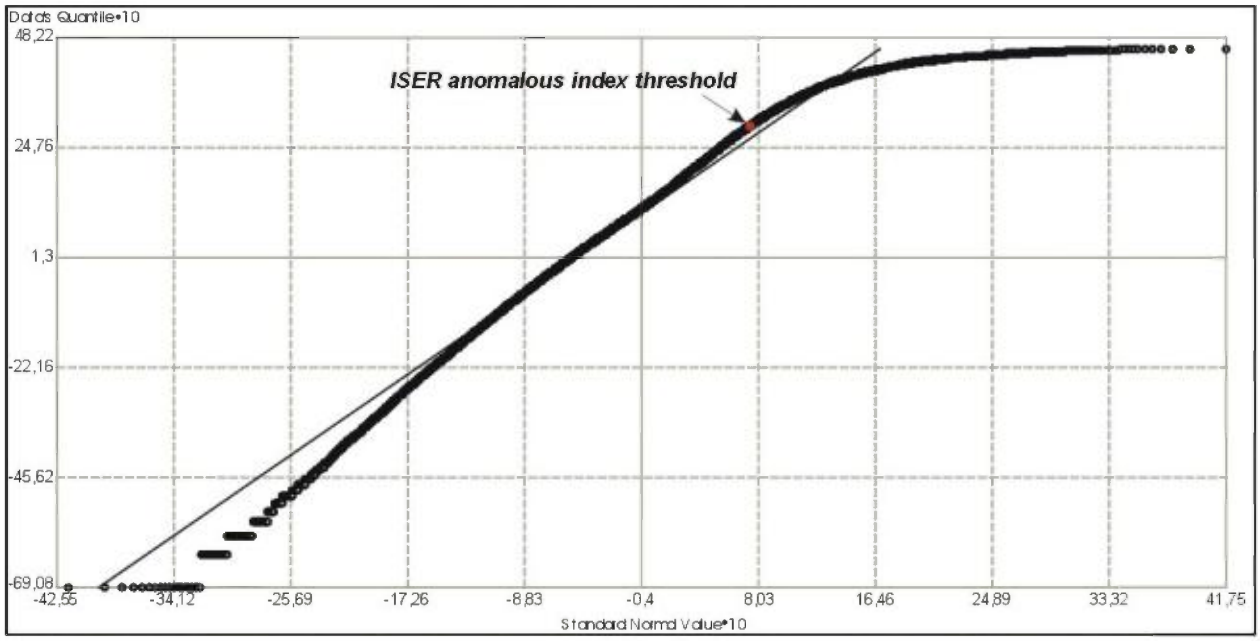

Figure 33 - Quantile-quantile plot of the $\log_n$ of the values of the ISER index. The threshold indicated on the plot corresponds to an ISER index of 19%.

Table 19 - *WofE* analysis of favourability. The contrast remains significant up to a distance of 1,000 m and becomes erratic beyond that point (see Table 3 for the definition of parameters).

Class	Area_km²	No_Points	W+	s(W+)	W-	s(W-)	C	s(C)	Stud(cnt)
100	55	13	5.7242	0.3173	-0.0752	0.0777	5.7993	0.3266	17.7547
200	94	3	3.4866	0.5868	-0.0164	0.0754	3.503	0.5916	5.9212
300	130	5	3.6849	0.4561	-0.0276	0.0758	3.7125	0.4624	8.0293
400	143	7	3.9315	0.3876	-0.0391	0.0763	3.9707	0.395	10.0526
500	178	3	2.8346	0.5823	-0.0159	0.0754	2.8505	0.5871	4.8549
600	166	6	3.6179	0.4158	-0.0332	0.0761	3.6511	0.4227	8.6366
700	211	4	2.9556	0.5048	-0.0214	0.0756	2.977	0.5105	5.8321
800	207	5	3.2008	0.4527	-0.0272	0.0758	3.2279	0.459	7.0322
900	222	3	2.6097	0.5813	-0.0157	0.0754	2.6254	0.5862	4.4789
1000	242	4	2.8139	0.5042	-0.0213	0.0756	2.8351	0.5098	5.561
1100	238	2	2.1288	0.7101	-0.0099	0.0752	2.1387	0.7141	2.9952
1200	239	1	1.4274	1.0021	-0.0043	0.075	1.4317	1.0049	1.4247
1300	270	0							
1400	261	2	2.0372	0.7098	-0.0098	0.0752	2.047	0.7138	2.8677
1500	277	6	3.0898	0.4127	-0.0326	0.0761	3.1224	0.4197	7.4396
1600	281	4	2.6624	0.5036	-0.021	0.0756	2.6834	0.5092	5.2694
1700	291	2	1.9267	0.7095	-0.0096	0.0752	1.9363	0.7135	2.7137
1800	289	2	1.9327	0.7096	-0.0096	0.0752	1.9424	0.7135	2.7222
1900	300	5	2.8219	0.451	-0.0267	0.0758	2.8485	0.4573	6.2288
2000	322	4	2.5238	0.5031	-0.0208	0.0756	2.5446	0.5088	5.0013
2100	305	4	2.5806	0.5033	-0.0209	0.0756	2.6015	0.509	5.1113
2200	325	0							
2300	312	3	2.2636	0.5801	-0.0152	0.0754	2.2787	0.585	3.8951
2400	325	1	1.1183	1.0015	-0.0038	0.075	1.1221	1.0043	1.1172
2500	340	2	1.7698	0.7092	-0.0093	0.0752	1.7791	0.7132	2.4947
2600	342	1	1.0686	1.0015	-0.0037	0.075	1.0723	1.0043	1.0678
2700	332	2	1.795	0.7092	-0.0094	0.0752	1.8044	0.7132	2.5299
2800	348	2	1.7454	0.7091	-0.0093	0.0752	1.7547	0.7131	2.4606
2900	345	1	1.0595	1.0015	-0.0037	0.075	1.0631	1.0043	1.0586
3000	346	5	2.6774	0.4505	-0.0264	0.0758	2.7038	0.4568	5.9187
3001	170044	77	-0.7997	0.114	2.5846	0.0997	-3.3843	0.1514	-22.3505

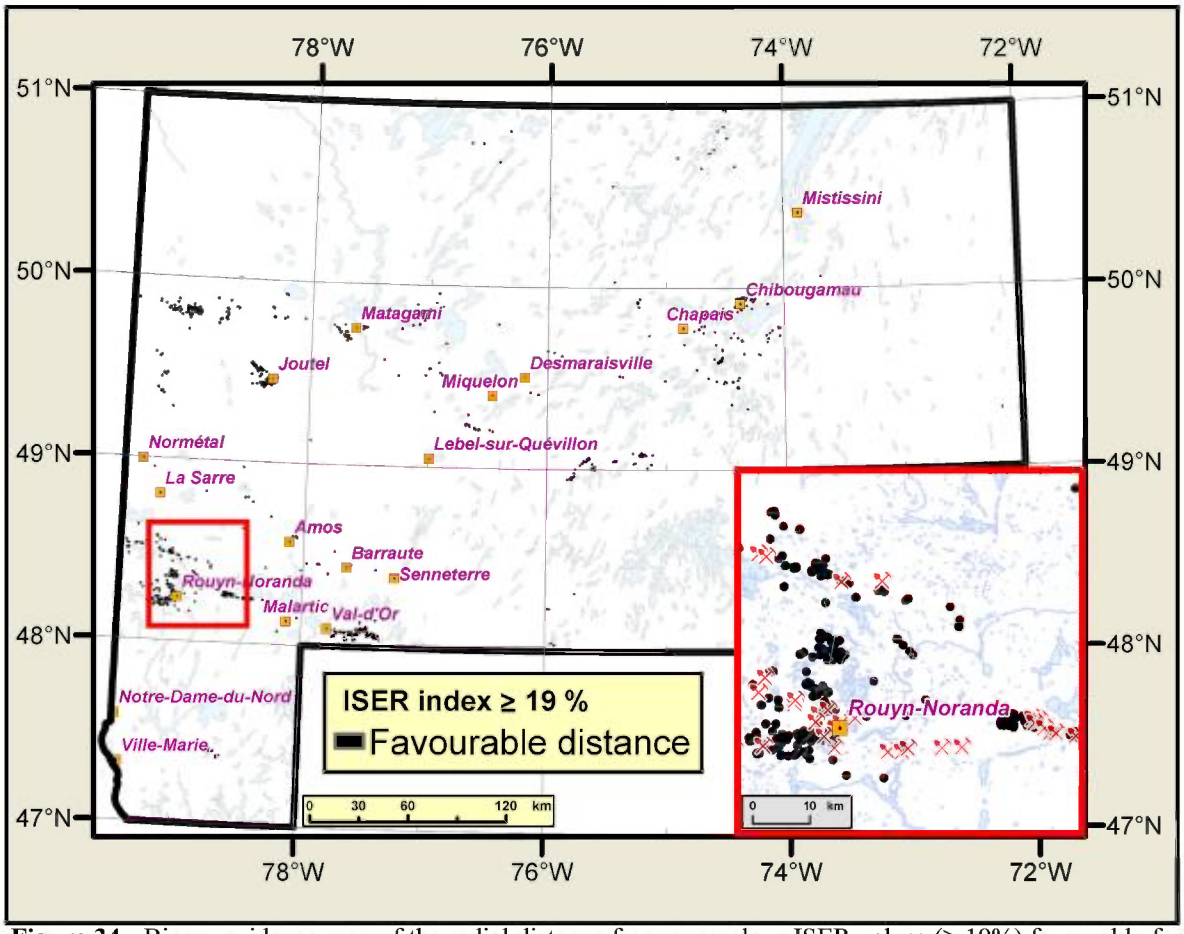

Figure 34 - Binary evidence map of the radial distance from anomalous ISER values (≥ 19%) favourable for gold mineralization.

4.5.2 Proximity to an anomalous ICHLO index

By using an approach similar to that for the ISER index, analyses with ICHLO indices greater than 28% are considered anomalous (Figure 35). This value is also very close to the 25% cut-off established by Piché (2000) for the Poirier mine.

The contrast values were calculated by the *WofE* method for proximity classes in 100-m intervals up to a distance of 3,000 m (Table 20). The contrast value decreases moderately after 200 m, becoming irregular beyond a distance of 1,200 m. Cells up to 1,200 m away from the anomalous ICHLO indices were used to create the binary evidence map (Figure 36).

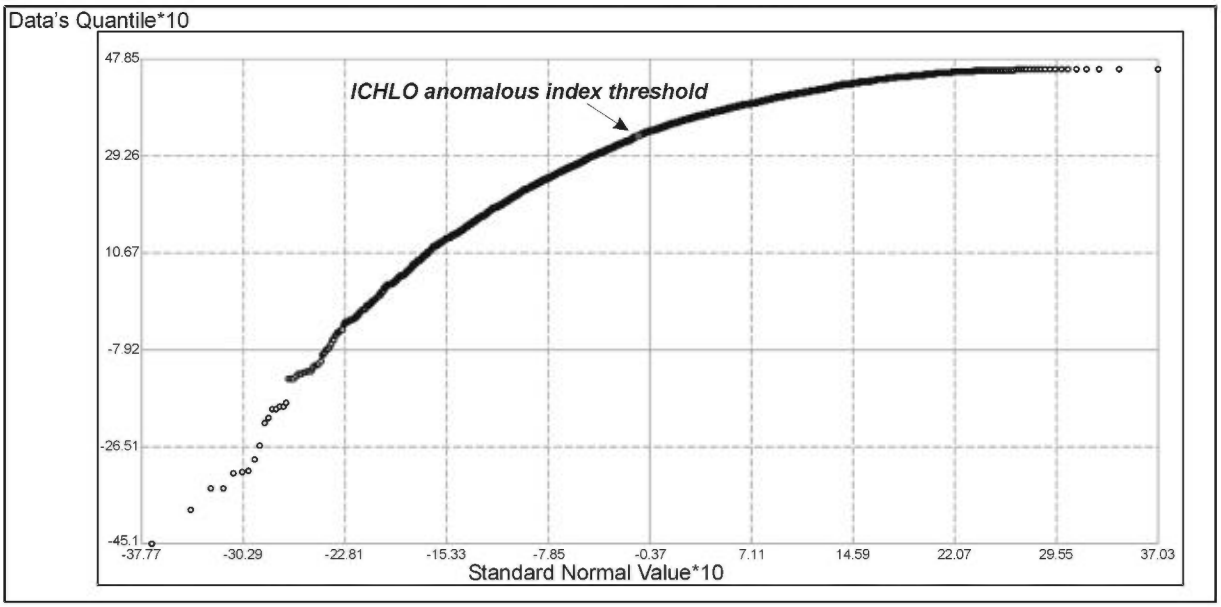

Figure 35 - Quantile-quantile plot of the $\log_n$ of the values of the ICHLO index. The threshold shown on the plot corresponds to an ICHLO index of 28%.

Table 20 - *WofE* analysis of favourability. The contrast value decreases moderately after a distance of 200 m, becoming irregular beyond a distance of 1,200 m (See Table 3 for the definitions of parameters).

Class	Area_km²	No_Points	W+	s(W+)	W-	s(W-)	C	s(C)	Stud(cnt)
100	31	10	6.1621	0.3845	-0.0574	0.077	6.2195	0.3921	15.8621
200	57	6	4.7599	0.4316	-0.0338	0.0761	4.7937	0.4382	10.9384
300	82	2	3.2137	0.7159	-0.0108	0.0752	3.2245	0.7199	4.4794
400	94	3	3.4887	0.5868	-0.0164	0.0754	3.5051	0.5916	5.9245
500	121	3	3.2316	0.5847	-0.0162	0.0754	3.2478	0.5895	5.5093
600	114	3	3.293	0.5851	-0.0163	0.0754	3.3093	0.59	5.6093
700	146	3	3.0348	0.5834	-0.0161	0.0754	3.0509	0.5882	5.1867
800	146	5	3.5592	0.4551	-0.0275	0.0758	3.5868	0.4613	7.7746
900	159	5	3.4698	0.4544	-0.0275	0.0758	3.4973	0.4607	7.5915
1000	177	7	3.7114	0.3857	-0.0389	0.0763	3.7504	0.3932	9.5393
1100	178	4	3.1294	0.5057	-0.0216	0.0756	3.151	0.5114	6.1621
1200	182	4	3.1069	0.5056	-0.0216	0.0756	3.1285	0.5112	6.1196
1300	208	1	1.5694	1.0024	-0.0044	0.075	1.5739	1.0052	1.5657
1400	202	7	3.5724	0.3847	-0.0388	0.0763	3.6112	0.3922	9.208
1500	216	3	2.6368	0.5814	-0.0157	0.0754	2.6525	0.5863	4.5243
1600	220	8	3.6217	0.3602	-0.0445	0.0765	3.6662	0.3682	9.9572
1700	229	2	2.1675	0.7102	-0.01	0.0752	2.1774	0.7142	3.0489
1800	229	0							
1900	240	5	3.0513	0.452	-0.027	0.0758	3.0783	0.4583	6.7172
2000	259	1	1.3471	1.0019	-0.0041	0.075	1.3513	1.0047	1.3449
2100	246	2	2.0959	0.71	-0.0099	0.0752	2.1058	0.714	2.9494
2200	263	4	2.7277	0.5038	-0.0211	0.0756	2.7488	0.5095	5.3953
2300	254	4	2.7636	0.504	-0.0212	0.0756	2.7848	0.5096	5.4644
2400	266	2	2.0158	0.7098	-0.0097	0.0752	2.0255	0.7137	2.8379
2500	279	4	2.671	0.5036	-0.0211	0.0756	2.6921	0.5093	5.2861
2600	280	2	1.9645	0.7096	-0.0097	0.0752	1.9742	0.7136	2.7665
2700	272	1	1.2993	1.0018	-0.0041	0.075	1.3033	1.0046	1.2973
2800	286	3	2.3544	0.5804	-0.0153	0.0754	2.3697	0.5853	4.0488
2900	282	2	1.958	0.7096	-0.0097	0.0752	1.9676	0.7136	2.7573
3000	283	2	1.9544	0.7096	-0.0097	0.0752	1.9641	0.7136	2.7524
3001	171780	71	-0.891	0.1187	2.9008	0.0971	-3.7918	0.1534	-24.7247

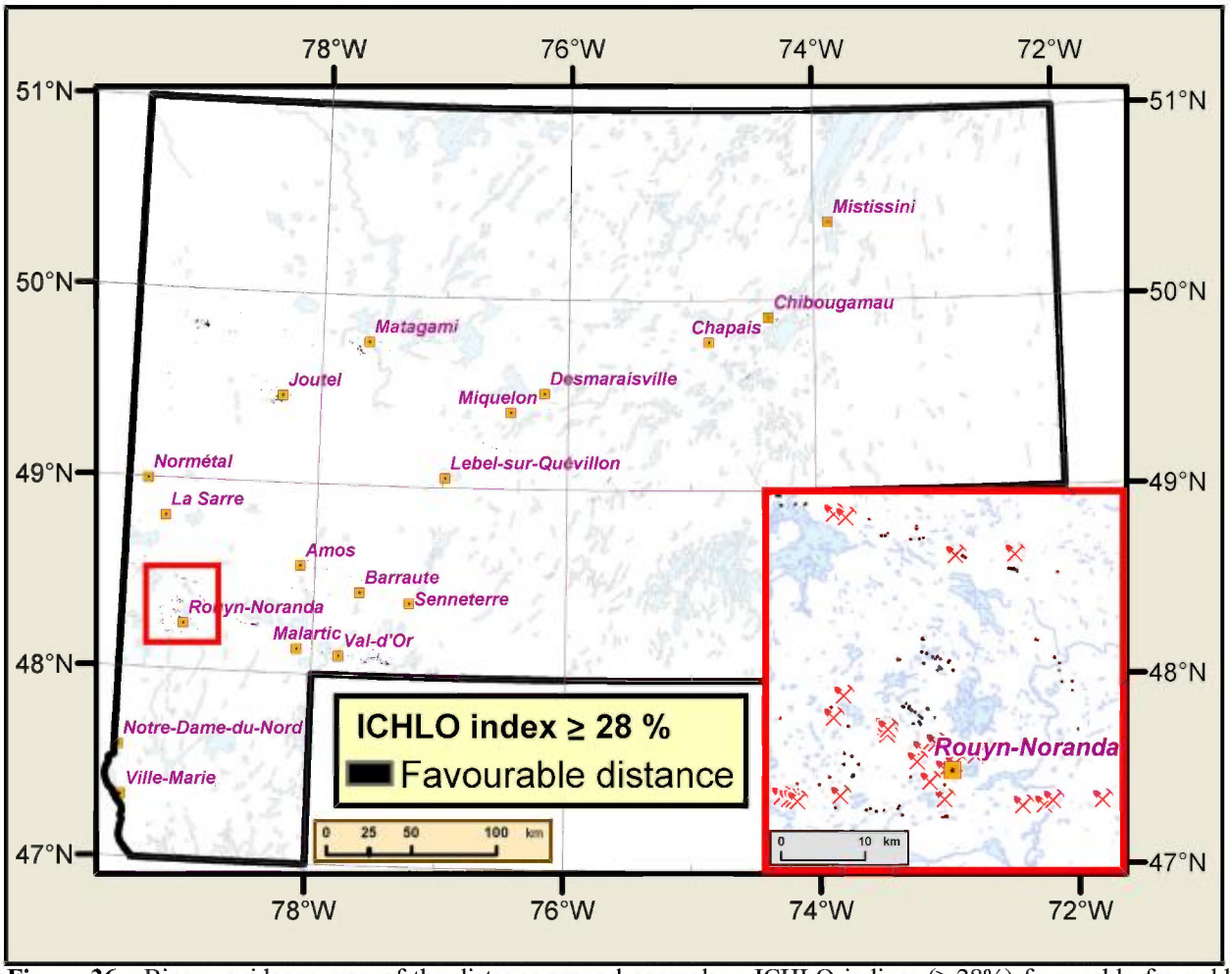

Figure 36 - Binary evidence map of the distance around anomalous ICHLO indices (≥ 28%) favourable for gold mineralization.

4.5.3 Proximity to an anomalous IPAF index

The IPAF index is a relative lithology-independent measure that expresses the ratio between the intensity of carbonatization and the maximum potential for carbonatization estimated by the loss-on-ignition value (Piché and Jébrak, 2004). An approach similar to that used for the ISER and ICHLO indices was used to determine the anomaly threshold for analyses exhibiting an IPAF index between 0 and 100%. Indices higher than 28% (Figure 37) were considered anomalous and buffered by 100-m intervals up to a distance of 3 km. Favourability associated with proximity was assessed by *WofE* (Table 21). Cells less than 300 m from analyses with an anomalous IPAF index were considered favourable and used to create the binary evidence map (Figure 38).

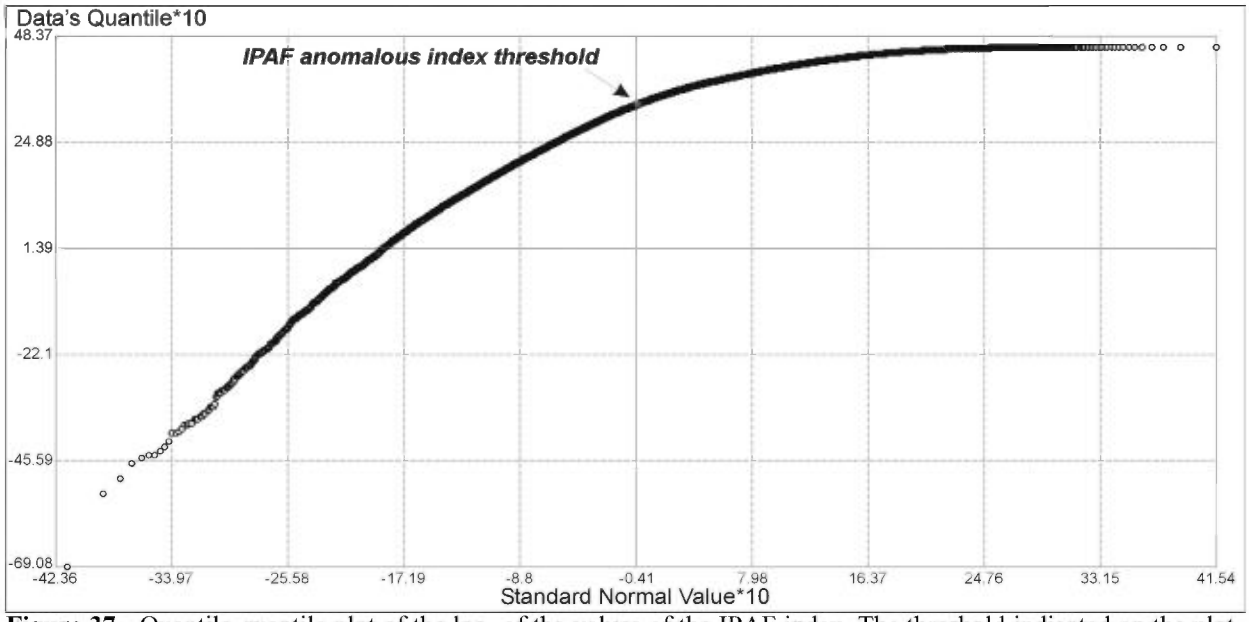

Figure 37 - Quantile-quantile plot of the $\log_n$ of the values of the IPAF index. The threshold indicated on the plot corresponds to an IPAF index of 28%.

Table 21 - *WofE* analysis of favourability. The contrast value decreases moderately after 200 m, becoming irregular beyond a distance of 1,200 m (See Table 3 for the definitions of parameters).

Classe	Aire_km²	No_Points	W+	s(W+)	W-	s(W-)	C	s(C)	Stud(Cnt)
100	167	34	5.3693	0.1921	-0.175	0.0752	5.5443	0.2063	26.8712
200	288	19	4.0843	0.2374	-0.0928	0.0722	4.1772	0.2481	16.8356
300	389	11	3.1971	0.3059	-0.0514	0.0708	3.2485	0.3139	10.3477
400	420	10	3.0221	0.3201	-0.0462	0.0706	3.0683	0.3278	9.3618
500	511	9	2.714	0.3363	-0.0408	0.0704	2.7548	0.3436	8.0175
600	466	6	2.3949	0.4109	-0.0263	0.0699	2.4211	0.4168	5.8089
700	580	8	2.4653	0.356	-0.0354	0.0702	2.5007	0.3629	6.8913
800	563	6	2.2038	0.4104	-0.0257	0.0699	2.2295	0.4163	5.355
900	594	6	2.1495	0.4103	-0.0255	0.0699	2.175	0.4162	5.2255
1000	640	6	2.0754	0.4102	-0.0253	0.0699	2.1006	0.4161	5.0486
1100	623	0							
1200	618	3	1.4128	0.5788	-0.0109	0.0694	1.4237	0.5829	2.4424
1300	686	9	2.4142	0.3355	-0.0398	0.0704	2.454	0.3428	7.1577
1400	651	4	1.6492	0.5015	-0.0155	0.0695	1.6647	0.5063	3.2877
1500	679	6	2.015	0.4101	-0.025	0.0699	2.04	0.416	4.9042
1600	676	7	2.1756	0.3799	-0.03	0.0701	2.2055	0.3863	5.7087
1700	686	7	2.1606	0.3799	-0.0299	0.0701	2.1905	0.3863	5.6703
1800	670	3	1.3315	0.5786	-0.0106	0.0694	1.3421	0.5828	2.3028
1900	683	2	0.9052	0.7081	-0.0057	0.0692	0.9109	0.7115	1.2803
2000	722	1	0.1547	1.0007	-0.0007	0.069	0.1553	1.0031	0.1549
2100	671	1	0.2282	1.0007	-0.001	0.069	0.2292	1.0031	0.2284
2200	705	3	1.2805	0.5786	-0.0104	0.0694	1.2908	0.5827	2.2151
2300	665	2	0.9316	0.7082	-0.0058	0.0692	0.9374	0.7115	1.3174
2400	680	2	0.909	0.7081	-0.0057	0.0692	0.9147	0.7115	1.2855
2500	698	4	1.5789	0.5014	-0.0152	0.0695	1.5941	0.5062	3.1489
2600	689	2	0.8966	0.7081	-0.0056	0.0692	0.9022	0.7115	1.2681
2700	655	5	1.8681	0.4489	-0.0203	0.0697	1.8884	0.4543	4.1566
2800	678	5	1.8331	0.4489	-0.0202	0.0697	1.8533	0.4543	4.0798
2900	662	1	0.2416	1.0008	-0.001	0.069	0.2426	1.0031	0.2419
3000	654	2	0.9486	0.7082	-0.0058	0.0692	0.9545	0.7116	1.3413
3001	159710	27	-1.9499	0.1925	2.1585	0.0741	-4.1083	0.2062	-19.9204

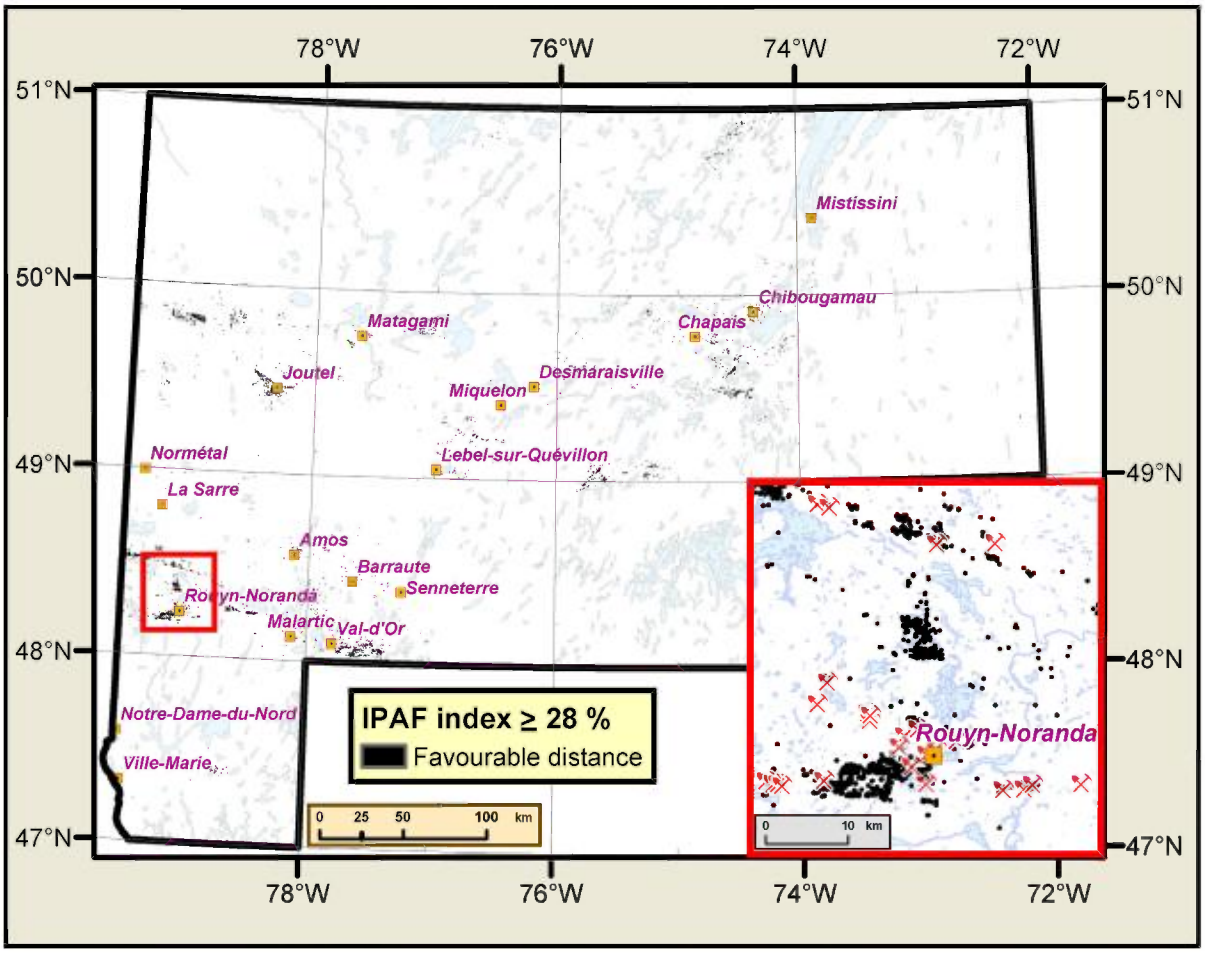

Figure 38 - Binary evidence map of the distance around anomalous IPAF indices (≥ 28%) favourable for gold mineralization.

4.5.4 Proximity to an indicator of mineralization

Gold deposits generally exhibit extensive lateral alteration zones whose mineral phases comprise proximal to distal assemblages. Among the routine indicator minerals, the following can be derived from the SIGEOM databases: gold, silica, sericite, chlorite, carbonates, tourmaline, pyrite, arsenopyrite, biotite and aluminosilicates (andalusite, kyanite) (Groves et al., 1998; Mickuki, 1998; Doucet and Lafrance, 2005). The point observations for these minerals were extracted from drill holes (position projected onto the surface), compilation outcrops and SIGEOM géofiches to create a vector file of relevant deposits (Figure 39). The favourability of the parameter remains significant up to a distance of 500 m (Table 22), and this value was used to create the binary evidence map (Figure 40).

Table 22 - *WofE* analysis of favourability. The contrast of the parameter remains significant up to a distance of 500 m (See Table 3 for the definitions of the parameters).

Class	Area_km²	No_Points	W+	s(W+)	W-	s(W-)	C	s(C)	Stud(cnt)
100	336	112	6.2084	0.1158	-0.9814	0.1222	7.1899	0.1683	42.7157
200	633	36	4.0921	0.1716	-0.2212	0.0837	4.3133	0.1909	22.5913
300	873	12	2.6268	0.2907	-0.0645	0.0774	2.6913	0.3008	8.9468
400	943	4	1.4416	0.5011	-0.0173	0.0756	1.4589	0.5067	2.8791
500	1139	5	1.4763	0.4482	-0.0219	0.0758	1.4982	0.4546	3.2958
600	1020	3	1.0741	0.5782	-0.0112	0.0754	1.0853	0.5831	1.8612
700	1246	0							
800	1177	1	-0.1698	1.0004	0.001	0.075	-0.1709	1.0032	-0.1703
900	1213	0							
1000	1275	3	0.8505	0.578	-0.0097	0.0754	0.8602	0.5829	1.4757
1001	167927	3	-4.0327	0.5774	2.8929	0.0761	-6.9257	0.5823	-11.8928

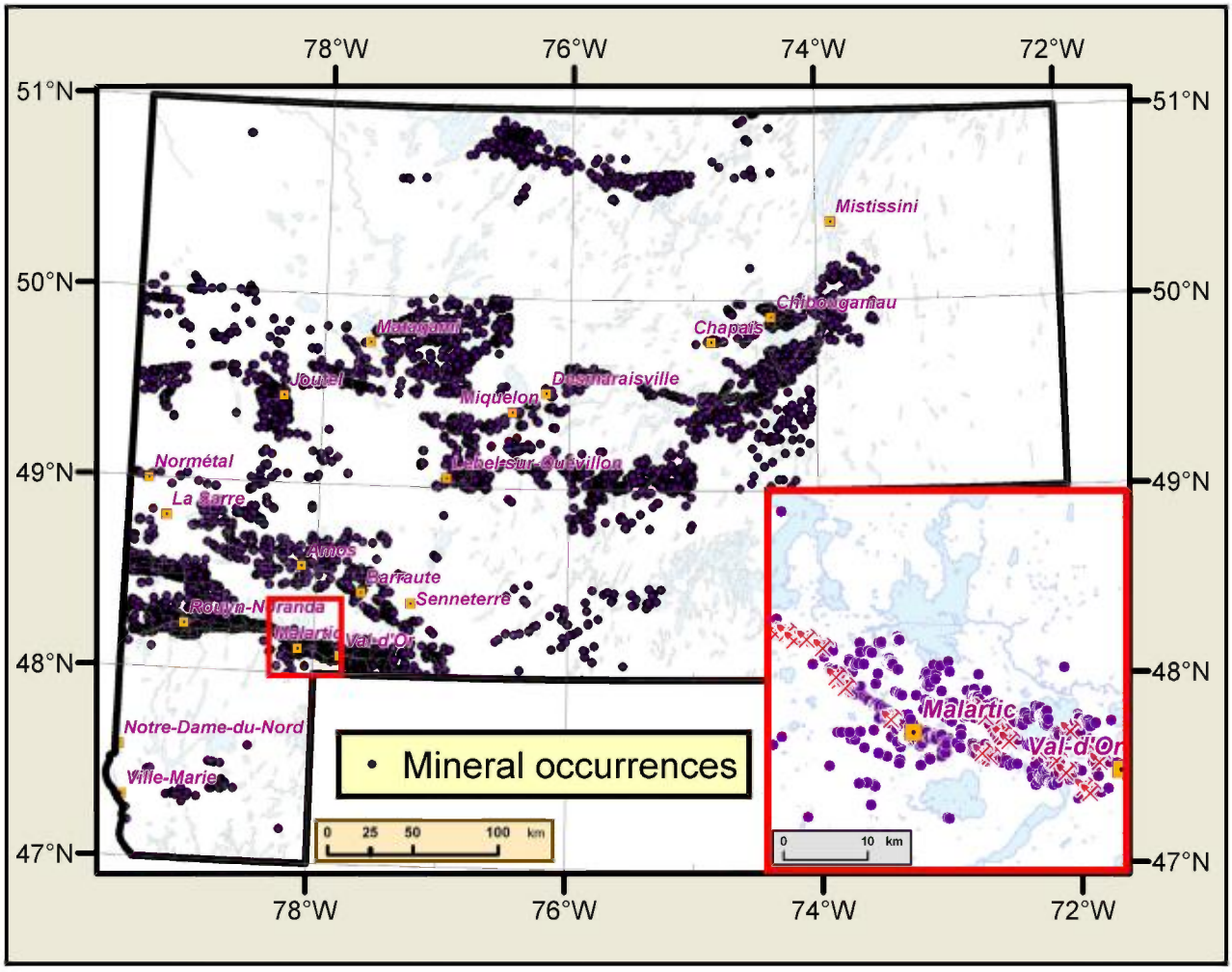

Figure 39 - Location of the mineral occurrences associated with gold deposits in the Abitibi.

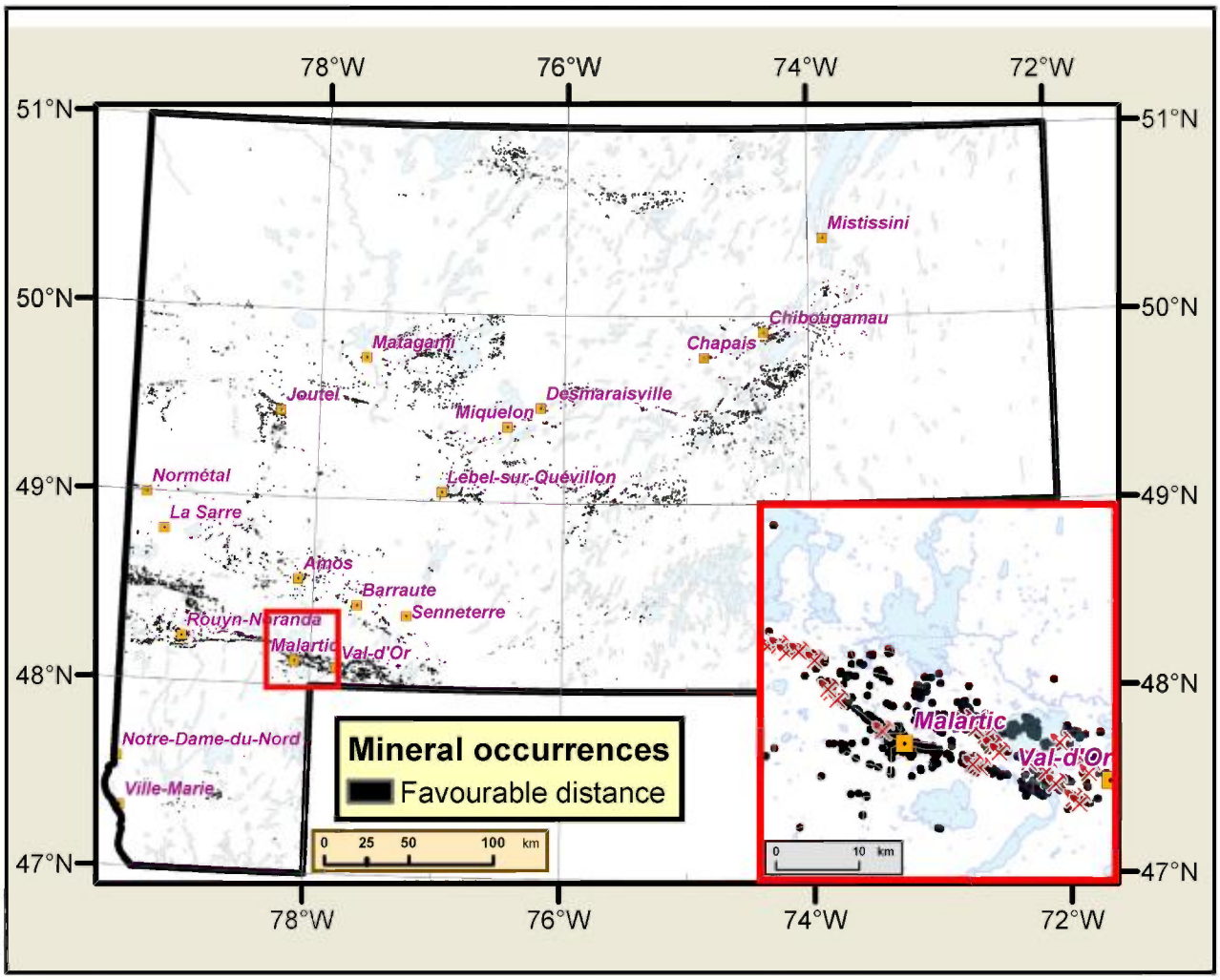

Figure 40 - Binary evidence map of radial distance from mineral occurrences favourable for gold mineralization.

4.6 Favourable metallogenic context

In the Abitibi, there are a number of VMS gold deposits, including the Horne, LaRonde, Bousquet and Doyon ones. These deposits account for a significant proportion (about 15%) of all gold production in the Abitibi (Robert, 1990). There is controversy related to their genesis, but for some deposits the gold enrichment can be explained by a secondary syntectonic replacement process, substantiated by the importance of structural control and the late paragenesis of gold, particularly in the Bousquet district (Poulsen and Hannington, 1996; Tourigny et al. 1989 et 1993). The potential that VMS deposits hold for orogenic gold is therefore a relevant parameter.

4.6.1 Association with a zone favourable for VMS

This processing step was aimed at assessing the spatial association between orogenic gold deposits and high-favourability zones for VMS deposits defined by Lamothe et al. (2005) for the Abitibi. These zones were identified by integrating 27 parameters relevant to VMS deposits through a hybrid fuzzy logic approach; they are distributed throughout the study region (shapefile) (Figure 41). *WofE* analysis showed a strong association between favourability zones and gold deposits, up to a distance of 200 m from the zones (Table 22); this 200 m distance was used to create the binary evidence map (Figure 42).

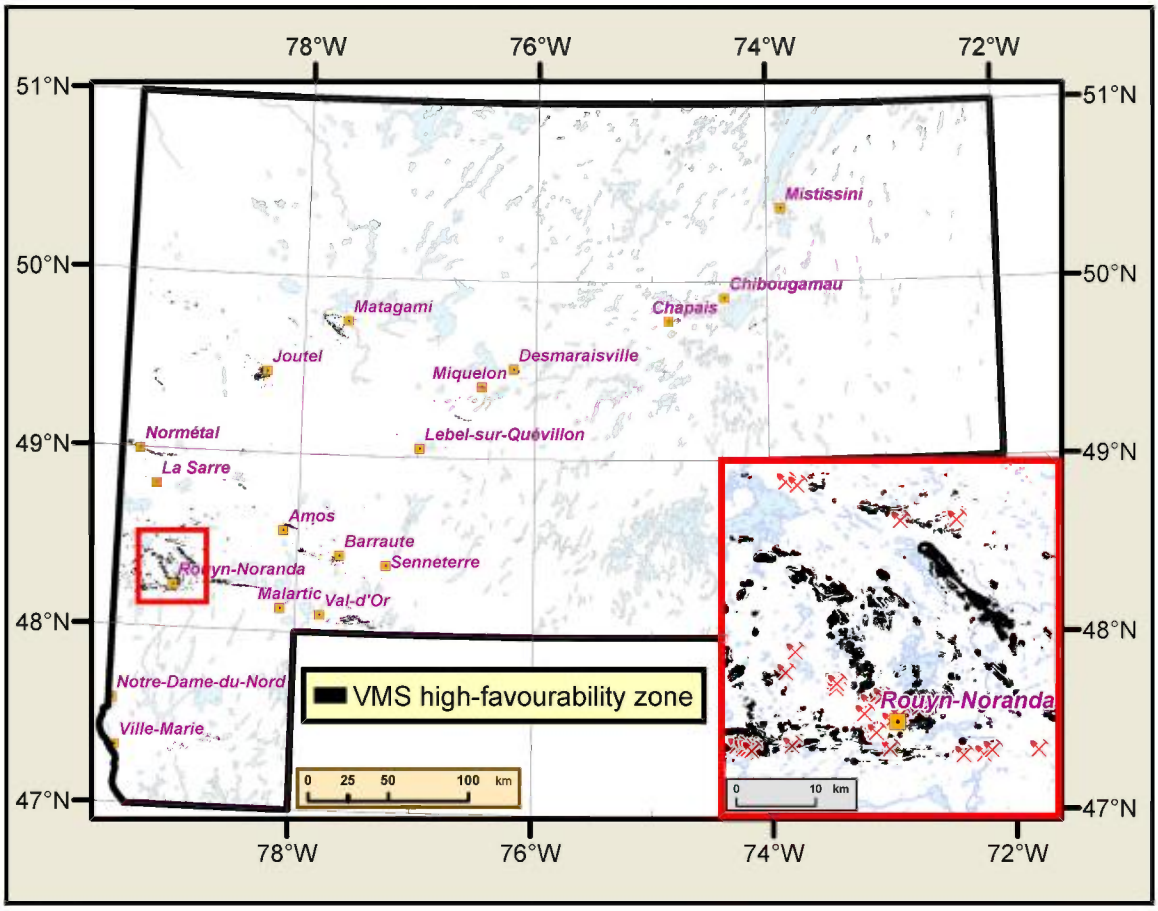

Figure 41 - Location of high-favourability zones for VMS-type deposits in the Abitibi.

Table 22 - *WofE* analysis of favourability. The contrast of the parameter remains significant up to a distance of 200 m, becoming irregular beyond that point. Class 1 corresponds to gold deposits located within a high-favourability zone for VMS deposits (See Table 3 for the definitions of parameters).

Class	Area_km²	No_Points	W+	s(W+)	W-	s(W-)	C	s(C)	Stud(cnt)
1	740	43	3.9499	0.1571	-0.224	0.0772	4.1739	0.1751	23.8413
100	306	10	3.346	0.3215	-0.0469	0.0706	3.3929	0.3292	10.3073
200	321	7	2.9313	0.3822	-0.032	0.0701	2.9632	0.3885	7.627
300	337	3	2.0225	0.5799	-0.0124	0.0694	2.0349	0.5841	3.484
400	320	6	2.7777	0.4121	-0.0271	0.0699	2.8048	0.418	6.7098
500	356	1	0.8629	1.0014	-0.0027	0.069	0.8656	1.0038	0.8624
600	307	1	1.0132	1.0016	-0.003	0.069	1.0162	1.004	1.0122
700	368	3	1.9353	0.5797	-0.0123	0.0694	1.9476	0.5839	3.3357
800	343	2	1.5955	0.7092	-0.0076	0.0692	1.6031	0.7125	2.2499
900	357	5	2.4822	0.4504	-0.022	0.0697	2.5042	0.4557	5.4948
1000	373	1	0.8161	1.0013	-0.0027	0.069	0.8188	1.0037	0.8157
1100	361	2	1.5439	0.7091	-0.0075	0.0692	1.5514	0.7124	2.1776
1200	351	0							
1300	392	6	2.5708	0.4114	-0.0267	0.0699	2.5975	0.4173	6.2245
1400	368	6	2.6367	0.4116	-0.0268	0.0699	2.6635	0.4175	6.3794
1500	383	6	2.5942	0.4115	-0.0267	0.0699	2.6209	0.4174	6.2795
1600	380	3	1.9024	0.5796	-0.0122	0.0694	1.9146	0.5838	3.2796
1700	386	2	1.4783	0.7089	-0.0074	0.0692	1.4857	0.7123	2.0857
1800	372	2	1.515	0.709	-0.0074	0.0692	1.5224	0.7124	2.1371
1900	383	8	2.8869	0.3573	-0.0365	0.0702	2.9234	0.3641	8.0284
2000	405	1	0.7327	1.0012	-0.0025	0.069	0.7352	1.0036	0.7326
2001	169870	93	-0.7744	0.1037	2.5452	0.0928	-3.3196	0.1391	-23.8572

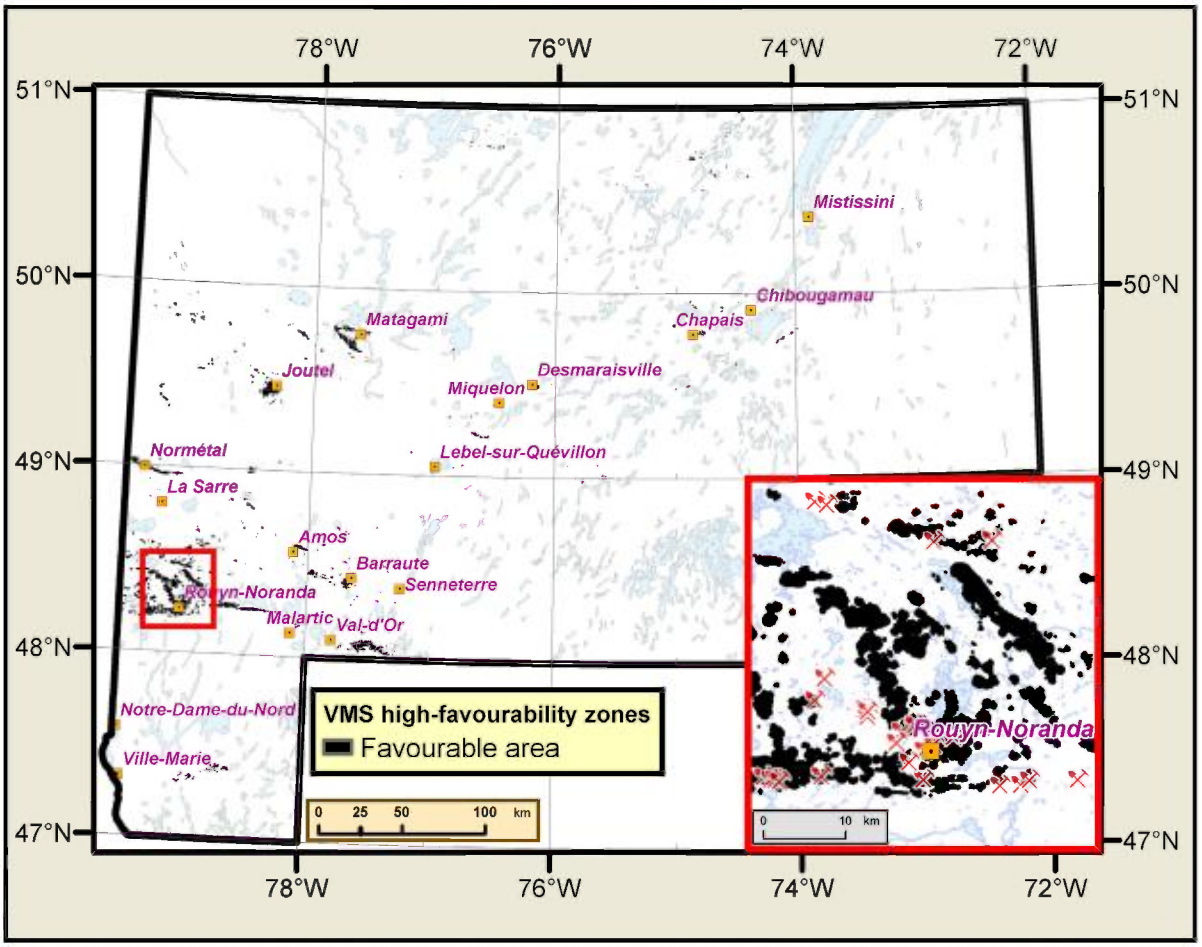

Figure 42 - Binary evidence map of zones favourable for gold mineralization as a function of proximity to a high-favourability zone for VMS deposits.

5 Overall favourability for orogenic gold mineralization in the Abitibi

The final favourability map (Figure 43) for orogenic gold deposits in the Abitibi was produced by the procedure described in Section 3.2. A version of this final map at 1:500,000 scale in PDF format is available on CD-ROM. The digital data are delivered in UTM projection, NAD83, zone 18 or in geographic coordinates.

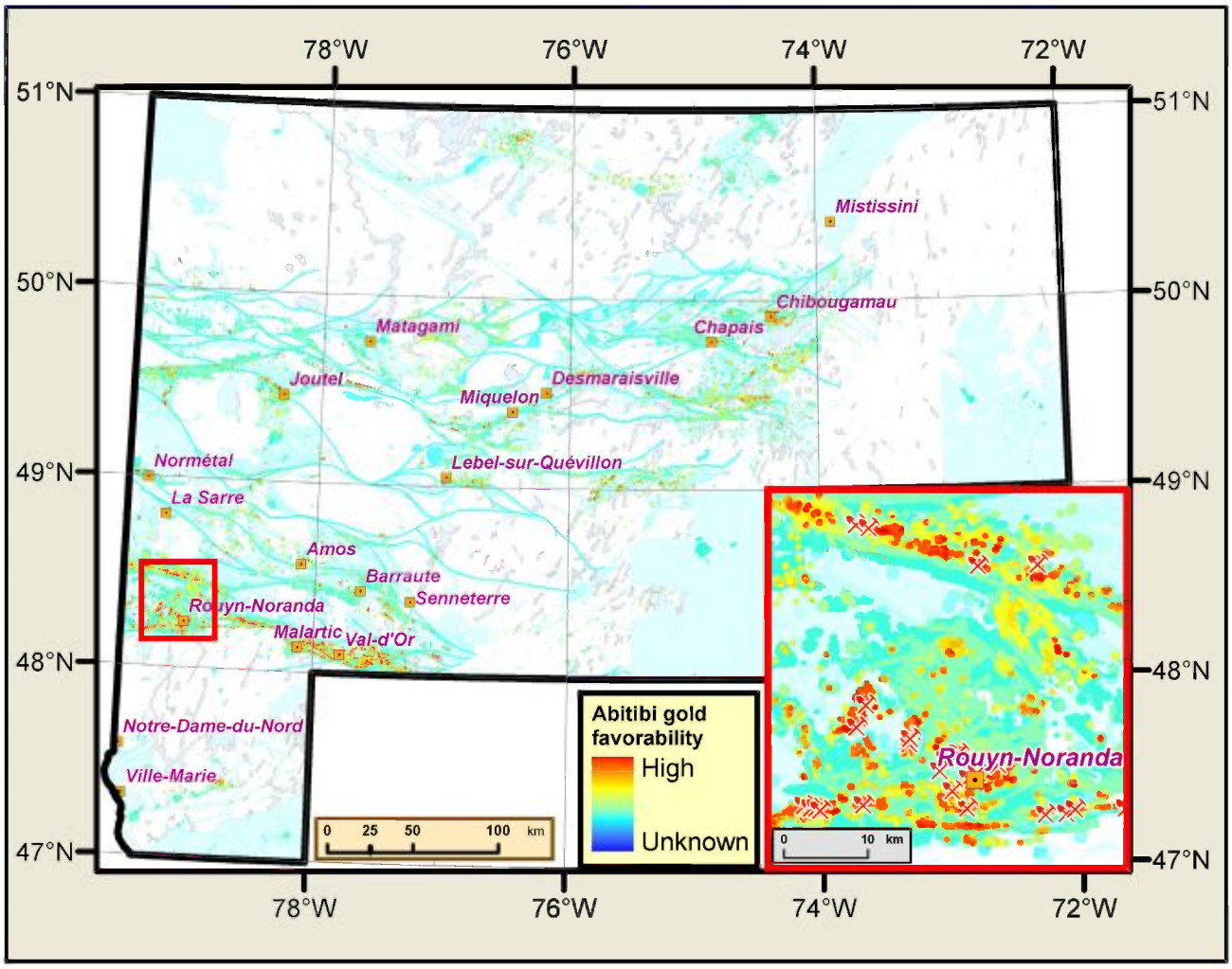

Figure 43 - Neural network analysis of favourability for orogenic gold mineralization in the Abitibi.

The colour pattern in this map is characterized by more or less linear clusterings of high-favourability values against a background of linear elements of moderate favourability. The clusterings are concentrated in a number of broad sectors:

- Cadillac Fault sector;
- Porcupine-Destor sector
- Joutel area;
- Western flank of the Mistaouac pluton;
- Southern flank of the Bell-Allard intrusion;
- Barry belt;
- Desmaraisville, Chapais and Chibougamau sectors;

- Sector north of Lake Caopatina (32G/07);
- Sector north of Lake Palmer (32G/09).

Appendix 1 shows the data processing steps leading to the production of the final favourability map for gold mineralization in the Abitibi. Readers can navigate through the different sections of the text by clicking on the parameters in the figure. The general 1:500,000-scale map can be visualized by clicking the figure on the right-hand side. The 132 maps at 1:50,000 scale on the CD-ROM can be visualized by clicking in the appropriate boxes of the index of mineral potential maps.

5.1 Determination of high-favourability zones and targets

Analysis of favourability for orogenic gold deposits in the Abitibi allows us to achieve two preliminary objectives: 1) to define, for the Abitibi, **high-favourability zones** for gold deposits that will help to focus mineral exploration; and 2) to define and document a certain number of targets not yet staked at the time of the study.

In order to define high-favourability zones, a minimal favourability threshold value must be determined, beyond which the favourability of a zone requires a significant predictability of the presence of orogenic gold occurrences belonging to the ore deposit category. To define this threshold, overall favourability values associated with the 179 mines and deposits with an estimated tonnage in the Abitibi (the training set) were plotted on a normal probability diagram (Figure 44). Two different normal populations were identified. The largest population, consisting of 158 (79%) of the 179 ore bodies used in the study, has a value exceeding the minimal threshold value of 0.947. The 38 bodies whose values were below the threshold form a second, distinct population which the favourability map does not target well, because the available data are insufficient or contradictory. Some important mines, plotted on the diagram, belong to this second category. The case of Horne mine, a world-class deposit of gold-bearing massive sulphides, can be explained by the absence in SIGEOM of analytical and drill hole data within a radius of about 500 m around the deposit. This isn't the case for the other three mines, whose favourability is underestimated in the study for various reasons (absence in SIGEOM of analytical data in drill holes and relevant geological data around Selbaie, absence of evidence for some parameters for Sigma and Doyon).

Using the minimum threshold value, a set of cells whose values are equal to or greater than 0.947 can be delineated based on the final favourability map, and the two groups of cells can be converted into polygons. These polygons constitute **high-favourability zones** (shapefile) (Figure 45).

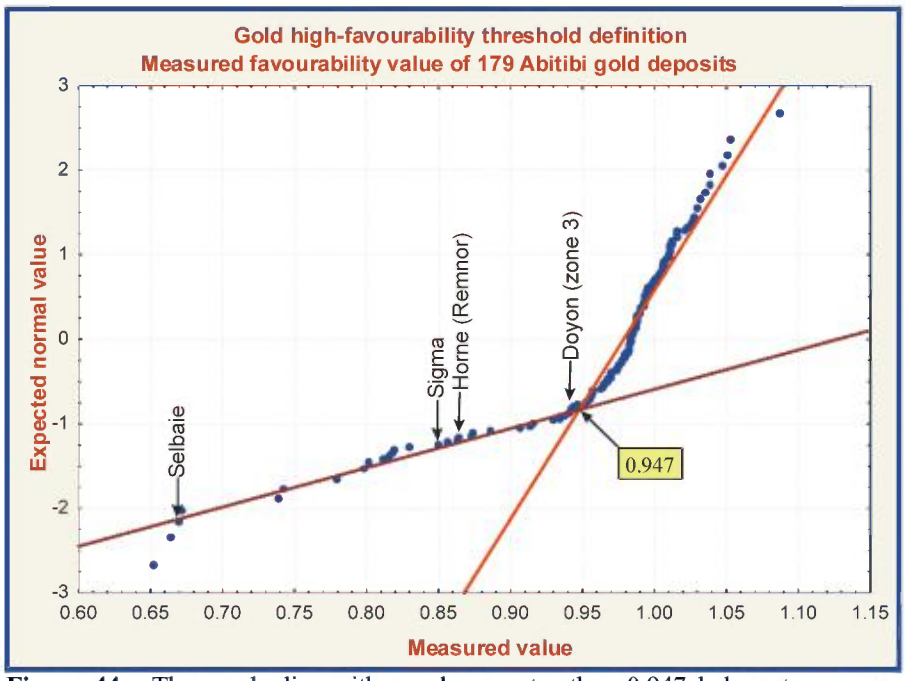

Figure 44 - The ore bodies with a value greater than 0.947 belong to a normal population. This is the minimal threshold value for high-favourability zones. A few important mines whose favourability is lower fall outside these zones, generally because of insufficient or contradictory data.

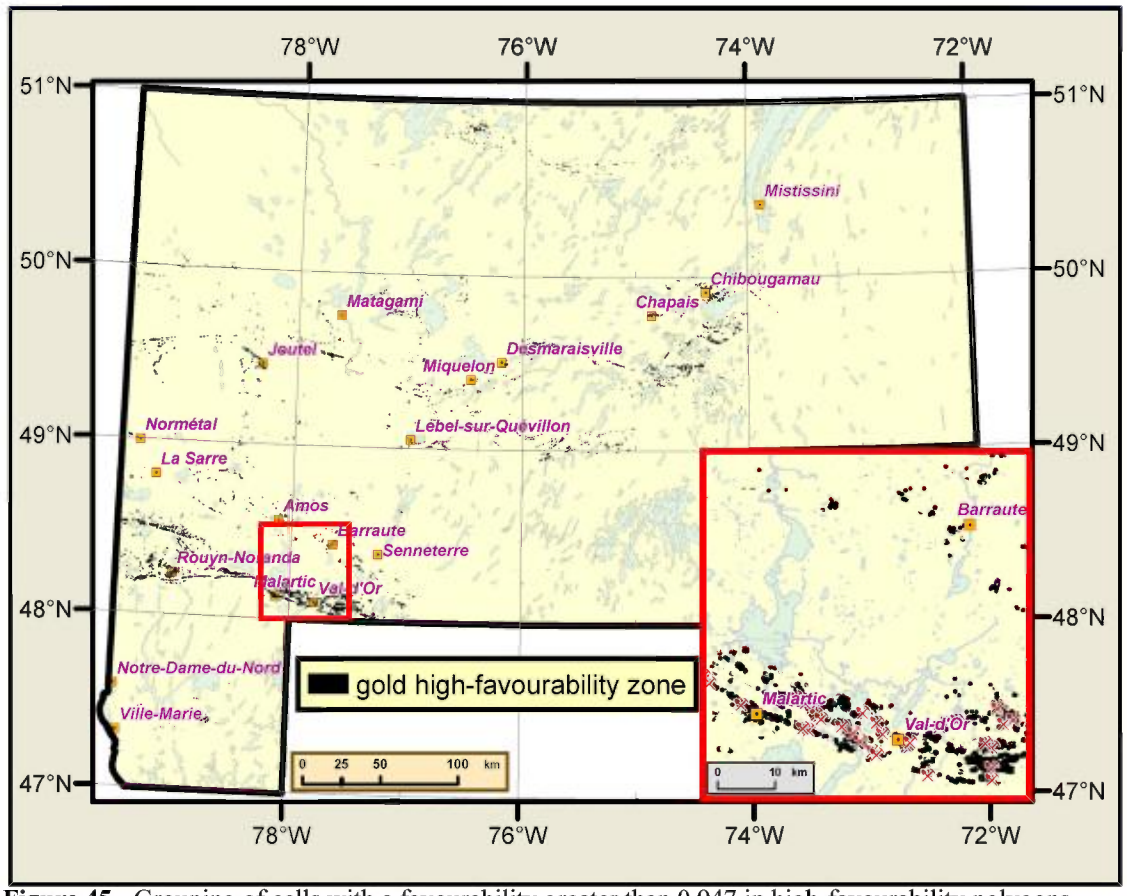

Figure 45 - Grouping of cells with a favourability greater than 0.947 in high-favourability polygons.

5.2 Validation of results

Figures 46a and 46b contain two comparative diagrams illustrating the predictability of the favourability map as a function of four types of orogenic gold occurrences in the Abitibi, namely: 1) the 179 mines and deposits with a tonnage estimate used to create the favourability map; 2) a control set of 32 mines and deposits with a tonnage estimate that were not used in processing; 3) a set of 638 deposits whose tonnage has not been evaluated; and 4) a set of 518 showings. The charts show the cumulative percentage of ore bodies (Y-axis) relative to the cumulative surface area corresponding to the favourability values sorted in descending order (X-axis). It can be seen that the mines and deposits with a tonnage estimate that were used to create the favourability map are predicted with an accuracy of 96.1%, with only 1% of the area showing a higher favourability—a result very comparable with that obtained for the control set (Figure 46b). The favourability map therefore shows a high predictive capacity, whose reliability is confirmed by the results of the control set of 32 points.

In comparison, only 69.1% of the deposits with no tonnage estimate and 42.7 % of showings are predicted for the same cumulative favourability value. This difference likely results from the fact that mines, and to a lesser extent, deposits with a tonnage estimate are generally characterized by an abundance of spatial data including drill holes and whole-rock analyses. The high volume of data aid in accurately defining their geological attributes. Conversely, deposits for which there is no tonnage estimate and showings have been studied less and their spatial characterization is more limited.

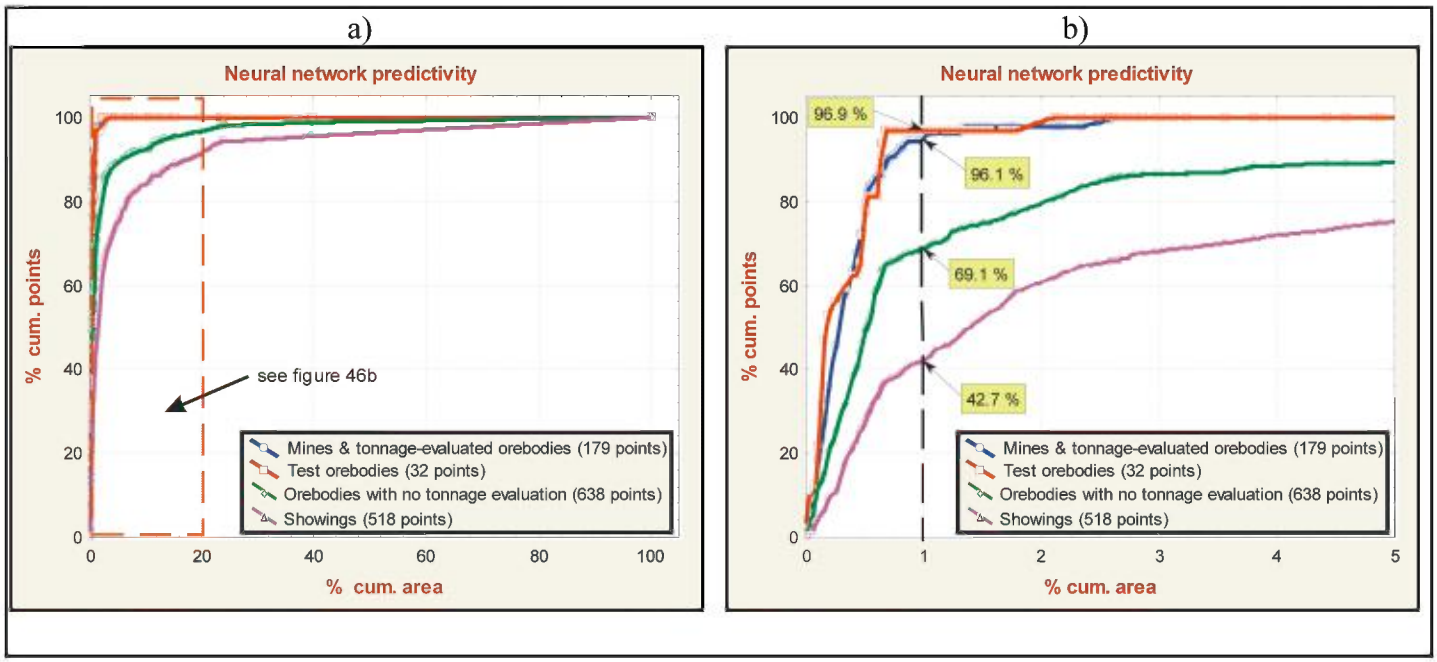

Figure 46 - a) and **b)** Comparison of the predictive performance, measured from the favourability map, for 4 sets of orogenic gold ore bodies in the Abitibi. The red line on the 2 diagrams corresponds to a control set of 32 points consisting of mines and deposits with a tonnage estimate that were not used to produce the favourability map.

6 References

AGTERBERG, F.P., 1989 - Systematic approach to dealing with uncertainty of geoscience information in mineral exploration. Proceedings 21st APCOM Symposium, Las Vegas, march 1989; Chapter 18, pages 165-178.

AGTERBERG, F.P. - BONHAM-CARTER, G.F. - WRIGHT, D.F., 1990 - Statistical pattern integration for mineral exploration. *In*: Computer Applications in Resource Estimation Prediction and Assessment for Metals and Petroleum (Gaal, G. and Merriam, D.F., editors). Pergamon Press, Oxford; pages 1-21.

AN, P. - MOON, W. - RENCZ, A.N., 1991 - Application of fuzzy theory for integration of geological, geophysical and remotely sensed data. Canadian Journal of Exploration Geophysics; Volume 27, pages 1-11.

AN, P. - MOON, W.M. - BONHAM-CARTER, G.F., 1992 - On a knowledge-based approach of integrating remote sensing, geophysical and geological information. Proceedings IGARSS'92; pages 34-38.

BOLENEUS, D.E. - RAINES, G.L. - CAUSEY, D. - BOOKSTROM, A.A. - FROST, T.P. - HYNDMAN, P.C., 2001 - Assessment method for epithermal gold deposits in northeast Washington State using weights-of-evidence GIS modelling. USGS; Open File report 01-501, 53 pages.

BONHAM-CARTER,G.F., 1994 - Geographic Information Systems for geoscientists: Modelling with GIS. Pergamon Press, Oxford; 398 pages.

BONHAM-CARTER, G.F. - AGTERBERG, F.P. - WRIGHT D.F., 1988 - Integration of geological datasets for gold exploration in Nova Scotia. Photogrammetric Engineering and Remote Sensing; Volume 54, No.77, pages 1585-1592.

BONHAM-CARTER, G.F. - AGTERBERG, F.P. - WRIGHT D.F., 1989 - Weights of evidence modelling : a new approach to mapping mineral potential. Statistical applications in the Earth Sciences; Geological Survey of Canada; Paper 89-9, pages 171-183.

BROWN, W.M. - GEDEON, T.D. - GROVES, D.I. - BARNES, R.G., 2000 - Artificial neural networks; a new method for mineral prospectivity mapping. Australian Journal of Earth Sciences, Volume 47, No.4, pages 757-770.

BROWN, W. - GROVES, D.I. - GEDEON, T., 2003a - Use of fuzzy membership input layers to combine subjective geological knowledge and empirical data in a neural network method for mineral-potential mapping. Natural Resources Research; Volume 12, No.3, pages 183-200.

BROWN, W.M. - GEDEON, T.D. - GROVES, D.I., 2003b - Use of noise to augment training data : A neural network method of mineral-potential mapping in regions of limited known deposit examples. Natural Resources Research; Volume 12, No.2, pages 141-152.

CHUNG, C.F. - AGTERBERG, F.P., 1980 - Regression models for estimating mineral resources from geological map data. Mathematical Geology; Volume 12, No.5, pages 473-488.

CHUNG, C.F. - MOON, W.M., 1991 - Combination rules of spatial geoscience data for mineral exploration. Geoinformatics; Volume 2, pages 159-169.

D'ERCOLE, C. - GROVES, D.I. - KNOX-ROBINSON C.M., 2000 - Using fuzzy logic in a Geographic Information System environment to enhance conceptually based prospectivity analysis of Mississippi Valley-type mineralization. Australian Journal of Earth Sciences; Volume 47, pages 913-927.

DE ARAUJO, C.C. - MACEDO, A.B., 2002 - Multicriteria geologic data analysis for mineral favourability mapping: Application to a metal sulphide mineralized area, Ribeira Valley Metallogenic Province, Brazil. Natural Resources Research. Volume 11, No. 1, pages 29-43.

DION, C. - LAMOTHE, D., 2002 - Évaluation du potentiel en minéralisations de sulfures massifs volcanogènes de la région de Chibougamau (32G) - Intégration de géodonnées par la technologie d'analyse spatiale. Ministère des Ressources naturelles; EP 2002-04, 1 cédérom.

DOUCET, P., - LAFRANCE, B., 2005 - Le potentiel aurifère en profondeur du camp minier de Cadillac. Ministère des Ressources naturelles et de la Faune; PRO 2005-01, 14 pages.

EISENLOHR, B.N. - GROVES, D.I. - PARTINGTON, G.A., 1989 - Crustal-scale shear zones and their significance to Archean gold mineralization in Western Australia. Mineralium Deposita; Volume 24, pages 1-8.

REFERENCES

FAURE, S., 2004 - Analyse des linéaments géophysiques en relation avec les minéralisations Au et de métaux de base de l'Abitibi : application aux camps miniers de Malartic et Val-d'Or. Site web du CONSOREM.

FRANKLIN, J.M., 1993 - Volcanic-associated Massive Sulphide Deposits. *In:* Mineral Deposits Modeling (Kirkham, R.D., Sinclair, W.D., Thorpe R.I. and Duke, J.M., editors). Geological Association of Canada Special Paper 40, pages 315-334.

GROVES, D.I., 2002 - Orogenic Gold Deposit Workshop. Matériel de l'atelier présenté à l'UQAM, avril 2002.

GROVES D.I. - BARLEY, M.E. - HO, S.E., 1989 - Nature, genesis and tectonic setting of mesothermal gold mineralization in the Yilgarn block, Western Australia. *In*: The geology of gold deposits : The perspective in 1988 (Kays, R.R., Ramsay W.R.H., Groves, D.I., editors). Economic Geology; Monograph 6, pages 71-85.

GROVES D.I. - GOLDFARB R.J. - GEBRE-MARIAM M. - HAGEMANN S.G. - ROBERT F., 1998 - Orogenic gold deposits: a proposed classification in the context of their crustal distribution and relationship to other gold deposit types. Ore Geology Reviews; Volume 13, pages 7-27.

GROVES D.I. - GOLDFARB R.J. - KNOX-ROBINSON C.M. - OJALA V.J. - GARDOLL S.J. - YUN G. Y. - HOLYLAND P.W., 2000 - Late-kinematic timing of orogenic gold deposits and significance for computer based exploration techniques with emphasis on the Yilgarn Block, Western Australia. Ore Geology Reviews; Volume 17, pages 1-38.

HAGEMANN, S.G. - CASSIDY, K.F., 2000 - Archean orogenic losde gold deposits. *In*: Gold in 2000 (Hagemann, S.G. and Brown, P.E., editors). Reviews in Economic Geology; Volume 13, pages 9-68.

HARRIS D.A. - PAN, R., 1999 - Mineral favourability mapping: a comparison of artificial networks, logistic regression and discriminant analysis. Natural Resources Research; Volume 8, No.2, pages 93-109.

HARRIS, J.R., 1989 - Data Integration for gold exploration in eastern Nova Scotia using a GIS. In Proceedings of Remote Sensing for Exploration Geology, Calgary, Alberta, pages 233-249.

HARRIS, J.R. - WILKINSON, L. - BROOME, J., 1995 - Mineral exploration using GIS-based favourability analysis, Swayze Greenstone Belt, Northern Ontario. *In*: Proceedings of the Canadian Geomatics Conference (CD-ROM), National Defense Canada.

HARRIS J.R. - WILKINSON, L. - GRUNSKY, G. - HEATHER, K., AYER, J., 1999 - Techniques for analysis and visualization of lithogeochemical data with applications to the Swayze greenstone belt, Ontario. Journal of Geochemical Exploration; Volume 67, No.1-3, pages 301-334.

HARRIS, J.R. - WILKINSON, L. - GRUNSKY, E., 2000 - Effective use and interpretation of lithogeochemical data in regional mineral exploration programs: Application of Geographic Information System (GIS) technology. Ore Geology Reviews; Volume 16, pages 107-143.

HARRIS, J.R. - WILKINSON, L. - HEATHER, K. - FUMERTON, S. - BERNIER, M.A. - AYER, J. - DAHN, R., 2001 - Application of GIS processing techniques for producing mineral prospectivity maps - A case study : Mesothermal Au in the Swayze greenstone belt, Ontario, Canada. Natural Resources Research; Volume 10, No.2, pages 91-124.

HARRIS, J.R. - SANBORN-BARRIE, M. - PANAGAPKO, D.A. - SKULSKI, T. - PARKER, J.R., 2005 - Gold prospectivity maps of the Red Lake greenstone belt: Application of GIS technology. Canadian Journal of Earth Sciences (in press).

HODGSON, C.J., 1993 - Mesothermal lode-gold deposits. *In*: Mineral Deposit Modeling (Kirkham, R.D., Sinclair, W.D., Thorpe R.I. and Duke, J.M., editors). Geological Association of Canada; Special Paper 40, pages 635-678.

JENKS, G.F., 1967 - The Data Model Concept in Statistical Mapping. International Yearbook of Cartography; volume 7, pages 186-190.

KNOX-ROBINSON, C.M., 2000 - Vectorial fuzzy logic: a novel technique for enhanced mineral prospectivity mapping, with reference to the orogenic gold mineralization potential of the Kalgoorlie Terrane, Western Australia. Australian Journal of Earth Sciences; Volume 57, No. 5, pages 929-942.

KOIKE, K. - MATSUDA, S. - SUZUKI, T. - OHMI, M., 2002 - Neural-network-based estimation of principal metal content in the Hokuroku district, Northern Japan, for exploring Kuroko-type deposits. Natural Resources Research; Volume 11, No. 2, pages 135-156.

REFERENCES

LABBÉ, J.-Y., 2002 - Évaluation du potentiel de découverte de kimberlites de la région du Grand-Nord du Québec - Intégration de géodonnées par la technologie d'analyse spatiale. Ministère des Ressources naturelles; EP 2002-05, 1 cédérom.

LAMOTHE, D. - BEAUMIER, M., 2001 - Évaluation du potentiel régional en minéralisations de type Olympic Dam-Kiruna dans la région du lac Manitou (SNRC 22I). Ministère des Ressources naturelles; EP 2001-01, 1 cédérom.

LAMOTHE, D. - BEAUMIER, M., 2002 - Évaluation du potentiel régional en minéralisations de type Olympic Dam-Kiruna dans la région du lac Fournier (SNRC 22P). Ministère des Ressources naturelles; EP 2002-01, 1 cédérom.

LAMOTHE, D. - HARRIS, J.R. - LABBÉ, J.-Y. - DOUCET, P. - HOULE, P. - MOORHEAD, J., 2005 - Évaluation du potentiel en minéralisations de type sulfures massifs volcanogènes (SMV) pour l'Abitibi. Ministère des Ressources naturelles, de la Faune et des Parcs; EP 2005-01, 1 cédérom.

LOONEY, C.G. - YU, H., 1999 - Special software development for neural network and fuzzy clustering analysis in geological information systems. Texte accompagnant le module ArcSDM.

MIHALASKI, M.J. - BONHAM-CARTER, G.F., 2001 - Lithodiversity and its spatial association with metallic mineral sites, Great Basin of Nevada. Natural Resources Research; Volume 10, No.3, pages 1-30.

MIKUCKI, E.J., 1998 - Hydrothermal transport and depositional processes in Archean lode-gold systems: A review. Ore Geology Reviews; Volume 13, pages 307-321.

PAGANELLI, F. - RICHARDS, J.P. - GRUNSKY, E.C., 2002 - Integration of Structural, Gravity and Magnetic Data Using the Weights of Evidence Method as a tool for Kimberlite Exploration in the Buffalo Head Hills, Northern Central Alberta, Canada. Natural Resources Research; volume 11, no. 3, pages 219- 236.

PHILLIPS, G.N. - GROVES, D.I., 1983 - The nature of archean gold-bearing fluids as deduced from gold deposits of Western Australia. Journal of the Geologic Society of Australia; Volume 30, pages 25-39.

PICHÉ, M., 2000 - Quantification de l'altération hydrothermale des roches du camp minier de Joutel à partir des analyses des éléments majeurs. Ministère des Ressources naturelles;, MB 2000-06, 34 pages.

PICHÉ, M. - JÉBRAK, M., 2004 - Normative minerals and alteration indices developed for mineral exploration. J. Geoch. Expl.; Volume 82, pages 59-77.

PORWAL, A. - CARRANZA E.J.M. - HALE, M., 2003a - Artificial neural networks for mineral-potential mapping: A case study from the Aravalli Province, western India. Natural resources Research; Volume 12, No. 3, pages 155-171.

PORWAL, A. - CARRANZA E.J.M. - HALE, M., 2003b - Knowledge-driven and data-driven fuzzy modlels for predictive mineral potential mapping. Natural resources Research; Volume 12, No. 1, pages 1-25.

POULSEN, K.H. - HANNINGTON, M.D., 1996 - Gîtes de sulfures massifs aurifères associés à des roches volcaniques. *Dans* : Géologie des types de gîtes minéraux du Canada (Ekstrand, O.R., Sinclair, W.D. et Thorpe, R.I., éditeurs). Commission géologique du Canada; Géologie du Canada Numéro 8, pages 202-217.

RAINES, G.L., 1999 - Evaluation of Weights of Evidence to predict epithermal gold deposits in the Great Basin of the western United States. Natural Resources Research; Volume 8, No.4, pages 257-276.

RENCZ, A.N. - HARRIS, J.R. - WATSON G.P. - MURPHY, B., 1994 - Data Integration for Mineral Exploration in the Antigonish Highlands, Nova Scotia. Canadian Journal of Remote Sensing; Volume 20, No.3, pages 258-267.

ROBERT, F., 1990 - An Overview of Gold Deposits in the Eastern Abitibi Belt. In The Northeastern Quebec Polymetallic belt: A Summary of 60 Years of Mining Exploration (Rive M., Verpaelst P., Gagnon Y., Lulin J., Riverin G. and Simard A., editors). Canadian Institute of Mining and Metallurgy; Special Volume 43, pages 93-105.

ROBERT, F., 2005 - Gold Metallogeny of the Superior (Canada) and Yilgarn (Australia) Cratons and Implications for Exploration. Québec Exploration 2005, résumé des conférences et photoprésentations, page 11.

SINGER, D.A. - KOUDA R., 1996 - Application of feedforward neural network in search for Kuoroko deposits in the Hokuroku district, Japan. Mathematical Geology; Volume 28, No.3, pages 1017-1023.

SINGER, D.A. - KOUDA R., 1997a - Use of a neural network to integrate geoscience information in the classification of mineral deposits and occurrences. *In:* Proceedings of Exploration 97: 4th Decennial International Conference on Mineral Exploration (Gubins A.G., editor). Pages 127-134.

REFERENCES

SINGER, D.A. - KOUDA R., 1997b - Classification of mineral deposits into types using mineralogy with a probabilistic neural network. Nonrenewable Resources; Volume 6, pages 27-32.

SINGER, D.A. - KOUDA R., 1999 - A comparison of the weights-of-evidence method and probabilistic neural networks. Natural Resources Research; Volume 8, No. 4, pages 287-298.

SPIEGELHALTER, D.J., 1986 - Uncertainty in expert systems. *In*: Artificial Intelligence and Statistics (Gale W. A. editor). Addison-Wesley, Reading, Massachusetts; pages 17-25.

TOURIGNY, G. - BROWN, A.C. - HUBERT, C. - CRÉPEAU, R., 1989 - Syn-volcanic and syntectonic gold mineralization at the Bousquet Mine, Abitibi greenstone belt, Québec. Economic Geology; Volume 84, pages 1875-1890.

TOURIGNY, G. - DOUCET, P. - BOURGET, A., 1993 - Geology of the Bousquet 2 Mine: an example of a deformed gold-bearing, polymetallic sulfide deposit. Economic Geology; Volume 88, pages 1578-1597.

WRIGHT, D.F., 1996 - Evaluating volcanic hosted massive sulphide favourability using GIS-based spatial data integration models, Snow Lake area, Manitoba. Unpublished Ph.D. thesis, University of Ottawa; 338 p.

WRIGHT, D.F. - BONHAM-CARTER, G.F., 1996 - VHMS Favourability Mapping with GIS-Based Integration Models, Chisel anLake-Anderson Lake Area. *In*: EXTECH I: A Multidisciplinary Approach to Massive Sulphide Research in the Rusty Lake- Snow Lake Greenstone Belts, Manitoba (Bonham-Carter G.F., Galley A.G., Hall G.E.M., editors). Geological Survey of Canada; Bulletin 426, pages 339 -376, 387-401.

Appendix 1

1/50 000 favourability map index

Each favourability map may be consulted by clicking on the appropriate SNRC reference number above.

Radial-based neural network

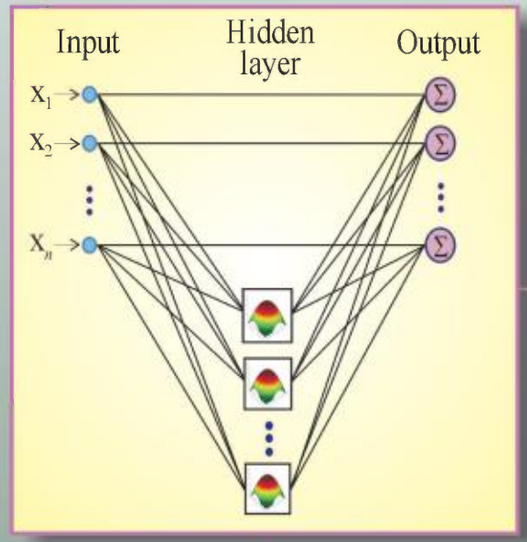

Abitibi gold potential

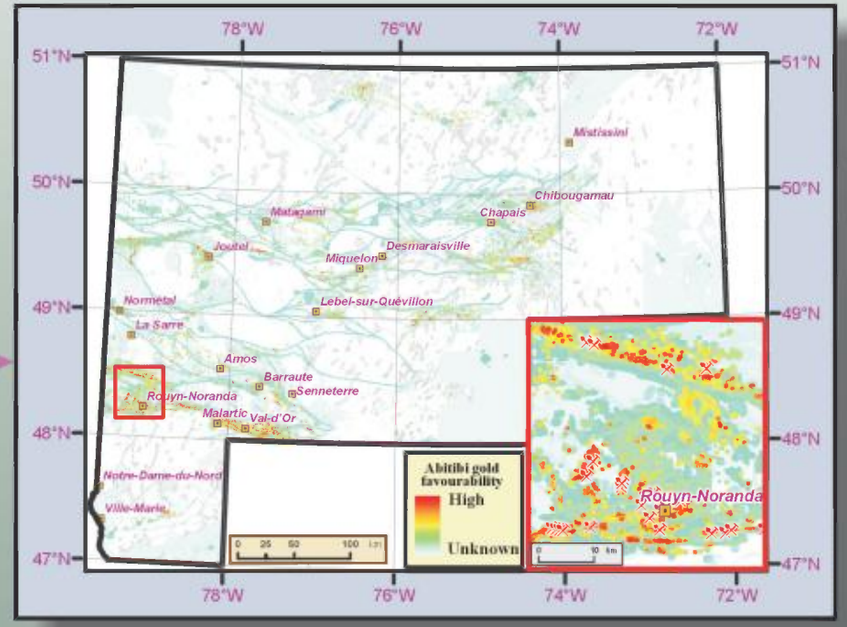

Favourable lithology	Litho-diversity	Competence contrast	Reac-tivity	Archean fault proximity	Archean fault density	Ductile linear element	Quartz vein	Gold	Arsenic	Antimony	Sulfur	MAG total field	MAG vertical gradient	ISER	IPAF	ICHLO	Mineral occurrence	VMS favourable zones
Lithological Control				*Structural Control*				*Metal Indicators*				*Geophysical signature*		*Alteration indicators*				*Favourable Context*

Parameters used for the evaluation of the Abitibi orogenic gold mineral potential. Text sections relevant to a specific parameter may be consulted by clicking on the appropriate box. Shapefiles and grids may be extracted by clicking on the relevant text elements.